ANL-ART-38

# Regulatory Technology Development Plan Sodium Fast Reactor

## Mechanistic Source Term – Metal Fuel Radionuclide Release

Nuclear Engineering Division

**About Argonne National Laboratory**
Argonne is a U.S. Department of Energy laboratory managed by UChicago Argonne, LLC under contract DE-AC02-06CH11357. The Laboratory's main facility is outside Chicago, at 9700 South Cass Avenue, Argonne, Illinois 60439. For information about Argonne and its pioneering science and technology programs, see www.anl.gov.

**DOCUMENT AVAILABILITY**

**Online Access:** U.S. Department of Energy (DOE) reports produced after 1991 and a growing number of pre-1991 documents are available free via DOE's SciTech Connect (http://www.osti.gov/scitech/)

**Reports not in digital format may be purchased by the public from the National Technical Information Service (NTIS):**
U.S. Department of Commerce
National Technical Information Service
5301 Shawnee Rd
Alexandria, VA 22312
**www.ntis.gov**
Phone: (800) 553-NTIS (6847) or (703) 605-6000
Fax: (703) 605-6900
Email: **orders@ntis.gov**

**Reports not in digital format are available to DOE and DOE contractors from the Office of Scientific and Technical Information (OSTI):**
U.S. Department of Energy
Office of Scientific and Technical Information
P.O. Box 62
Oak Ridge, TN 37831-0062
**www.osti.gov**
Phone: (865) 576-8401
Fax: (865) 576-5728
Email: **reports@osti.gov**

**Disclaimer**
This report was prepared as an account of work sponsored by an agency of the United States Government. Neither the United States Government nor any agency thereof, nor UChicago Argonne, LLC, nor any of their employees or officers, makes any warranty, express or implied, or assumes any legal liability or responsibility for the accuracy, completeness, or usefulness of any information, apparatus, product, or process disclosed, or represents that its use would not infringe privately owned rights. Reference herein to any specific commercial product, process, or service by trade name, trademark, manufacturer, or otherwise, does not necessarily constitute or imply its endorsement, recommendation, or favoring by the United States Government or any agency thereof. The views and opinions of document authors expressed herein do not necessarily state or reflect those of the United States Government or any agency thereof, Argonne National Laboratory, or UChicago Argonne, LLC.

ANL-ART-38

# Regulatory Technology Development Plan
# Sodium Fast Reactor

Mechanistic Source Term – Metal Fuel Radionuclide Release

---

Prepared by
David Grabaskas, Matthew Bucknor, James Jerden
Nuclear Engineering Division, Argonne National Laboratory

February, 2016

# Acknowledgements

The authors would like to express their appreciation to the members of the Regulatory Technology Development Plan (RTDP) project at Idaho National Laboratory for their assistance with the project development and report creation.

***Wayne Moe***
***Jim Kinsey***
***Mark Holbrook***

The authors would also like to thank the technical reviewers of the report.

***Thomas King (Ret., Nuclear Regulatory Commission)***
***Leonard Leibowitz (Senior Chemist, Argonne National Laboratory)***
***Candido Pereira (Principal Chemical Engineer, Argonne National Laboratory)***

The authors would like to thank those technical experts who provided insight and assistance throughout the course of the project.

***Steve Hayes***
***Steve Frank***
***Francine Rice***
***Mark Williamson***
***Walid Mohamed***
***Aydin Karahan***
***Gerard Hofman***

# Executive Summary

The development of an accurate and defensible mechanistic source term will be vital for the future licensing efforts of metal fuel, pool-type sodium fast reactors. To assist in the creation of a comprehensive mechanistic source term, the current effort sought to estimate the release fraction of radionuclides from metal fuel pins to the primary sodium coolant during fuel pin failures at a variety of temperature conditions. These release estimates were based on the findings of an extensive literature search, which reviewed past experimentation and reactor fuel damage accidents. Data sources for each radionuclide of interest were reviewed to establish release fractions, along with possible release dependencies, and the corresponding uncertainty levels.

Although the current knowledgebase is substantial, and radionuclide release fractions were established for the elements deemed important for the determination of offsite consequences following a reactor accident, gaps were found pertaining to several radionuclides. First, there is uncertainty regarding the transport behavior of several radionuclides (iodine, barium, strontium, tellurium, and europium) during metal fuel irradiation to high burnup levels. The migration of these radionuclides within the fuel matrix and bond sodium region can greatly affect their release during pin failure incidents. Post-irradiation examination of existing high burnup metal fuel can likely resolve this knowledge gap. Second, data regarding the radionuclide release from molten high burnup metal fuel in sodium is sparse, which makes the assessment of radionuclide release from fuel melting accidents at high fuel burnup levels difficult. This gap could be addressed through fuel melting experimentation with samples from the existing high burnup metal fuel inventory.

# Table of Contents


1 INTRODUCTION ..... 1
1.1 SCOPE ..... 2
1.2 METHODOLOGY ..... 4
2 LITERATURE REVIEW SUMMARY ..... 5
2.1 EXPERIMENTS AND REPROCESSING ..... 5
2.1.1 MELT REFINING EXPERIENCE ..... 5
2.1.1.1 PRE-OPERATIONAL FUEL MELT TESTS ..... 6
2.1.1.2 FCF MELT REFINING EXPERIENCE ..... 9
2.1.2 FUEL MELT EXPERIMENTS ..... 9
2.1.2.1 OAK RIDGE FUEL MELT TESTING ..... 9
2.1.2.2 HANFORD FUEL MELT TESTING ..... 11
2.1.2.3 ATOMICS INTERNATIONAL FUEL MELT TESTING ..... 12
2.1.3 CLADDING BREACH EXPERIMENTS AT EBR-II ..... 12
2.1.3.1 LEAKER EXPERIMENTS ..... 13
2.1.3.2 RUN-BEYOND-CLADDING-BREACH TESTS ..... 13
2.1.4 TREAT M-SERIES ..... 14
2.1.5 METAL FUEL POST-IRRADIATION EXAMINATION (PIE) ..... 16
2.1.5.1 FISSION GAS RELEASE EXPERIMENTS ..... 16
2.1.5.2 EBR-II PIE ..... 17
2.1.5.3 FFTF PIE ..... 22
2.1.5.4 METAPHIX PIE ..... 23
2.1.5.5 AFC SERIES PIE ..... 24
2.2 FUEL DAMAGE ACCIDENTS ..... 26
2.2.1 SODIUM REACTOR EXPERIMENT (SRE) ACCIDENT ..... 26
2.2.2 FERMI 1 ACCIDENT ..... 27
2.2.3 EBR-II FAILED EXPERIMENTAL CAPSULE ..... 28
2.3 OTHER SOURCES ..... 28
2.3.1 EBR-I INCIDENT ..... 28
2.3.2 DOUNREAY FAST REACTOR ..... 28
3 CHEMISTRY MODELING SUMMARY ..... 29
3.1 OVERVIEW OF MODELING EFFORT ..... 29
3.2 MODEL SCENARIOS AND ASSUMPTIONS ..... 30
3.3 CONCLUSIONS OF INITIAL CHEMISTRY MODELING EFFORT ..... 32
4 ESTIMATED RADIONUCLIDE RELEASE FRACTION FROM METAL FUEL ..... 33
4.1 RESULTS ..... 33
4.1.1 NOBLE GASES ..... 36
4.1.2 HALOGENS ..... 37
4.1.3 ALKALI METALS ..... 38
4.1.4 TELLURIUM GROUP ..... 39
4.1.5 BARIUM, STRONTIUM ..... 40
4.1.6 NOBLE METALS ..... 42
4.1.7 LANTHANIDES ..... 43
4.1.8 CERIUM GROUP ..... 44
4.2 GAPS AND POSSIBLE CLOSURE PATHWAYS ..... 46
4.2.1 EXPANDED METAL FUEL PIE ..... 46
4.2.2 HIGH BURNUP METAL FUEL MELT TESTS ..... 47
5 CONCLUSION ..... 48
BIBLIOGRAPHY ..... 49

**APPENDIX A: RADIONUCLIDE RELEASE FRACTION DETERMINATION** ..... **53**
A.1 NOBLE GASES ..... 53
A.2 HALOGENS ..... 55
A.3 ALKALI METALS ..... 58
A.4 TELLURIUM GROUP ..... 61
A.5 BARIUM, STRONTIUM ..... 63
A.6 NOBLE METALS ..... 67
A.7 LANTHANIDES ..... 69
A.6 CERIUM GROUP AND URANIUM ..... 71
**APPENDIX B: LITERATURE REVIEW INFORMATION TABLES** ..... **75**
**APPENDIX C: CHEMISTRY MODELING DETAILS** ..... **82**

# Acronyms & Abbreviations

| | |
|---|---|
| AI | Atomics International |
| ALMR | Advanced Liquid Metal Reactor |
| Argonne | Argonne National Laboratory |
| AT | Applied Technology |
| ATR | Advanced Test Reactor |
| BNL | Brookhaven National Laboratory |
| CEA | Commissariat a l'Energie Atomique |
| CRIEPI | Central Research Institute of Electric Power Industry |
| DFR | Dounreay Fast Reactor |
| DOE | U.S. Department of Energy |
| EBR-I | Experimental Breeder Reactor I |
| EBR-II | Experimental Breeder Reactor II |
| EMPA | Electron Micro Probe Analysis |
| FCF | Fuel Cycle Facility |
| FFTF | Fast Flux Test Facility |
| HFEF | Hot Fuel Examination Facility |
| IFR | Integral Fast Reactor |
| INL | Idaho National Laboratory |
| ITU | Institute of Transuranium Elements |
| KEWB | Kinetics Experimental Water Boiler |
| LWR | Light Water Reactor |
| MA | Minor Actinide |
| MST | Mechanistic Source Term |
| ORNL | Oak Ridge National Laboratory |
| PIE | Post-Irradiation Examination |
| QA | Quality Assurance |
| RBCB | Run Beyond Cladding Breach |
| RE | Rare Earth |
| RTDP | Regulatory Technology Development Plan |
| SFR | Sodium Fast Reactor |
| SRE | Sodium Reactor Experiment |
| STR | Submarine Thermal Reactor |
| TREAT | Transient Reactor Test Facility |

# 1 Introduction

To license and operate a commercial nuclear power plant, it is vital to ensure the safety of the public and environment by providing protections against the release of radionuclides. As part of the process to assess the safety of a nuclear plant design, the source term expected to occur during normal reactor operation and accident sequences is analyzed, where a source term is considered to be the types and amounts of radionuclides that could be released to the environment. Not only is this a fundamental part of the design process, but it is a requirement for regulatory licensing [1]. While past nuclear plant power source term analyses often utilized a deterministic, bounding, and conservative assessment of radionuclide release, over the past 25 years there has been an increased interest in the development of more realistic evaluations that also consider important uncertainties.

This work is part of continuing series of projects to assist in the development of a mechanistic source term (MST) for sodium fast reactors (SFRs). In general, an MST attempts to realistically model the release and transport of radionuclides from the source to the environment for a specific accident scenario, while accounting for retention or transmutation phenomena and their associated uncertainties. Significant knowledge and modeling capabilities regarding complex radionuclide transport phenomena are necessary for the determination of an accurate MST, as multiple chemical and physical interactions are occurring simultaneously. However, development of a technically sound assessment of the source term is a responsibility of reactor vendors who are seeking to design, license, and build commercial nuclear power plants within the U.S.

***Objective:*** *Determine the release fraction of radionuclides from metal fuel pins to the primary sodium following pin failure under different temperature conditions.*

The current work, outlined below, focuses on the determination of radionuclide release fractions from metal fuel pins into the primary sodium of an SFR following pin failure. Available information is used as the basis of this analysis, with the goal of identifying existing gaps in the current knowledgebase. This work begins with an overview of the project scope and methodology in Section 1. The next section reviews the findings of a literature search to determine relevant past experiments and reactor fuel damage accidents. Section 3 describes attempts to supplement the current knowledgebase through the use of modern chemistry modeling tools. The main findings of the report, the radionuclide release fractions and established gaps, are summarized in Section 4. Lastly, Section 5 presents general conclusions from the project. A series of appendices provide additional details regarding the literature reviewed, the determined release fractions, and chemistry code analysis.

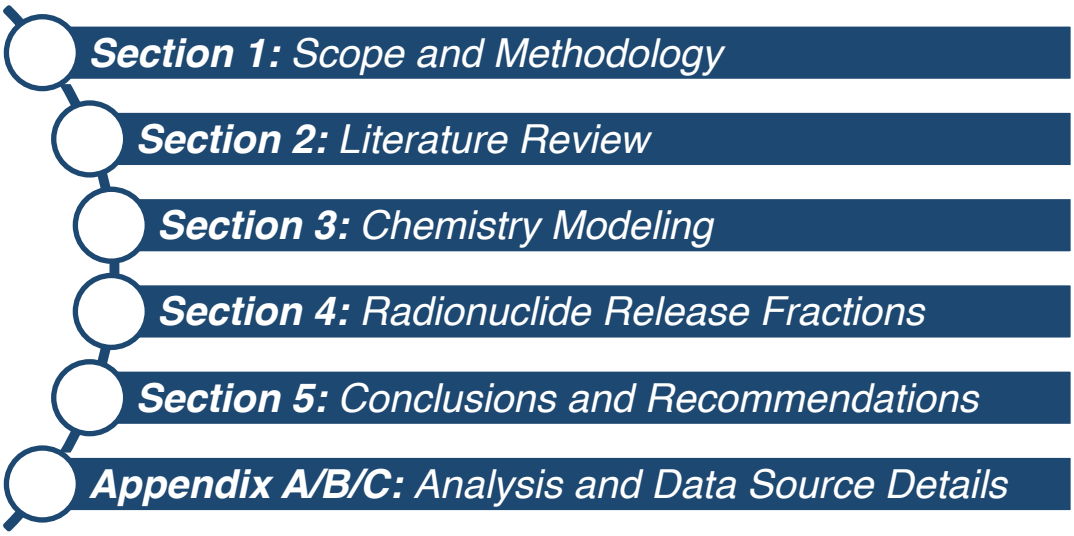

### *1.1 Scope*

The main objective of this work is to determine radionuclide release fractions from metal fuel to the primary sodium during fuel pin failure. Figure 1–1 shows where the current effort falls within the overall development of an MST. This figure represents a stylized process, as there are design-specific factors that would need to be considered by particular licensees. A previous project report, ANL-ART-3 [2], examined the first two steps of the MST development process. The current work is part of the third step, as determining radionuclide release fractions from the fuel to the primary sodium is the initial step in modeling the transport of radionuclides to the environment, as shown in Figure 1–2.

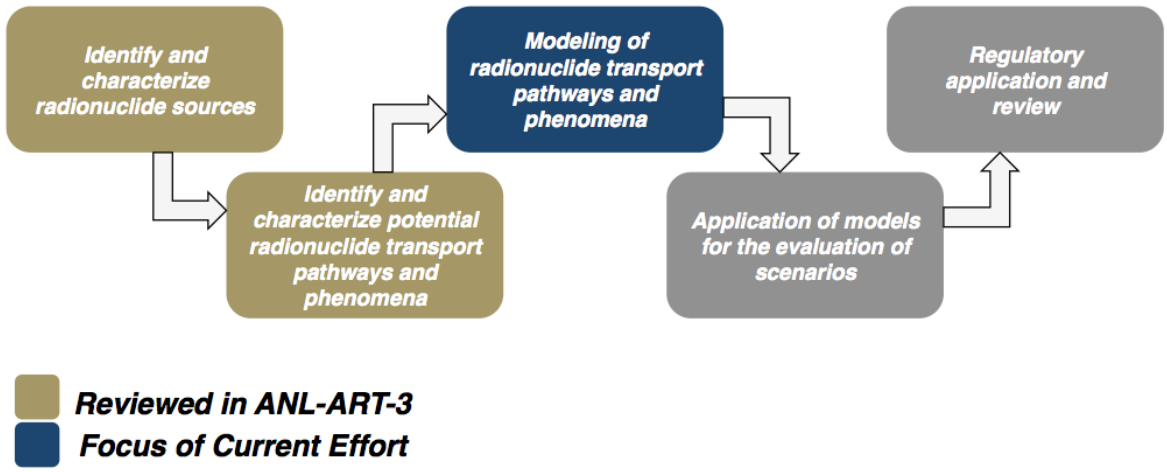


**Figure 1–1: Mechanistic Source Term Development Pathway and Current Focus Area**

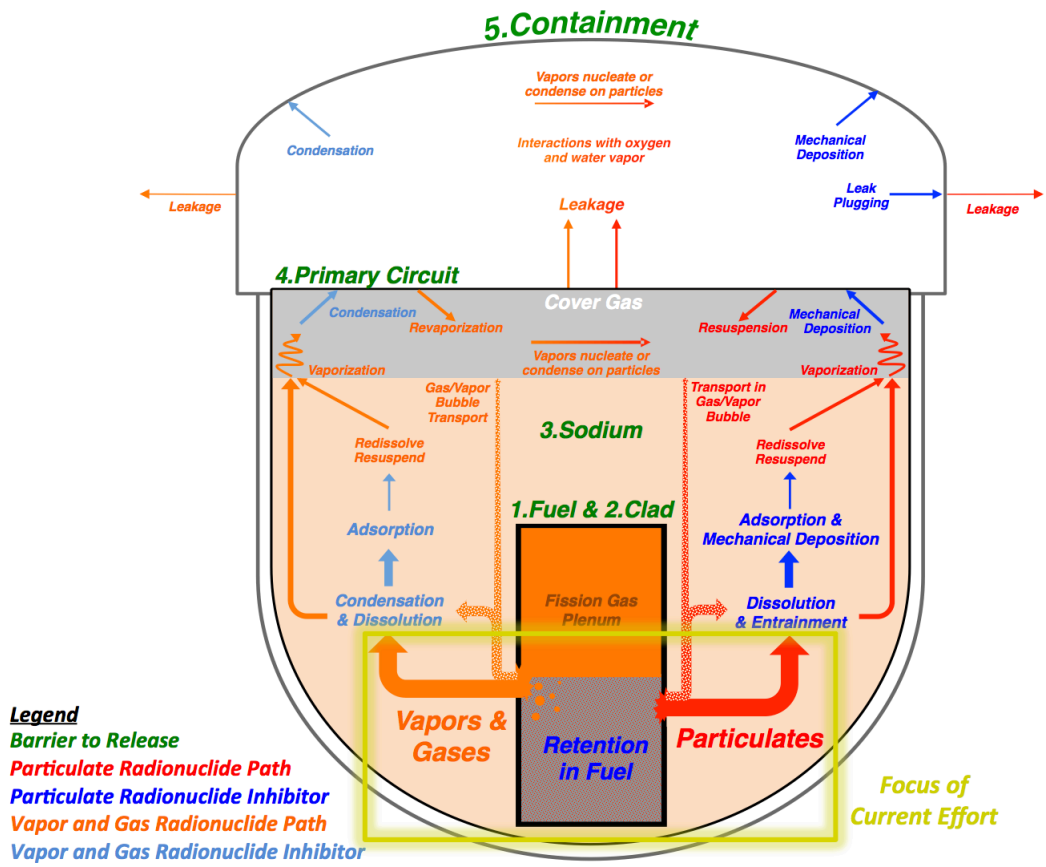


**Figure 1–2: SFR Radionuclide Transport Pathways and Current Focus Area**

The project scope was split into six main elements, as listed below. The first four elements (*a* – *d*) describe the review to be performed of past experiments, accidents, and studies, and the proper documentation of their results, along with pertinent associated information, such as quality assurance protocol and range of applicability. The fifth element (*e*) notes that modern chemistry modeling techniques will be examined for their capability to address gaps where no data exist. The final element (*f*) states that the findings of the previous five elements will be used to determine radionuclide release fractions.

a. Identify and compile a list of existing metal fuel experiments that will yield data applicable to determination of the type and quantity of radionuclides released from melted metal fuel into sodium coolant.

b. The melted metal fuel experiment list will include important identifying information (when available), such as 1) facility where experiments were performed, 2) identifying experiment numbers or designations, 3) dates that experiments were performed, 4) fuel burnup levels at the time of the experiments, 5) current location of experimental data/results, 6) the entity that controls access to the experimental data/results, and 7) comments on the quality assurance processes that were in place when the experiment was conducted.

c. Radionuclide release information from past metal fuel accidents will also be reviewed, consolidated, and assessed for applicability to SFR MST calculations. The accident list is expected to include (at a minimum) the Sodium Reactor Experiment (SRE) meltdown, the Fermi 1 meltdown, and the failed experimental fuel capsule at the Experimental Breeder Reactor II (EBR-II).

d. A review shall be conducted to analyze and assess the available metal fuel radionuclide release information. This review should focus on quantification of the amounts of actinides, halogens, alkali metals, alkaline earths, and noble metals that would be released to the primary sodium during fuel melting.

e. In conjunction with the review of past metal fuel experiment and accident information, mechanistic models of metal fuel behavior (such as chemical equilibrium codes) will be examined to gauge their applicability for determining radionuclide release fractions from molten metal fuel. This task consists of assessing the ability, and accuracy, of the mechanistic models to properly simulate radionuclide transport from the metal fuel pin to the primary sodium coolant.

f. Based on the reviews of the available metal fuel information described above, develop estimates for individual radionuclide release fractions from molten metal fuel into the sodium coolant. The task shall identify all necessary documentation and information resources used to support the release fractions estimate. Clearly identify the analysis codes used in the examination and provide insights as appropriate regarding weaknesses and uncertainties in the calculation methodology and associated estimates.

*Radionuclide release from metal fuel to the primary sodium is examined for fuel conditions typical of design basis and beyond design basis accidents at metal fuel, pool-type SFRs.*

This analysis involves the examination of radionuclide release from metal fuel under conditions that would be typical of design basis and beyond design basis accidents for metal fuel, pool-type SFRs. This includes pin breach under normal operation due to defects, cladding failure at elevated temperatures due to eutectic penetration, and fuel melting conditions due to loss of heat sink/loss of flow scenarios or transient overpowers. Fuel conditions for accident scenarios that typically fall in the residual risk category or beyond for metal fuel, pool-type SFRs, such as core energetics, hypothetical core disruption accidents, or loss of sodium accidents, are not examined, as these accidents may involve very high fuel temperatures, and the possibility of fuel vaporization.

### *1.2 Methodology*

The project methodology consisted of two parallel paths, as shown in Figure 1–3. The first path involved an extensive literature review of past experiments, accidents, and analyses for pertinent information (Section 2 and Appendix B). The second path included an examination of chemistry modeling techniques as an avenue of providing additional radionuclide release information, in conjunction with the literature review (Section 3 and Appendix C). The original intent was to leverage existing chemistry modeling tools to complement the findings of the literature review and to assist in filling gaps in the knowledgebase. However, as will be described in Section 3, initial investigations utilizing modern chemistry codes indicated limited applicability for determining quantitative radionuclide release fractions. This fact is largely due to the complex phenomena regarding radionuclide behavior within the fuel pin and matrix, and the simplifying assumptions necessary to utilize chemistry codes within the confines of the current databases. Therefore, the literature review was the primary data source utilized for the metal fuel radionuclide release fractions provided in this report, with only supporting insight from chemistry modeling tools.

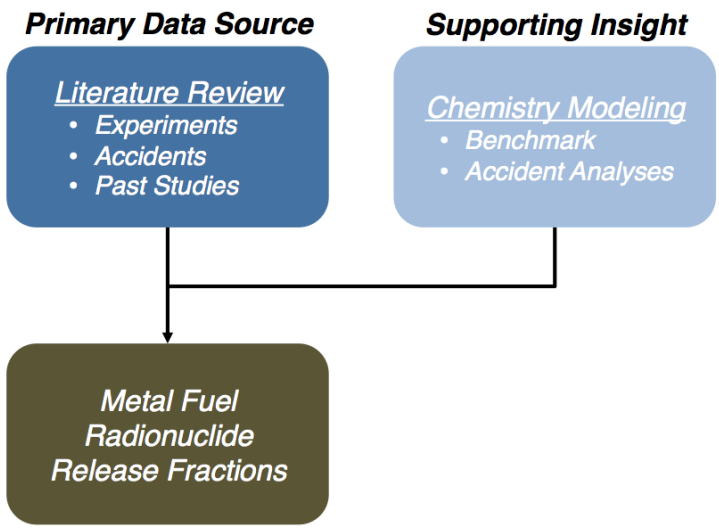


**Figure 1–3: Metal Fuel Radionuclide Release Fraction Strategy**

# 2 Literature Review Summary

This section provides an overview of the data sources utilized to establish radionuclide release fractions from metal fuel to the primary sodium during accident conditions. Due to the substantial differences in fuel chemistry and radionuclide behavior between oxide and metal fuel in SFRs, this review focused on data pertaining only to metal reactor fuel (metallic uranium, U-Fs, U-Mo, U-Zr, U-Pu, and U-Pu-Zr[1]). The first subsection describes past experimental and reprocessing experience, while the second subsection details past accidents. Only a summary of each source is provided in this section, highlighting the most pertinent results. The focus of the literature search was on U.S. metal fuel experience, although some international data, such as Dounreay Fast Reactor information and Japanese metal fuel post-irradiation examinations, is also included.

*The focus of the literature review was on available metal fuel data, as there are significant differences between metal and oxide fuel behavior in SFRs, particularly during fuel failure incidents.*

***Appendix B** provides additional details on each source reviewed, including source document numbers, dates, locations, metal fuel types, access limitations, and quality assurance protocol.*

Details for each individual source reviewed in this section are available in Appendix B. A series of tables provides expanded information on the source documents, including the location of the experiment or accident, dates, document numbers, metal fuel type involved, access limitations, and quality assurance protocol. These tables are provided to assist with knowledge preservation of metal fuel data and to offer insight regarding the applicability of the data for future SFR licensing efforts. As will be seen, the available data spans over a 60-year period and originates from a variety of laboratories and reactor sites.

## *2.1 Experiments and Reprocessing*

### *2.1.1 Melt Refining Experience*

The original objective of EBR-II was to demonstrate the operation of an SFR with on-site metal fuel reprocessing. Reprocessing was to be conducted at the Fuel Cycle Facility (FCF) located at the EBR-II site utilizing melt refining (also known as oxide slagging or drossing). Experiments in preparation for fuel reprocessing, along with five years of melt reprocessing experience at FCF (1964 – 1969) provide valuable insight into metal fuel composition and melting behavior.

While considered somewhat crude by today's reprocessing standards, melt refining uses high temperatures to separate various fuel and fission product elements to create new fuel. Melt refining reprocessing can be split into three main steps [3]:

1) De-cladding: The cladding of the used fuel is removed by peeling through a spiral de-cladding machine.
2) Chopping: The de-cladded fuel is chopped into smaller pieces (about 1.5" in length).
3) Melting: The chopped fuel is melted at high temperatures (~1400°C) for several hours in an oxide crucible within an inert gas atmosphere to separate unwanted fission products from the used fuel.

By melting the used fuel at high temperatures in an oxide crucible, unwanted fission products can be separated through volatilization and oxide reactions with the crucible. As shown in Figure 2–1, used fuel is placed into the crucible and melted. Reactive elements bond with the crucible and form a "skull," while non-reactive elements remain in the ingot. Table 2-1 describes three categories of fission products based on their behavior during melt refining. The first category of fission products, which includes noble gases,

[1] Additional metal fuel types, such as U-Al were also investigated, but initial analyses indicated behavioral differences between these fuel types and the metal fuel types listed here.

halogens, and alkali metals, amongst others, is volatized at high temperatures and removed through gas filtering processes and deposition. The second group reacts with the oxide crucible to form fission product oxides that create the "skull" on the crucible. The last group does not react with the oxide crucible and does not volatize from the fuel, even at the elevated temperatures. These elements remain within the uranium/plutonium ingot formed during the melting (and subsequent cooling) process and become part of the new fuel element. This element grouping is known as fissium – Fs.

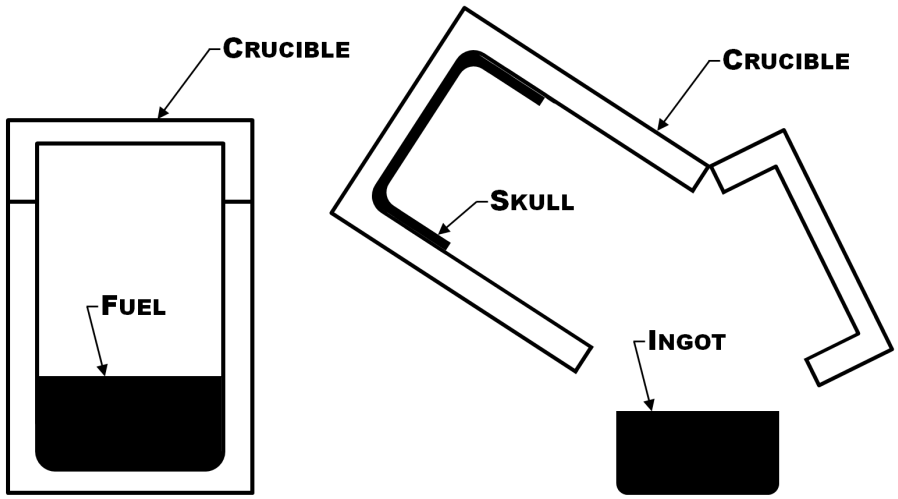


**Figure 2–1: Melt Refining Crucible Elements[2]**

**Table 2-1: Fission Product Group Behavior During Melt Refining[3] [3]**

| *1st Group: Volatile and Gaseous Fission Products* | *2nd Group: Reactive Fission Products* | *3rd Group: Noble Fission Products* |
|---|---|---|
| *Br*[1] | *Sr* | *Ze* |
| *Kr* | *Y* | *Nb* |
| *Rb* | *Te* | *Mo* |
| *Cd*[1] | *Ba* | *Tc* |
| *I* | *La* | *Ru* |
| *Xe* | *Ce* | *Rh* |
| *Cs* | *Pr* | *Pd* |
| | *Nd* | *Ag*[1] |
| | *Pm* | *In*[1] |
| | *Sm* | *Sn*[1] |
| | *Eu*[1] | *Sb*[1] |

[1]The grouping of these elements is unimportant because of their low fission yields. A few fission products of very low yield have been omitted.

#### 2.1.1.1 Pre-Operational Fuel Melt Tests

Before reprocessing could begin at FCF, a series of experiments were performed to identify how the fission products would behave during the melt process, and to identify any possible radiological health hazards that would need addressed at the FCF. These experiments, performed in the late 1950s and early 1960s, sought to determine what fraction of each radionuclide

*Fuel melt tests with fission product volatilization in an inert gas atmosphere may underestimate the fission product release fraction during a fuel melt accident at an SFR, as complete volatilization may not be necessary for radionuclide release to the sodium.*

[2] Not shown in the diagram is the off-gas filtering mechanism that removes the volatile fission products of the first group of Table 2-1 during the melting process.

[3] Reprinted from ref [3] with permission from the American Nuclear Society.

would be volatized, reacted with the crucible, or remain within the fuel ingot when heated to between 1300°C and 1400°C, which was the planned operational temperature range of the FCF. These tests were conducted in an inert atmosphere using an oxide crucible.

Many fuel melt tests were conducted to investigate the behavior of iodine, as it posed a potential radiological hazard for FCF workers. Two sets of melt refining tests were conducted. The first set, summarized in Table 2-2, explored the percentage of iodine volatized from a U-Fs when held at various temperatures. As the results show, the percentage of iodine remaining in the fuel ingot, crucible, or skull decreased significantly as the melt temperature was increased from 1250°C to 1400°C. A second set of experiments, shown in Table 2-3, performed additional melting tests at 1400°C, and reaffirmed the conclusion that almost complete iodine volatilization would be expected at that temperature.

**Table 2-2: Retention of Iodine in Melt Refining Experiments [4]**

| *Experiment* | *Temperature* | *Time (hours)* | *Iodine Inventory Percentage Remaining*[1] |
|---|---|---|---|
| *2A* | *1250°C* | *4* | *>99%* |
| *36A* | *1300°C* | *2.3* | *55.5%* |
| *44A* | *1300°C* | *3* | *67%* |
| *52A*[2] | *1300°C* | *3* | *44.3%* |
| *74A*[2] | *1400°C* | *3* | *1.9%* |
| *67A*[2] | *1400°C* | *3* | *1.6%* |

[1]Includes skull, ingot, and crucible.
[2]$UI_3$ spike added.

**Table 2-3: Retention of Iodine in Additional Melt Refining Experiments [5]**

| *Experiment* | *Fuel* | *Burnup (%)* | *Temperature* | *Time (hours)* | *Iodine Inventory Percentage Remaining*[1] |
|---|---|---|---|---|---|
| *III* | *U-Fs (10%-$U^{235}$)* | *0.74* | *1400°C* | *1* | *0.3 ± 0.1%* |
| *IV* | *U-Fs (10%-$U^{235}$)* | *0.87* | *1400°C* | *1* | *0.3 ± 0.1%* |
| *V* | *U-Fs (10%-$U^{235}$)* | *1.75* | *1400°C* | *1* | *0.3 ± 0.1%* |
| *VI* | *U-Fs (10%-$U^{235}$)* | *1.18* | *1400°C* | *1* | *2.8%* |
| *VII* | *U-Fs (10%-$U^{235}$)* | *1.18* | *1400°C* | *1* | *~0.25%*[2] |
| *IX* | *U-5Fs w/ KI*[note 3)] | *Synthetic* | *1400°C* | *1* | *0.11%* |
| *X* | *U-5Fs w/ CsI*[note 3)] | *Synthetic* | *1400°C* | *1* | *0.6%* |

[1]Includes skull, ingot, and crucible.
[2]Only from ingot and skull, crucible not analyzed.
[3]Natural uranium

Similar tests were performed regarding cesium volatilization, shown in Table 2-4. At 1200°C, the volatilization of cesium appears to depend on time at temperature and initial concentration. Subsequent operational experience at the FCF found that essentially complete cesium volatilization occurred during actual melt refining conditions, which were at slightly higher temperatures (~1400°C for 3 – 4 hours) [6].

Melt refining tests were also performed for many of the elements within the "reactive" group (Te, Sr, Ba, La, Y, Ce, etc.). However, since these elements formed oxides with the crucible, their behavior during testing and melt refining reprocessing is not necessarily indicative of a metal fuel SFR accident, since there would be a very limited amount of oxygen available. Limited insight from these experiments is still possible, and is discussed in greater detail regarding release fraction estimates in Appendix A.

Noble metals, such as those seen in Table 2-5, did not react with the oxide crucible during melt testing, which makes the results pertinent to the current work. As Table 2-5 shows, very high retention of noble metals within the fuel matrix was observed.

**Table 2-4: Retention of Cesium in Melt Refining Experiments [6]**

| Fuel | Cs Concentration (ppm) | Temp. | Time (hours) | Number of Experiments | Iodine Inventory Percentage Remaining | |
|---|---|---|---|---|---|---|
| | | | | | Ingot[1] | Skull |
| U-Fs with 7wt% Ce & Irradiated U | 0.7 | 1200°C | 4 | 2 | 6 ± 4% | 35 ± 11% |
| Irradiated U | 1.1 | 1200°C | 0.5 | 2 | 16 ± 3% | 57± 1% |
| | | | 4 | 5 | 3 ± 1% | 43 ± 2% |
| Irradiated U | 5.65 | 1200°C | 4 | 6 | 0.16 ± 0.08% | 7 ± 1% |
| Irradiated U-1.7Zr (burnup 0.4%) | 426.0 | 1200°C | 4 | 1 | 0.001% | 0.07% |

[1]Variation believed to be due to variation in initial charge (fuel) geometry [6].

**Table 2-5: Ru, Mo, Rh, and Pd Melt Refining Test Results [7]**

| Fuel | Crucible | Temp. | Number of Experiments | Percentage Remaining in Ingot | | | |
|---|---|---|---|---|---|---|---|
| | | | | Ru | Mo | Rh | Pd |
| Irradiated U | $ThO_2$ | 1200°C | 4 | 100% | | | |
| | $Al_2O_2$ | 1200°C | 3 | 107% | 95% | | |
| | $Al_2O_2$ | 1310°C | 1 | 104% | 96% | | |
| Irradiated U-1.7Zr | MgO | 1200°C | 1 | 104% | 95% | | |
| Fs-0.5Ce | MgO | 1300°C | 1 | 96% | 96% | | |
| | $ZrO_2$ | 1300°C | 3 | 100% | 99% | | |
| | $ZrO_2$ | 1400°C | 2 | 103% | 103% | | |
| Fs | $ZrO_2$ | 1385°C | 10 | | | 97 ± 3.9% | 97.4 ± 3.8% |

The melt refining experiments conducted as part of EBR-II reprocessing raised questions regarding the chemical form of iodine when volatized from melted metal fuel. The EBR-II experiments appeared to indicate that iodine was volatized as CsI (as this compound was found on the upper walls and structure of the melt facility) [5]. This result appeared theoretically reasonable, as CsI is the thermodynamically preferential compound of iodine within the fuel matrix. However, in the mid to late 1960s, experimentation at Brookhaven National Laboratory (BNL) [8] [9] identified uranium iodides, rather than CsI, as the most likely volatized form of iodine at the temperature range of melt refining. Table 2-6 summarizes the findings of the experiments, which melted irradiated U-3.5Mo in an inert gas atmosphere. As the table shows, CsI was not identified as a probable volatized iodine state, despite the presence of cesium in the irradiated fuel [9]. Release fractions of iodine were not recorded for these experiments.

**Table 2-6: Summary of Studies of Metallic Uranium in Inert Atmospheres [8]**

| Probably Volatized Iodine State | Conditions and Remarks |
|---|---|
| UI (note 1) | ~1200 – 2000°C |
| UI + I | ~2100 – 2500°C |
| $U_xI$ + I | >2500°C |

[1]UI does not imply only uranium iodide was found, but a compound of uranium and iodine (the exact ratio of uranium to iodine was not determined).

#### 2.1.1.2 FCF Melt Refining Experience

In addition to the melt testing performed before EBR-II operation, the five years of successful melt refining reprocessing experience at the FCF also provide valuable insight into metal fuel composition at high burnup values. Table 2-7 provides an overview of the metal fuel characteristics seen by operators of the FCF, including the approximate location of radionuclides after fuel irradiation, and for the noble gases, the stages of melt refining reprocessing where they were usually released. It was also noted that tellurium interaction with the cladding was also observed. It is important to note that the fuel reprocessed by melt refining at the FCF had a burnup limit of approximately 1.2% [10]. About 35,000 fuel pins were reprocessed using melt refining.

**Table 2-7: Typical Used Metal Fuel Composition, Based on EBR-II FCF Reprocessing Experience [11]**

| *Element* | *Details* |
|---|---|
| *Fission gases (noble gases)* | *75wt% released during pin chopping*<br>*20wt% released during melting* |
| *I* | *90% in fuel*<br>*10% in upper plenum Na bond* |
| *Cs* | *85% in fuel*<br>*15% in upper plenum Na bond* |
| *Se* | *100% in fuel* |
| *Ba* | *100% in fuel* |
| *Sr* | *100% in fuel* |
| *Na bond* | *60wt% in upper plenum*<br>*40wt% in fuel matrix* |

### *2.1.2 Fuel Melt Experiments*

During the late 1950s, in parallel to the reprocessing experimentation being conducted at EBR-II, several research institutions (Oak Ridge National Laboratory – ORNL, Hanford, and Atomics International - AI) were conducting fuel-melting tests to determine fission product volatilization during reactor accidents. While many of these experiments focused on fission product release when different types of uranium metal fuel were oxidized, which is unlikely to occur during a metal fuel, pool-type SFR core damage accident[4], other tests investigated fission product volatilization in inert atmospheres. As mentioned in the preceding section, release fractions determined by volatilization of fission products into an inert gas may underestimate the release of radionuclides from metal fuel into sodium during an SFR accident, as some radionuclides may be soluble in sodium in their solid or liquid states. However, these tests do provide insight into the mobility and transport of radionuclides from the fuel matrix at high temperatures.

#### 2.1.2.1 Oak Ridge Fuel Melt Testing

Figure 2–2 provides the results of one such experiment conducted at ORNL that melted irradiated (0.1% burnup) metallic uranium in flowing helium [12]. The goal of this experiment was to determine the relationship between the release fraction of the noble gases and temperature. As can be seen, essentially all of the $Kr^{85}$ was released after 15 minutes above the fuel melting point.

[4] Many fuel melting experiments focused on fuel oxidization at high temperatures. The motivation for these tests was the early concern of reactor loss of coolant accidents that would result in the core exposed to an air or steam environment. Oxygen in the air or steam would then interact with the high temperature fuel causing oxidation. This phenomenon is very unlikely for design basis or beyond design basis metal fuel, pool-type SFR accidents, where the core will remain immersed in the primary sodium.

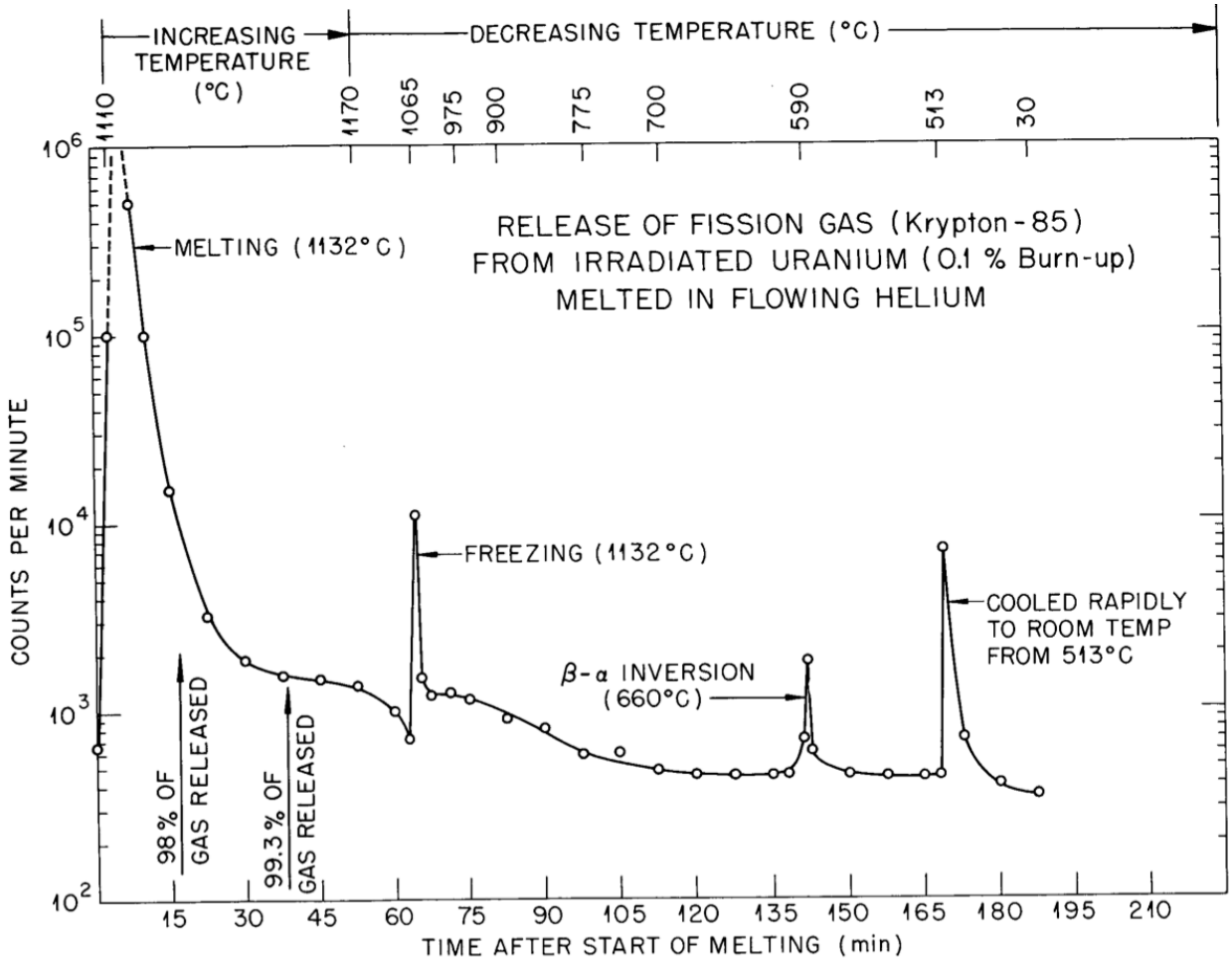


**Figure 2–2: Release of $Kr^{85}$ from Irradiated Uranium (0.1% burnup) Melted in Flowing Helium [12]**

ORNL also conducted melt experiments of U-Zr fuel plates, which were used in the Submarine Thermal Reactor (STR) [13]. The fuel elements had been irradiated to 15% burnup[5]. The melting experiments were performed using punched disks of the STR fuel plate in a quartz ($SiO_2$) crucible. The results of the first set of tests were considered unreliable due to the exposed edges of the fuel disk [13]. However, subsequent tests, which melted the U-Zr fuel in air and in steam, addressed these concerns by encapsulating the exposed fuel edges. The results of these tests can be found in Table 2-8. It is important to note that oxidization was likely to occur in air and in steam at such elevated temperatures, although the short test period likely limited the oxidization amount. Oxidization has been shown to increase the release fraction of fission products from uranium metal (see Table 4.3 and 4.4 of ref [12]).

[5]Unlike SFR U-Zr fuel, the U-Zr fuel in STR did not use a sodium bond.

**Table 2-8: Radionuclide Volatilization by Melting Encapsulated U-Zr Punched Disks, 15% Burnup[6] [13]**

| Run No. | Atmosphere During Melting | Heating Time[a] (sec) | Maximum Temperature[b] (°C) | Per Cent of Total Activity Released | | | | | | |
|---|---|---|---|---|---|---|---|---|---|---|
| | | | | Rare Gases | Gross Gamma | $I_2$ | Cs | Sr | Ba | Ce |
| 10-10 | Air | 12.5 | 1705 | 100 | 2 | 28.0 | 10.0 | | | |
| 10-15 | Air | 16 | | 100 | 2.2 | 32.4 | 11.3 | | | |
| 10-16[c] | Air | 12 | 1750 | 100 | 6.4 | | 11.7 | | | |
| 11-25 | Air | 30 | 1705 | 100 | 2.5 | 14.4 | 7.3 | 0.9 | 0.11 | 0.0047 |
| 11-26 | Air | 30 | 1800 | 100 | 4.1 | 30.0 | 12.9 | 0.8 | 0.3 | 0.004 |
| | | Av 20.1 | 1740 | 100 | 3.4 | 26.2 | 10.6 | 0.85 | 0.2 | 0.0043 |
| 10-20 | Steam | 33 | | 100 | 5.3 | 12.8 | 8.9 | 2.4 | 0.25 | 0.05 |
| 10-22 | Steam | 32 | 1775 | 100 | 5.5 | 52.4 | 23.0 | 3.1 | 1.2 | 0.01 |
| 11-11 | Steam | 18 | | 100 | 7.8 | 66.4 | 21.8 | 4.8 | | |
| 11-12 | Steam | 31 | 1750 | 100 | 7.2 | 55.8 | 24.4 | 1.3 | | |
| 11-14 | Steam | 35 | 1750 | 100 | 4.8 | 57.4 | 12.9 | 0.2 | | |
| 11-21 | Steam | 30.5 | 1750 | 100 | 8.0 | 45.2 | 19.4 | 0.2 | 0.049 | |
| 11-24 | Steam | 31.5 | 1730 | 100 | 5.7 | 36.3 | 20.3 | 0.8 | 0.20 | |
| | | Av 30 | 1750 | 100 | 6.3 | 46.6 | 18.7 | 1.8 | 0.4 | 0.03 |

[a]Optical pyrometer temperature.
[b]Punched disk not reirradiated.
[c]Sample usually melted in approximately 12 sec.

### 2.1.2.2 Hanford Fuel Melt Testing

Other melt testing, conducted at Hanford in the late 1950s, also demonstrates the effects of oxidization on fission product release and provides another dataset for fission product volatilization [14]. This test melted uranium metal (irradiated to $2.4 \times 10^{14}$ n/cm$^2$) samples at 1215°C for 25 minutes in both air and helium in a zirconia ($ZrO_2$) boat. The results of this test can be seen in Table 2-9, and generally show lower release fractions for the melt in helium. However, the release fraction of iodine is much higher than what was observed in EBR-II melt refining tests at similar temperatures for much longer time periods. There is very little supporting documentation regarding this melt test, and the experiment was not repeated to validate the results. Despite these limitations, the data is included here for completeness.

**Table 2-9: Fission Product Release in Air and Helium for Metallic Uranium[7] [14]**

| *Atmosphere* | *Percentage Release from Specimen* | | | | | | |
|---|---|---|---|---|---|---|---|
| | *$I^{131}$* | *$Te^{132}$* | *$Xe^{133}$* | *$Sr^{89}$* | *Cs* | *$Ru^{103}$* | *$Ba^{140}$* |
| *Air* | *65* | *60* | *50* | *0.04* | *1.0* | *0.65* | *0.09* |
| *Helium* | *41* | *4.2* | *10* | *0.18* | *1.2* | *0.09* | *0.08* |

[6]Some oxidization likely occurred due to air and steam atmosphere.

[7]Specimen heated 25 minutes at 1215°C.

#### 2.1.2.3 Atomics International Fuel Melt Testing

Lastly, AI conducted a series a fuel melt experiments in stagnant sodium following the accident at SRE (described in Section 2.2.1), which was operated by AI. Four in-pile fuel melt tests were conducted, known as IP-1 through IP-4. The tests involved placing a small metallic uranium disc in a capsule filled with sodium and a helium cover gas. The fuel disc was then ruptured using neutron burst heating in the Kinetics Experimental Water Boiler (KEWB) reactor at Santa Susana Field Laboratory [15]. While the main purpose of these tests was to examine the retention of fission products in sodium, they also provide insight into fission product release from molten metallic uranium into sodium at very high temperatures.

Table 2-10 provides a summary of the fuel and sodium conditions for the four in-pile experiments. IP-3 and IP-4 are particularly applicable to SFR fuel melt accidents, as the sodium temperatures are similar to typical SFR core outlet temperatures. The exact temperature of the fuel discs during the neutron burst is unknown, but estimates place the peak temperature at 2300 – 3900°C, which resulted in complete destruction of the fuel discs into very small particles (on average 75 – 125 microns) with some fuel vaporization also occurring [15]. It is thought that the fuel experienced very high temperatures for less than 20ms [15].

**Table 2-10: Summary of AI In-Pile Fuel Melt Tests [15]**

| *Experiment* | *Uranium Sample* | *Sodium Temperature* |
|---|---|---|
| *IP-1* | *93% Enriched, Non-irradiated Uranium* | *260°C (500°F)* |
| *IP-2* | *93% Enriched, Irradiated Uranium* | *260°C* |
| *IP-3* | *93% Enriched, Irradiated Uranium* | *538°C (1000°F)* |
| *IP-4* | *93% Enriched, Irradiated Uranium* | *538°C* |

Table 2-11 presents the radionuclide release percentages into sodium for IP-3 and IP-4. It is important to note that these release fractions are representative of fuel at extremely high temperatures (possibly vaporized) and in very small fragments in sodium. Together, these factors likely increased the release of radionuclides from the fuel. No cesium was found in the sodium following IP-3 and IP-4 [15] [16]. It is also noteworthy that IP-2 saw the complete release of xenon from the fuel disc during melting [15].

**Table 2-11: Summary of Fission Product Behavior for IP-3 and IP-4 [15]**

| *Isotope* | *Fraction of Isotope Released to Sodium (%)* | |
|---|---|---|
| | *IP-3*[1] | *IP-4* |
| *$ZrNb^{95}$* | *24* | *10.3* |
| *$Ru^{103}$* | *0.66* | *1.9* |
| *$I^{131}$* | *72* | *44* |
| *$BaLa^{140}$* | *5.4* | *2.1* |

[1]Activity from sodium, plating strip and activity remaining in capsule after rinsing.

### *2.1.3 Cladding Breach Experiments at EBR-II*

Two series of tests concerning the behavior of metal fuel pins following cladding failure were conducted at EBR-II. The first set, referenced here as the "leaker experiments", was performed in the late 1960s after a series of fission product releases due to pin failure (see section I of ref [17]). The second set of tests, known as the Run-Beyond-Cladding-Breach (RBCB) tests, began in 1985[8] as part of the Integral Fast Reactor (IFR) project.

[8] Prior to 1985, oxide fuel RBCB tests had been performed at EBR-II, which are not reviewed here.

#### 2.1.3.1 Leaker Experiments

The goal of the leaker experiments was to determine techniques to identify "leaking" fuel pins during normal operation at EBR-II, including the difference between a "top" and "bottom" leaker[9] [18]. Two tests were performed, one with a predetermined weakness at the top of the fuel pin, and one with a prepared leak at the bottom. Unfortunately, the top leaker test did not fail as planned in the reactor. The focus of the bottom leaker test was on the behavior of xenon and iodine after clad failure. More information on the bottom leaker test can be found in ref [13], but the main result of note for the current work is that xenon and iodine were both found to be released from the fuel pin after cladding failure. It also appears that the release of iodine may have some dependence on the primary sodium flowrate (likely due to internal pin pressures and bond sodium movement), but sampling equipment failures makes a quantitative conclusion impossible [18].

**Table 2-12: EBR-II "Leaker" Experiment Results [18]**

| *Experiment* | *Fuel* | *Notes* |
|---|---|---|
| *Top Leaker* | *U-5Fs, 1.52% Avg. Burnup (Mk-IA)* | *No Clad Failure Occurred* |
| *Bottom Leaker* | *U-5Fs, 0.55% Avg. Burnup (Mk-IA)* | *Test focused on iodine and xenon behavior. Xenon found in cover gas, and iodine found in primary sodium. Some degree of flowrate dependence seen for radionuclide release* |

#### 2.1.3.2 Run-Beyond-Cladding-Breach Tests

The goal of the RBCB tests was to analyze the behavior of metal fuel after a cladding breach and to demonstrate the compatibility between metal fuel and sodium. The RBCB tests were initiated by grinding down an area of the cladding surface of a pre-irradiated fuel pin until only 30-40 μm of the cladding remained [19]. The pin was then reinserted into the reactor, with cladding failure occurring shortly after reinsertion, as the pin pressure increased. The reactor would then continue to operate with the failed pin in the core.

RBCB Tests were performed with U-Fs, U-Zr, and U-Pu-Zr fuel elements, as seen in Table 2-13. As the table shows, many of the failed fuel pins remained in EBR-II for over 100 days after cladding failure. Post-irradiation examination of the fuel pins included radiological analysis to determine the radionuclides released from the fuel. These results, seen in Table 2-14, focused on the area around the defect. No quantitative release fraction calculations for these tests were located.

**Table 2-13: Summary of RBCB Tests [20]**

| *Experiment* | *Scoping Tests Phase I* | | | *IFR Prototypic Phase II* | | | *Natural Breach* |
|---|---|---|---|---|---|---|---|
| *ID* | *UXY-21/22A* | *XY-24* | *XY-27* | *X482* | *X482A* | *X482B* | *X420B* |
| *Composition* | *U-5Fs* | *U-19Pu-10Zr* | *U-8Pu-10Zr* | *U-19Pu-10Zr* | *U-10Zr* | *U-19Pu-10Zr* | *U-19Pu-10Zr* |
| *Final Burnup* | *~9.3%* | *~7.5%* | *~6.0%* | *14.4%* | *13.5%* | *14.0%* | *17.0%* |
| *Days Breached* | *54* | *233* | *131* | *168* | *~100* | *~190* | *150* |

[9] The tests were designed to model pin leakage from a failure of the top or bottom weld of the Mk-IA fuel pin design.

**Table 2-14: Analytical Results of RBCB Experiments [20]**

| S/A# | ELEMENT | SMEAR NUMBER | S/A# | ELEMENT | WEIGHT LOSS(G) | BURNUP (A/O) | Composition (Wt%) | Uranium µg/sm or samp | Plutonium µg/sm or samp | Nb-95 | Zr-95 | Ru-106 | Cs-134 |
|---|---|---|---|---|---|---|---|---|---|---|---|---|---|
| X-482 | T-139 | #69(µCi/smear) | X-482 | T-139 | 4.04 | 12.2 | U-19Pu-10Zr | | 0.6 | | | | 2 |
| X-482 | T-139 | Samp.Vial(µCi/samp) | X-482 | T-139 | 4.04 | 12.2 | U-19Pu-10Zr | | 64 | | | | 1700 |
| XY-21A | RT-95 | #J-382(µCi/smear) | XY-21A | RT-95 | 2.07 | 9.3 | U-5Fs | | | 0.765 | 0.437 | 1.08 | 0.062 |
| XY-21A | RT-95 | #J-331(µCi/smear) | XY-21A | RT-95 | 2.07 | 9.3 | U-5Fs | | | n.d. | 3.06 | n.d. | 0.139 |
| XY-21A | RT-95 | #J-386(µCi/smear) | XY-21A | RT-95 | 2.07 | 9.3 | U-5Fs | | | 0.137 | n.d. | n.d. | 0.061 |
| XY-21A | RT-95 | #J-327(µCi/smear) | XY-21A | RT-95 | 2.07 | 9.3 | U-5Fs | | | 0.176 | 0.178 | n.d. | n.d. |
| XY-21A | RT-95 | "Blob"(µCi/samp) | XY-21A | RT-95 | 2.07 | 9.3 | U-5Fs | 350 | 0.2 | | | | |
| XY-24 | J-516 | #M-445(µCi/smear) | XY-24 | J-516 | 0.00 | 7.5 | U-19Pu-10Zr | <3.0 | 0.007 | | | | n.d. |
| XY-24 | J-507 | #M-401(µCi/smear) | XY-24 | J-507 | 2.73 | 7.5 | U-19Pu-10Zr | <3.0 | 0.95 | | | | 42 |
| XY-24 | J-507 | Can#S2(µCi/samp) | XY-24 | J-507 | 2.73 | 7.5 | U-19Pu-10Zr | <150 | 6.2 | | 390 | | |
| XY-27 | J-432 | #M-408(µCi/smear) | XY-27 | J-432 | 2.45 | 6 | U-8Pu-10Zr | 7 | 0.15 | | | | 40 |
| XY-27 | J-432 | #M-44(µCi/smear) | XY-27 | J-432 | 2.45 | 6 | U-8Pu-10Zr | <300 | 7.3 | | | | 60 |
| XY-27 | J-486 | #M-405(µCi/smear) | XY-27 | J-486 | 2.60 | 6 | U-8Pu-10Zr | <3 | 0.15 | | | | 24 |
| XY-27 | J-486 | #M-43(µCi/smear) | XY-27 | J-486 | 2.60 | 6 | U-8Pu-10Zr | <3 | 1.6 | | | | 400 |

| S/A# | ELEMENT | SMEAR NUMBER | S/A# | ELEMENT | Cs-137 | Ba-140 | La-140 | Ce-141 | Ce-144 | Eu-154 | Eu-155 | Others | |
|---|---|---|---|---|---|---|---|---|---|---|---|---|---|
| X-482 | T-139 | #69(µCi/smear) | X-482 | T-139 | 19 | 3.2 | 3.8 | | 4.4 | 0.2 | 1.9 | | |
| X-482 | T-139 | Samp.Vial(µCi/samp) | X-482 | T-139 | 16000 | 3600 | 4600 | | 1800 | 600 | 5100 | | |
| XY-21A | RT-95 | #J-382(µCi/smear) | XY-21A | RT-95 | 0.865 | n.d. | 0.114 | n.d. | 4.27 | n.d. | 0.103 | | |
| XY-21A | RT-95 | #J-331(µCi/smear) | XY-21A | RT-95 | 3.75 | 34.8 | 41 | 0.46 | 2.52 | 6.6 | 25.2 | | |
| XY-21A | RT-95 | #J-386(µCi/smear) | XY-21A | RT-95 | 1.14 | 1.38 | 1.45 | n.d. | 0.466 | 0.277 | 1.09 | | |
| XY-21A | RT-95 | #J-327(µCi/smear) | XY-21A | RT-95 | 0.31 | 0.5 | 0.7 | n.d. | 0.92 | 0.093 | 0.341 | | |
| XY-21A | RT-95 | "Blob"(µCi/samp) | XY-21A | RT-95 | 2 | 188 | 239 | | | 10 | 28 | | |
| XY-24 | J-516 | #M-445(µCi/smear) | XY-24 | J-516 | 0.2 | 0.6 | 0.7 | | | n.d. | 0.3 | .2(Mn-54) | .9(Co-58) |
| XY-24 | J-507 | #M-401(µCi/smear) | XY-24 | J-507 | 700 | 1100 | 1400 | | | 360 | 4000 | | 40(Co-58) |
| XY-24 | J-507 | Can#S2(µCi/samp) | XY-24 | J-507 | 520 | 2600 | 3700 | | | 5100 | 48000 | 2100(Na-22) | |
| XY-27 | J-432 | #M-408(µCi/smear) | XY-27 | J-432 | 540 | 290 | 390 | | | n.d. | 120 | | |
| XY-27 | J-432 | #M-44(µCi/smear) | XY-27 | J-432 | 800 | 630 | 830 | | | 25 | 330 | | |
| XY-27 | J-486 | #M-405(µCi/smear) | XY-27 | J-486 | 310 | 520 | 700 | | | 14 | 190 | | |
| XY-27 | J-486 | #M-43(µCi/smear) | XY-27 | J-486 | 4100 | 19000 | 26000 | | | n.d. | 5300 | | |

### *2.1.4 TREAT M-Series*

The M-Series Tests (M2 through M7) were performed at the Transient Reactor Test Facility (TREAT) between 1984 and 1987. The goals of these tests were to study cladding failure thresholds and IFR fuel behavior during simulated transient overpower accidents. The source of irradiated fuel for the M-Series Tests was EBR-II. However, due to the unavailability of irradiated U-Pu-Zr IFR fuel at the time, EBR-II U-Fs driver fuel was utilized for early tests (M2, M3, and M4). Later tests (M5, M6, and M7) utilized prototypic U-Pu-Zr and U-Zr IFR fuel that had been irradiated in EBR-II. Table 2-15 summarizes the fuel pin characteristics for each of the M-Series Tests. Nineteen pins were utilized during the tests; five experienced cladding failure. In each test, pins were subjected to overpower conditions usually exceeding four times nominal power (pin failure was not observed to occur at power levels significantly below this level). All overpower transient tests resulted in significant melting in the test fuel (~50% of the fuel matrix[10]) even if the cladding remained intact [21].

In tests where fuel pin failure occurred (M2, M4, M6, and M7), test loop sodium had to be purified to remove any fission products and fuel fragments that had been released. Prior to sodium purification efforts, gamma scans of the test loop were performed at TREAT. The purpose of the gamma scans was to identify the quantity and location of fuel fragments in the test loop. The elements detected during these gamma scans provide insight into the fission products that were released into the test loop sodium following fuel pin failure. The results of the gamma scans were found in communications between Argonne West and Argonne East in the form of memorandums (described in Appendix B). A list of the isotopes identified from the gamma scans of the test loops are provided in Table 2-16. It is important to note that the gamma scans were not performed immediately following the tests; in most cases, they were

[10] Based on the results of post-experiment examinations and thermal analysis.

performed months after the tests. The delay provides an explanation for why some of the shorter-lived fission products (such as $I^{131}$) were not detected.

Following the gamma scans, the test loops were sent to the Hot Fuel Examination Facility (HFEF) where the sodium was filtered. Before the filtering process was performed, sodium and gas samples from the test loops were taken and analyzed. Technicians at HFEF recorded the results of the samples in process work sheets that provided step-by-step instructions for handling of the test loops. A list of the isotopes identified in the process work sheets is provided in Table 2-16. As noted previously, shorter-lived fission products had most likely decayed before these samples were taken.

**Table 2-15: TREAT M-Series Tests Summary**

| Test | Fuel | Cladding Material | Burnup | Cladding Failure | Date of Test |
|---|---|---|---|---|---|
| M2 | U-5Fs | Type 316 stainless steel | 0.3% | No | March 1985 |
| | U-5Fs | Type 316 stainless steel | 4.4% | Yes | |
| | U-5Fs | Type 316 stainless steel | 7.9% | Yes | |
| M3 | U-5Fs | Type 316 stainless steel | 0.3% | No | April 1985 |
| | U-5Fs | Type 316 stainless steel | 4.4% | No | |
| | U-5Fs | Type 316 stainless steel | 7.9% | No | |
| M4 | U-5Fs | Type 316 stainless steel | 0.0% | No | January 1986 |
| | U-5Fs | Type 316 stainless steel | 2.4% | Yes | |
| | U-5Fs | Type 316 stainless steel | 7.9% | No | |
| M5 | U-19Pu-10Zr | D9 | 0.8% | No | August 1986 |
| | U-19Pu-10Zr | D9 | 1.9% | No | |
| M6 | U-19Pu-10Zr | D9 | 1.9% | No | February 1987 |
| | U-19Pu-10Zr | D9 | 5.3% | Yes | |
| M7 | U-19Pu-10Zr | D9 | 9.8% | Yes | October 1987 |
| | U-10Zr | HT9 | 2.9% | No | |

**Table 2-16: Radionuclides Detected after TREAT M-Series[11]**

| Isotopes Identified During Gamma Scans (TREAT) | Isotopes Identified From Sodium and Gas Samples (HFEF) |
|---|---|
| $Na^{22}$ | U |
| $Cr^{51}$ | Pu |
| $Fe^{59}$ | $Na^{22}$ |
| $Co^{60}$ | $Kr^{85}$ |
| $Nb^{95}$ | $Nb^{95}$ |
| $Zr^{95}$ | $Zr^{95}$ |
| $Ru^{103}$ | $Ag^{110}$ |
| $Rh^{106}$ | $Sb^{125}$ |
| $Sb^{125}$ | $Xe^{133}$ |
| $Cs^{134}$ | $Cs^{134}$ |
| $Cs^{137}$ | $Cs^{137}$ |
| $La^{140}$ | $Ce^{144}$ |
| $Ce^{144}$ | $Eu^{144}$ |
| $Pr^{144}$ | $Eu^{154}$ |
| | $Eu^{155}$ |

[11] Measurements taken several months after M-Series tests were conducted.

### *2.1.5 Metal Fuel Post-Irradiation Examination (PIE)*

The following section reviews relevant metal fuel post-irradiation examination (PIE) results. There is significant PIE analysis available from EBR-II, FFTF, foreign sources, and recent INL irradiations. Only a sample of the most pertinent results is presented here.

*Although originally conducted to assess fuel pin integrity and fuel performance, there is considerable metal fuel PIE available, which provides valuable insight into the behavior of fission products during irradiation.*

#### 2.1.5.1 Fission Gas Release Experiments

The behavior of fission gases is particularly important to metal fuels, as their release from the fuel matrix can lead to high internal pin pressures. Many studies have been performed to determine how fission gases are created and are transported within the fuel matrix. While the focus of the experiments reviewed here was usually on ensuring structural integrity of the fuel pin, the findings can be interpreted to provide insight into fission gas (particularly noble gas) release.

In the 1960s, a series of tests were performed at EBR-II with U-Fs, U-Pu-Fs, and U-Pu-Zr fuel pins to determine the percentage of fission gas released as fuel volume increased [22]. The results, which are provided in Figure 2–3, show that all three fuels types demonstrate similar behavior. Once the fuel volume increase exceeds 20%, the fission gases begin to escape the fuel matrix through the interconnection of fuel porosities. Even with a volume increase of close to 100%, only about 80% of the fission gas is released. These findings can be translated to specific fuel types, if the fuel volume increase over time (or burnup) is known.

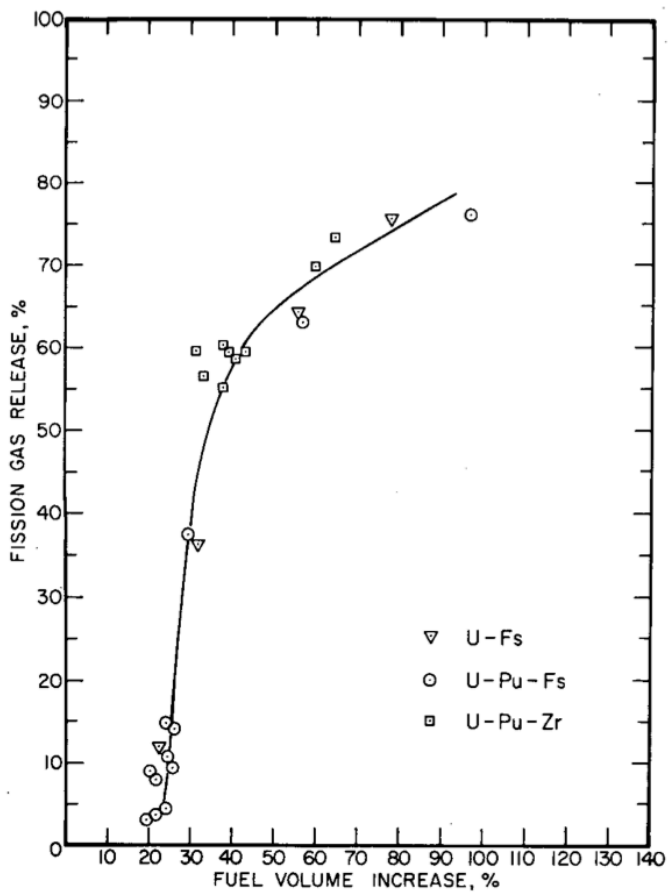


**Figure 2–3: Fission Gas Release versus Fuel Volume Increase [22]**

There was renewed interest in the phenomena of fuel volume increase and fission gas release in the 1980s as part of the IFR project, which sought to achieve burnup levels over 15%. Results of testing with U-10Zr, U-8Pu-10Zr, and U-19Pu-10Zr at EBR-II are provided in Figure 2–4 [23]. Fission gas release begins to occur around 1% burnup, as the fuel matrix expands. By approximately 5% burnup, the fission gas release approaches an asymptotic release of approximately 70% to 80%. Increasing to higher burnup levels does not appear to result in any significant additional fission gas release. As will be seen, many of the experiments reviewed in the following subsections also had fission gas release analyses performed.

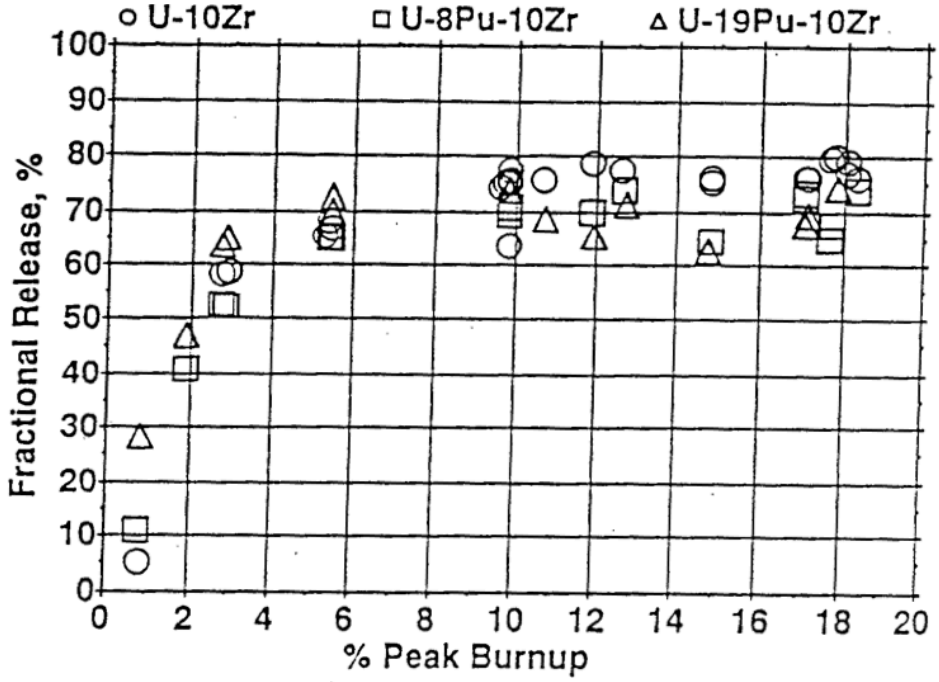


**Figure 2–4: Burnup Dependence on Fission Gas Release[12] [23]**

2.1.5.2 EBR-II PIE

Over its 30-year lifespan, EBR-II was the site of numerous metal fuel experiments (in addition to its normal metal driver fuel). The metal fuel experiments were subjected to a variety of PIE techniques, such as gamma scans, metallography, and destructive examinations. Table 2-17 provides a list of notable experiments whose PIE included axial gamma scans. While the purpose of the gamma scans was to assess fuel behavior and integrity during irradiation, they can also provide insight into fission product migration. The remainder of this subsection highlights several important EBR-II experiments and findings.

Experiment X430 was conducted at EBR-II in the late 1980s through the early 1990s. The purpose of the experiment was to examine the behavior of advanced HT-9 cladding. However, there are several notable results relevant to the current work. First, detailed PIE was performed regarding constituent migration within the fuel matrix. For example, Figure 2–5 shows an optical micrograph of the fuel cross-section, with an overlay of the X-ray measurements from uranium, plutonium, and zirconium. As the figure demonstrates, even at 1.9% burnup, uranium becomes concentrated in an annular region, while zirconium migrates to the center and periphery of the fuel matrix.

[12] Reprinted from ref [23] with permission from the American Nuclear Society.

**Table 2-17: EBR-II Experiments with Axial Gamma Scans[13] [24]**

| *Experiment*[1] | *Fuel* | *Peak Burnup* | *Notes* |
|---|---|---|---|
| *X419* | *U-10Zr, U-8Pu-10Zr, U-19Pu-10Zr* | *12.0%* | *Lead test* |
| *X420* | *U-10Zr, U-8Pu-10Zr, U-19Pu-10Zr* | *17.1%* | *Lead test* |
| *X421* | *U-10Zr, U-8Pu-10Zr, U-19Pu-10Zr* | *18.4%* | *Lead test* |
| *X423* | *U-10Zr, U-3Pu-10Zr, U-8Pu-10Zr, U-19Pu-10Zr, U-22Pu-10Zr, U-26Pu-10Zr* | *5.0%* | *Lead test* |
| *X425* | *U-10Zr, U-8Pu-10Zr, U-19Pu-10Zr* | *19.3%* | *IFR lead test* |
| *X429* | *U-10Zr, U-8Pu-10Zr, U-19Pu-10Zr* | *14.4%* | *Fabrication test* |
| *X430* | *U-10Zr, U-19Pu-10Zr, U-22Pu-10Zr, U-26Pu-10Zr* | *11.5%* | *Advanced HT9 test* |
| *X431* | *U-2Zr, U-6Zr, U-10Zr* | *3.8%* | *HT9 blanket test* |
| *X441* | *U-19Pu-6Zr, U-19Pu-10Zr, U-19Pu-14Zr* | *12.7%* | *Variable Zr: 6/10/12%* |
| *X447* | *U-10Zr* | *10.1%* | *Mk-III high temperature* |
| *X448* | *U-10Zr* | *14.8%* | *Mk-IV qualification* |
| *X501* | *U-20.2Pu-9.1Zr-1.2Am-1.3Np* | *5.9%* | *Actinide burner* |

[1]The experiment number refers to the fuel pin assembly irradiated in EBR-II.

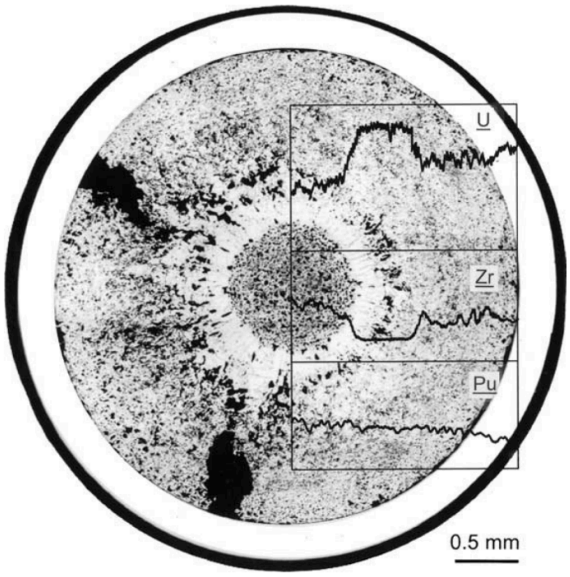


**Figure 2–5: Constituent Redistribution Radially at 1.9% Burnup (T179 of X419)[14] [25]**

Secondly, an analysis of two X430 fuel pins was recently conducted by INL as part of pyrometallurgical reprocessing operations of EBR-II fuel [26]. This examination focused on the migration of iodine within the fuel pin, as it is an environmental concern during reprocessing operation. The two U-19Pu-10Zr fuel pins selected, T659 and T660, had been irradiated to approximately 11.5% burnup. For the first fuel pin, T659, the amount of iodine located in the upper plenum, lower plenum, and end cap was measured (through plasma-mass spectrometry of $I^{129}$, a long-lived iodine isotope). The results of this analysis, shown in Table 2-18, found only ~9% of the predicted total iodine inventory in these three regions. To confirm these results, the second fuel pin (T660) was analyzed in both the plenum (upper, lower, and end cap) and fuel regions. As the results show, approximately 10% of the iodine was found in the plenum regions, with

13 This list is likely not exhaustive, as gamma scanning of EBR-II fuel elements has continued for many years post-operation.

14 Reprinted from ref [25] with permission from Elsevier.

the remainder accounted for in the fuel region of the pin. It is important to note that while these results indicate that approximately 90% of the iodine inventory remains in the fuel region of the pin at ~11% burnup, they do not specify whether the iodine was within the fuel matrix, or part of the bond sodium that has been dispersed within inclusions in the fuel matrix.

**Table 2-18: X430 Iodine Measurements[15] [26]**

| Pin | Iodine Concentration | | | Total Measured Iodine | Total Iodine Expected[2] |
|---|---|---|---|---|---|
| | Fuel Region | Plenum Sodium and End Cap | Plenum Gas | | |
| T659 | NA[1] | 6.9mg | NA | 6.9mg | 78.9mg |
| T660 | 78mg | 7.3mg | 0.02mg | 85.3mg | 78.9mg |

[1]Not analyzed.
[2]Based on neutronics calculation.

Also at EBR-II in the late 1980s, testing of a U-10Zr subassembly (X447) was conducted to examine the performance of HT9 cladding at high temperatures [27]. This subassembly was irradiated to a maximum burnup of 10.0%. Subsequent analyses indicated that two of the fuel elements (DP70 and DP75) had breached between 9.5% and 10% burnup, as they had a weight defect of 2.9g and 2.7g. Gamma scans for $Cs^{134}$ and $Cs^{137}$ showed that the intact fuel pins had about twice the cesium activity as the breached elements, indicating that the breached elements had lost approximately 50% of their total cesium inventory. Based on this information, and other details given in ref [27], the calculation shown in Table 2-19 was conducted as part of the current work. As the table shows, if it assumed that 100% of the bond sodium was released, than the release percentage for fission gas and cesium are consistent with the measured gamma scan (for cesium) and past fission gas release experiments (Section 2.1.5.1).

**Table 2-19: X447 Release Calculation (Based on Data in Ref [27])**

| Source | Mass |
|---|---|
| Total Weight Loss (Measured) | 2.7 & 2.9g |
| Initial bond sodium loading | ~1.7g |
| Fission gas production (75%)[1] | ~0.7g |
| Cesium (50%)[2] | ~0.4g |
| **Calculated Total Weight Loss** | **~2.8g** |

[1] ~0.9g, assuming 75% of inventory in upper plenum and available for release (additional analyses on similar X447 pins confirmed this assumption).
[2] ~0.8g, 50% estimate based on gamma scans.

Other fuel pins of the X447 experimental assembly were subjected to radial profilometry[16] to investigate constituent migration. Figure 2–5 and Figure 2–6 provide two example radial profile results for pin DP-11. The first figure shows the interaction between elements in the fuel and the cladding, as cerium and neodymium transport into the cladding matrix. Perhaps more relevant for the current work, Figure 2–7 demonstrates that there is little radial dependence on cesium concentration, and small barium concentrations are observed, but mass migration to one area is not apparent.

[15] Measurement uncertainty of ±10% at the 2σ level.

[16] Using Electron Probe Micro Analysis (EPMA).

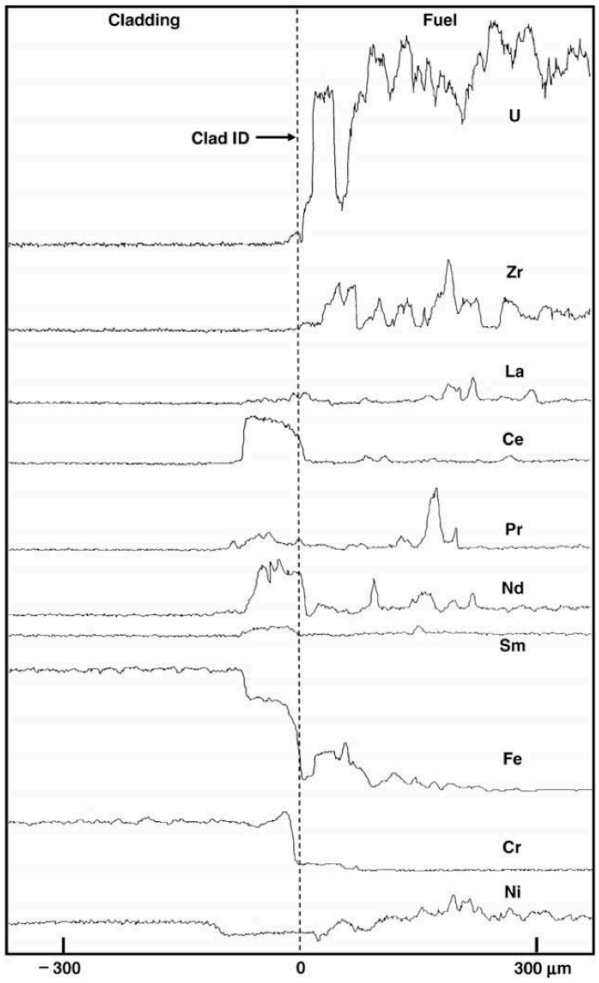


**Figure 2–6: EBR-II X447 (DP-11) Radial Profile, ~10% Burnup[17] [28]**

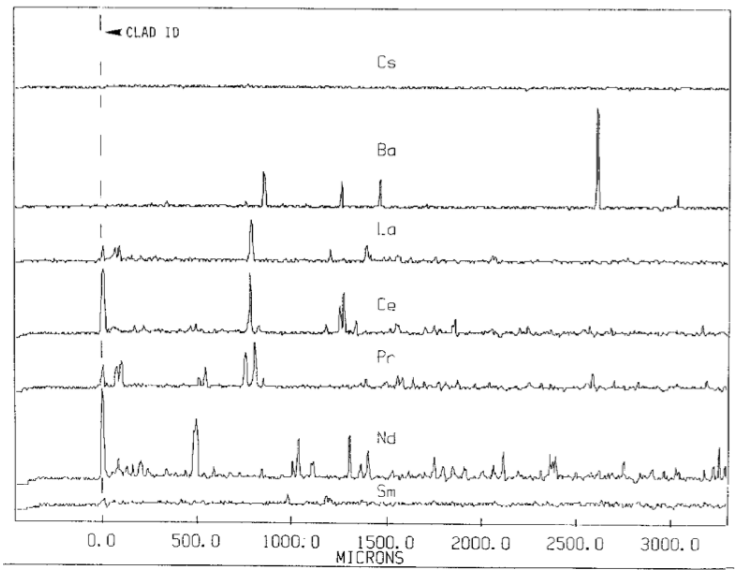


**Figure 2–7: EBR-II X447 (DP-11) Radial Profile, ~10% Burnup[18]**

[17] Reprinted from ref [28] with permission from Elsevier.

[18] Fuel center at approximately 3000 microns.

As part of the IFR project, examinations were made regarding minor actinide burning with metal fuel. Near the end of EBR-II operation, experiment X501 (U-20.2Pu-9.1Zr-1.2Am-1.3Np) was irradiated to 7.6% heavy metal burnup [29]. Subsequent PIE and gamma scans found the $Cs^{137}$ distribution provided in Figure 2–8. The fuel matrix length was 13.5 in, and the spike of cesium activity above 13.5 in is due to cesium collection in the bond sodium, which has relocated to the fission gas plenum due to fuel expansion. An approximate calculation indicates about 40% of the cesium inventory was present in the bond sodium in the fission gas plenum. Additional radial scans were performed on X501 elements to investigate constituent migration. Figure 2–9 provides an illustrative result, again demonstrating uranium and zirconium migration.

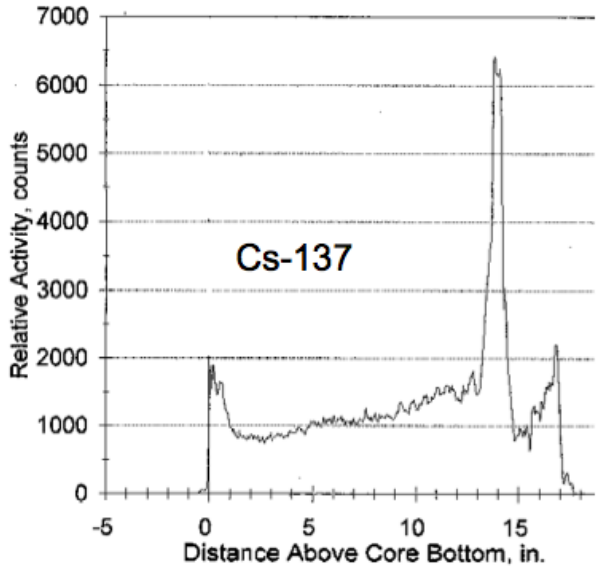


**Figure 2–8: X501 PIE $Cs^{137}$ Axial Gamma Scan[19] [29]**

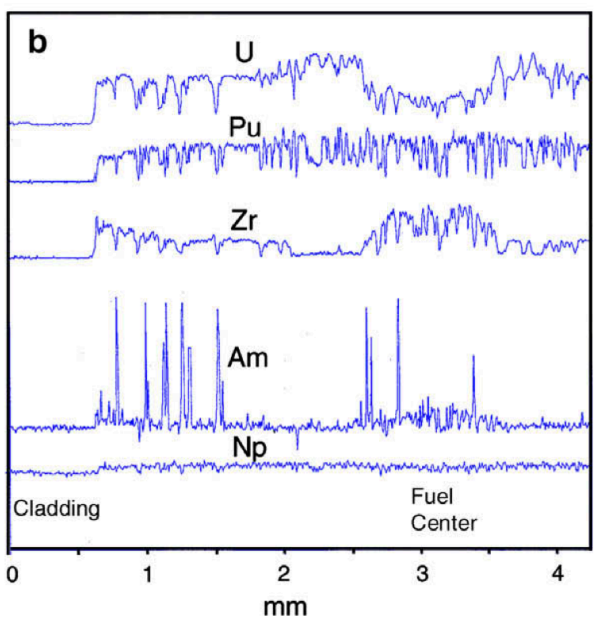


**Figure 2–9: Radial Profile of X501 at ~6% Burnup[20] [28]**

[19] Fuel length is 13.5 in, with fission gas plenum above.

[20] Reprinted from ref [28] with permission from Elsevier.

#### 2.1.5.3 FFTF PIE

In the late 1980s and early 1990s, a series of experiments were conducted at the Fast Flux Test Facility (FFTF) regarding the performance of prototypic IFR U-Pu-Zr metal fuel [30]. Of the 169 fuel pins irradiated as part of the IFR-1 tests at FFTF, eight were gamma scanned following irradiation. Table 2-20 reviews the characteristics of five of the scanned pins. The gamma scans focused on $Rh^{106}$, which is typically immobile and will stay within the fuel matrix, $Cs^{137}$, which can migrate to the bond sodium, and $Ce^{144}$, which appears to be mobile within the fuel matrix. An example axial gamma scan for pin 181193 is provided in Figure 2–10. The fission gas release percentages given in Table 2-20 are consistent with previous findings from studies at EBR-II. The gamma scan results provide qualitative (and potentially quantitative) data regarding the transport and migration of cesium, rhodium, and cerium.

**Table 2-20: FFTF IFR-1 Pin Summary [30]**

| *Characteristic* | *Pin Number* | | | | |
|---|---|---|---|---|---|
| | *181193* | *181165* | *181154* | *181180* | *181175* |
| *Fuel Type* | *U-19Pu-10Zr* | *U-19Pu-10Zr* | *U-8Pu-10Zr* | *U-10Zr* | *U-10Zr* |
| *Peak Burnup %* | *9.42* | *9.65* | *9.60* | *9.72* | *9.66* |
| *Avg. Burnup %* | *7.85* | *8.04* | *8.00* | *8.10* | *8.05* |
| *Fission Gas Release* | *72%* | *69%* | *71%* | *73%* | *69%* |

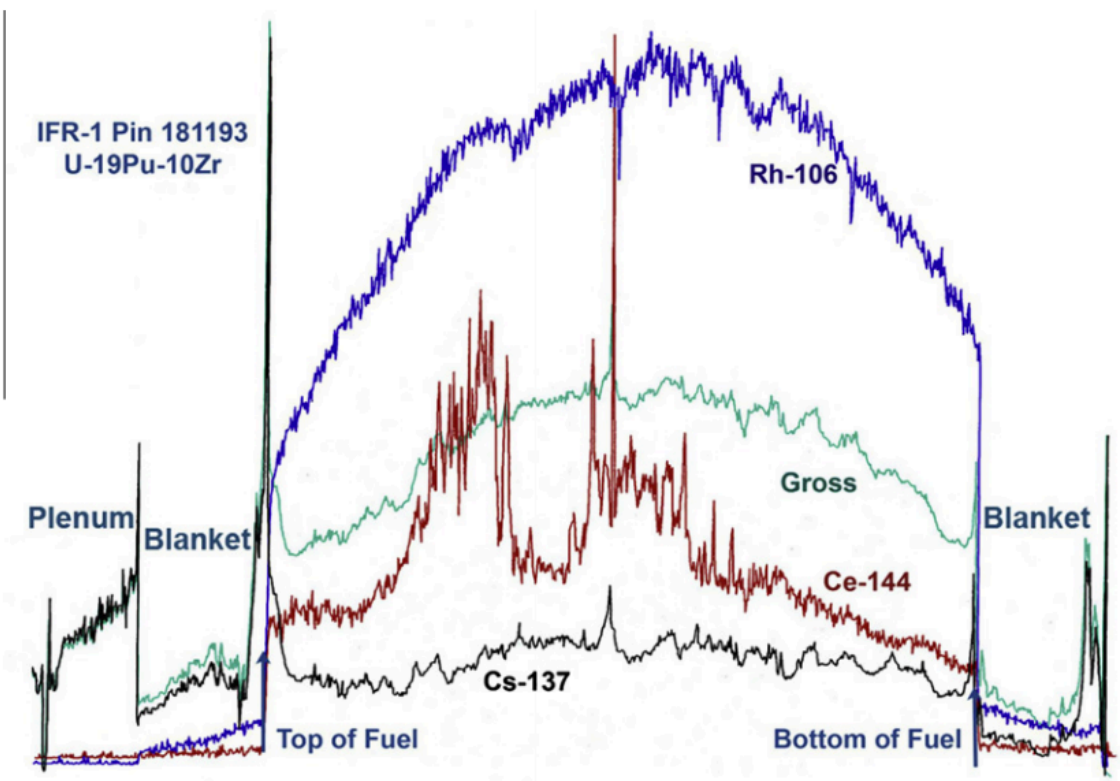


**Figure 2–10: Example FFTF IFR-1 Axial Gamma Scan Result[21] [30]**

[21] Different y-scale for each isotope. Reprinted from ref [30] with permission from Elsevier.

#### 2.1.5.4 METAPHIX PIE

METAPHIX, a series of metal fuel experiments containing transuranics, was performed by the Central Research Institute of the Electric Power Industry (CRIEPI), the Institute of Transuranium Elements (ITU), and the Commissariat a l'Energie Atomique (CEA) [31]. The experiments, with noteworthy results shown in Table 2-21, examined the behavior of metal fuel consisting of a variety of uranium, plutonium, zirconium, minor actinide (MA), and rare earth (RE) combinations. These tests were repeated at different burnup levels.

**Table 2-21: METAPHIX Sodium Bond and Cesium Redistribution Results [31]**

| *Experiment* | *Peak Burnup* | *Pin[1]* | *Ratio of Bond Sodium in Upper Plenum[2]* | *$Cs^{137}$ Percentage in Upper Plenum (within sodium)* |
|---|---|---|---|---|
| *METAPHIX-1* | *2.5 – 2.7%* | *#1* | *75%* | *30%* |
| | | *#2* | *80%* | *38%* |
| | | *#3* | *83%* | *32%* |
| *METAPHIX-2* | *6.6 - 7.2%* | *#1* | *83%* | *40%* |
| | | *#2* | *86%* | *43%* |
| | | *#3* | *88%* | *46%* |
| *METAPHIX-3* | *9.3 – 10.2%* | *#1* | *92%* | *53%* |
| | | *#2* | *87%* | *52%* |
| | | *#3* | *89%* | *48%* |

[1]Pin #1 – U-19Pu-10Zr
Pin #2 – U-19Pu-10Zr/U-19Pu-10Zr-2MA-2RE/U-19Pu-10Zr
Pin #3 – U-19Pu-10Zr/ U-19Pu-10Zr-5MA-5RE/U-19Pu-10Zr-5MA/U-19Pu-10Zr
[2](Volume of bond sodium extruded to upper plenum)/(Volume of bond sodium filling in fuel-cladding gap before irradiation) × 100 (%)

There are two notably relevant results from the analysis for the current study. First, an examination of bond sodium movement showed that the majority (75 - 83%) of the bond sodium migrated to the upper plenum after only 2% burnup[22]. The fraction of bond sodium in the upper plenum increases slightly with further burnup, reaching approximately 90% of the total bond sodium inventory by 10% burnup. The second major finding is the percentage of cesium found in the upper plenum, and hence in the bond sodium, at various burnup levels. The results show a dependence on burnup, with approximately 35% migration at 2.5% burnup, 45% migration at 7% burnup, and 50% migration at 10% burnup. These percentages were found through gamma scans (an example gamma scan is provided in Figure 2–11). These results appear consistent with EBR-II melt refining experience, and PIE experience at EBR-II/FFTF. However, taken together, the results appear to demonstrate that the migration of cesium to the upper plenum bond sodium is not directly linked to the migration of the bond sodium itself, as the percentage of cesium in the upper plenum sodium almost doubles from 2% to 10% burnup, but the percentage of bond sodium in the plenum only increases from ~80% to ~90%

There are several other pertinent findings of the METAPHIX project. Fission gas behavior and release was shown to be consistent with previous studies at EBR-II (reviewed in Section 2.1.5.1). Also, europium was found to migrate to the bond sodium, and subsequently the upper plenum, in the same fashion as cesium. However, release fraction calculations for europium were not reported.

[22] This percentage appears consistent with the FCF experience (reviewed in Section 2.1.1.2), which typically found approximately 60% of the bond sodium in the upper plenum with ~1% burnup.

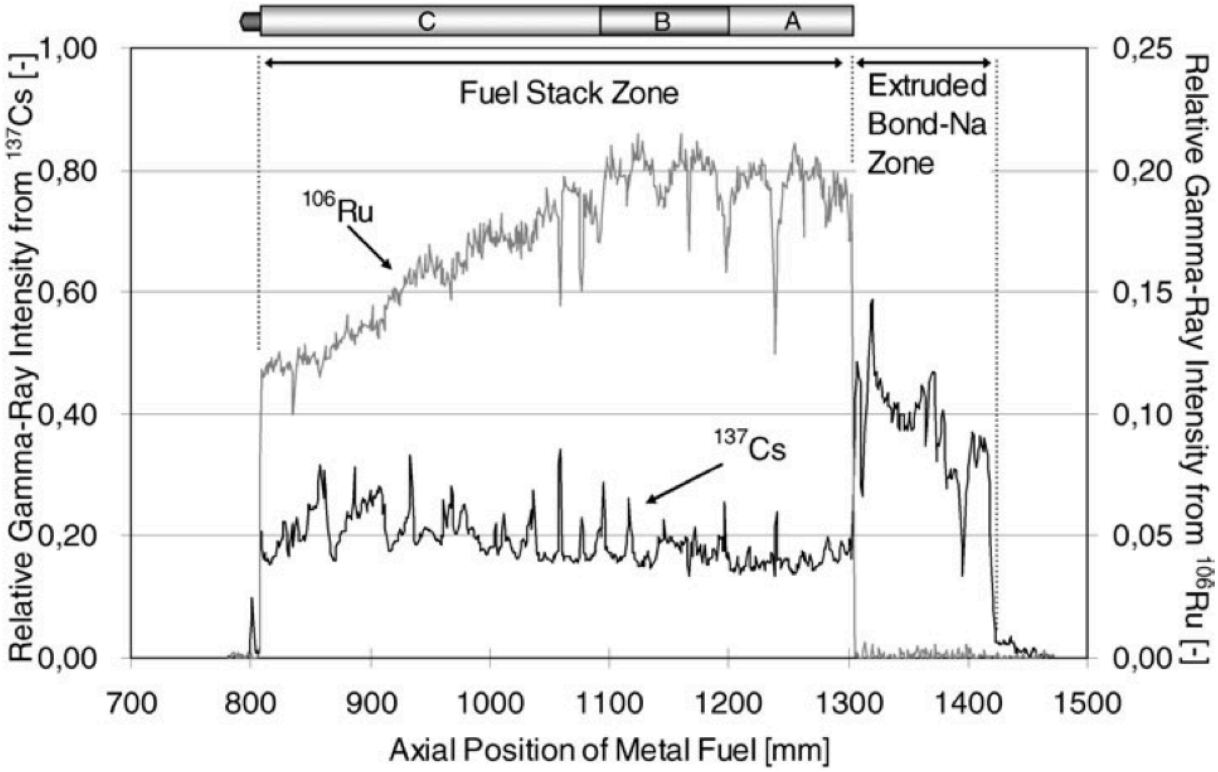


**Figure 2–11: Example Gamma Scan for METAPHIX-1, Pin 3[23] [32]**

2.1.5.5 AFC Series PIE

Lastly, recently a sequence of tests, known as the AFC series, have examined the performance of metal fuel using the Advanced Test Reactor (ATR) [33]. In particular, the AFC-1F, 1H, 2A, and 2B experiments investigated the behavior of a variety of metal fuel alloys of U, Pu, Np, Am, and Zr, at burnup ranges from several percent to greater than 25%. Table 2-22 contains details on each AFC series. Figure 2–12 shows an example experimental "rodlet" for the AFC-1 tests. The sodium bonded metallic fuel slug has a height of 38.1mm (1.5 in), with a large gas plenum above the fuel matrix [34].

After irradiation, the experimental fuel rodlets undergo detailed PIE, including axial gamma scans. These scans can identify the location of fission products within the fuel pin, such as the results shown in Figure 2–13, for a U-29Pu-4Am-2Np-30Zr fuel pin irradiated to 26.68% heavy metal burnup. As can be seen, at these very high burnup levels, the majority of the cesium inventory has transferred to the sodium bond located in the upper plenum. An estimate based on the figure indicates approximately 70% of the cesium inventory is located in the bond sodium in the upper plenum. The AFC tests also demonstrate that fission gas release at very high burnup appears to follow the trend of earlier EBR-II tests and achieves an asymptote at approximately 80% release [35].

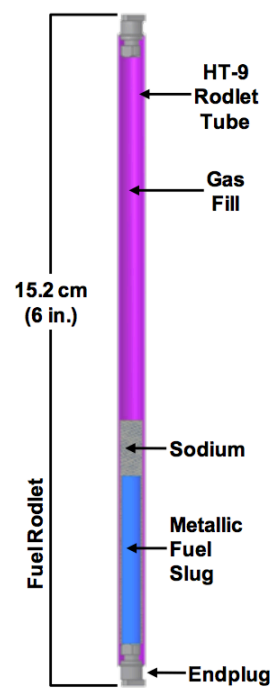


**Figure 2–12: AFC-1 Experimental Rodlet [34]**

[23] Reprinted from ref [32] with permission from the American Nuclear Society.

**Table 2-22: AFC Metal Fuel Test Summary [36]**

| *Experiment* | *Peak Burnup* | *Rodlet* | *Composition*[1] |
|---|---|---|---|
| *AFC-1F & AFC-1H* | *~7% - 1F* | *1* | *U-29Pu-4Am-2Np-30Zr* |
| | *~30% - 1H* | *2* | *U-34Pu-4Am-2Np-20Zr* |
| | | *3* | *U-25Pu-3Am-2Np-40Zr* |
| | | *4* | *U-29Pu-4Am-2Np-30Zr* |
| | | *5* | *U-89Pu-7Am-30Zr* |
| | | *6* | *U-25Pu-3Am-2Np-40Zr* |
| *AFC-2A* | *~10%* | *1* | *U-20Pu-3Am-2Np-15Zr* |
| | | *2* | *U-20Pu-3Am-2Np-1.0RE-15Zr* |
| | | *3* | *U-20Pu-3Am-2Np-1.5RE-15Zr* |
| | | *4* | *U-20Pu-3Am-2Np-1.5RE-20Zr* |
| | | *5* | *U-20Pu-3Am-2Np-1.0RE-20Zr* |
| | | *6* | *U-20Pu-3Am-2Np-20Zr* |
| *AFC-2B* | *~25%* | *1* | *U-20Pu-3Am-2Np-15Zr* |
| | | *2* | *U-20Pu-3Am-2Np-1.0RE-15Zr* |
| | | *3* | *U-20Pu-3Am-2Np-1.5RE-15Zr* |
| | | *4* | *U-20Pu-3Am-2Np-1.5RE-20Zr* |
| | | *5* | *U-20Pu-3Am-2Np-1.0RE-20Zr* |
| | | *6* | *U-20Pu-3Am-2Np-20Zr* |

[1]RE – Rare Earth composition (6% La, 16% Pr, 25% Ce, 53% Nd)

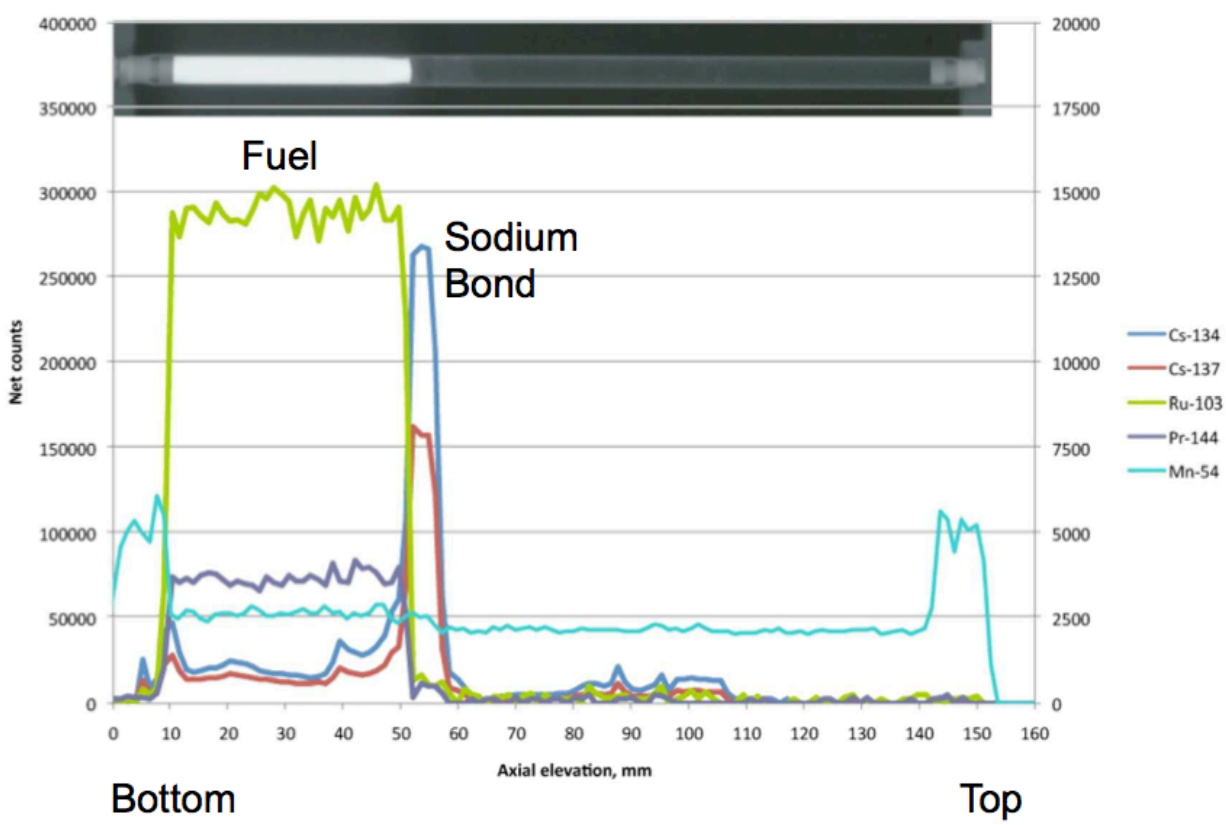


**Figure 2–13: Axial Gamma Scan of AFC-1H Rod 4[24] [35]**

[24]Mn-54 is an activation product of the cladding.

## *2.2 Fuel Damage Accidents*

The following subsection provides an overview of three U.S. metal fuel sodium reactor accidents. The focus here is on the release of radionuclides from the fuel to the primary sodium. Additional details on each accident can be found in ref [2].

*There have been three U.S. sodium reactor fuel damage accidents involving metal fuel. However, all three incidents occurred at very low fuel burnup levels, which limits the available insights*

### *2.2.1 Sodium Reactor Experiment (SRE) Accident*

The Sodium Reactor Experiment (SRE) was a 20 $MW_{th}$ sodium-cooled thermal reactor that experienced fuel failure around July 12th, 1959 due to a tetralin[25] leak into the primary sodium coolant. The tetralin reacted to form a particulate that accumulated and restricted coolant flow though the core region. Despite abnormal temperature and radioactivity readings, the reactor was not shutdown for almost two weeks.

During the SRE accident, 13 of the 43 fuel assemblies experienced pin failures, but no significant melting, beyond that seen due to eutectic formation with the cladding, was observed. Of the failed fuel elements, 11 contained unalloyed uranium metal, enriched to 2.8%, while two of the failed fuel elements contained alloyed uranium fuel (U, Zr, Th, Mo combinations). On average, the fuel was at ~0.1% burnup [37]. Subsequent analyses indicated that the fuel pin failures likely occurred due to repeated cycling through the α - β phase transformation temperature for uranium. This resulted in significant fuel expansion and eventual cladding burst. It is also possible that the NaK pin bond boiled[26], causing additional pin pressure increase. It is estimated that peak fuel temperatures reached ~ 940°C, although the highest thermocouple reading was ~ 800°C [38].

Following the accident, samples of the primary sodium were taken to determine the radionuclides released from the fuel pins. Using this data, SRE staff developed the release fractions provided in Table 2-23. However, the first primary sodium sample was delayed until about seven days after the accident due to $Na^{24}$ activity, which means some portion of the original fission product activity was likely lost. In ref [39], an attempt was made by SRE staff to account for these factors, although no details on the calculation were given. The revised release estimates were Cs/Sr ~ 1%, I/Ba-La/Ce ~0.7%, Zr-Nb ~ 0.4%, and Ru ~ 0.2%. In addition to the isotopes listed in Table 2-23, the following isotopes were identified, but not quantified in the analysis: $Xe^{133}$, $Kr^{85}$ (both were detected in the cover gas).

**Table 2-23: SRE Estimated Radionuclide Release Fraction (Based on Ref [39])[27]**

| *Isotope* | *Estimated Release Percentage of Damage Fuel Inventory* |
|---|---|
| $Cs^{137}$ | 1.05% |
| $Cs^{134}$ | 0.66%[1] |
| $Sr^{89}$ | 0.92% |
| $Sr^{90}$ | 0.87% |
| $I^{131}$ | 0.32% |
| $Ce^{141}$ | 0.25% |
| $Ce^{144}$ | 0.22% |
| $Ba(La)^{140}$ | 0.22% |
| $Zr^{95} + Nb^{95}$ | 0.18% |
| $Ru^{103}$ | 0.09% |

[1]From neutron capture in $Cs^{133}$; estimated.

[25] Tetralin is an oil-like hydrocarbon that was used to cool the primary pump seals.

[26] NaK has a lower boiling point than sodium (785°C vs. 883°C at atmospheric pressure).

[27] The release fractions given in ref [39] were multiplied by 43/13 to account for only the failed fuel elements.

### *2.2.2 Fermi 1 Accident*

Fermi 1, a commercial SFR, located at the current site of the Enrico Fermi Nuclear Generating Station outside of Detroit, experienced significant fuel melting on October 5th, 1966 due to fuel assembly flow blockage. U-10Mo fuel pins (enriched to 25.6% $U^{235}$) with zirconium cladding fueled the $200MW_{th}/66MW_e$ reactor. The blockage was caused by a Zircaloy baffle that broke loose from the melt-down section liner located below the core and transported to the entrance of the core region by primary sodium flow. Four of the 150 subassemblies experienced damage and two of those four subassemblies experienced significant fuel melting. The estimated burnup of the fuel in the four subassemblies was less than 0.05 a/o [40].

Subsequent analyses were performed to assess the recorded sodium temperature rise [41], and to estimate the approximate fuel temperature during the incident [42]. Although there are no recorded fuel temperatures from the melted assemblies, based on analyses of the fuel behavior, it is thought that fuel pins failed soon after exceeding ~1100°C, with a maximum temperature of ~1400°C, before slumping and being cooled by lower fuel assembly structure or an infusion of sodium vapor once the fuel assembly can failed [42]. Immediately following the accident, it was unknown how many fuel elements had failed or melted. Table 2-24 presents an initial analysis of radionuclide release conducted by Fermi 1 staff based on the measured activity of the system [40]. As can be seen in the table, a range of release fractions were assumed to provide bounds on the number of melted pins. In addition to the isotopes listed in Table 2-24, the following isotopes were identified, but not quantified in the analysis: $Xe^{135}$, $Sr^{90}$, Ba-$La^{140}$, $Ce^{141}$, $Ce^{144}$, $I^{133}$, $Ru^{103}$, Zr-$Nb^{95}$.

**Table 2-24: Fermi 1 – Fuel Failure Analysis for Radioactivity [40]**

| *Region* | *Isotope* | *Activity in System (Ci)* | *Activity in Average Pin (Ci)* | *Number of Fuel Pins Melted per Assumed Release Fraction* | | |
|---|---|---|---|---|---|---|
| | | | | *10%* | *50%* | *100%* |
| *Cover Gas* | *Kr-85* | *1.43* | *0.02* | | *142* | *71* |
| | *Xe-133* | *6.4* | *0.118* | | *109* | *54* |
| | | | | | *240*** | *170** |
| *Primary Na* | *Cs-137* | *2.75* | *0.17* | *162* | *32.4* | *16.2* |
| | *Sr-89* | *1570* | *5* | *3140* | *628* | *314* |
| | *I-131* | *5.04* | *0.33* | *153* | *30.6* | *15.3* |

* 100% release of $^{133}Xe$ and 0% release of $^{133}I$ (which would lead to additional $^{133}Xe$)
** 50% Release of $^{133}Xe$, 10% release of $^{133}I$

Once the damaged fuel assemblies were removed, it was estimated that the amount of fuel melting was equivalent to one or two assemblies worth of pins (140 pins per assembly) [40,43][28]. Table 2-25 presents the estimated release fractions based on both cases. The release fractions in Table 2-25 likely err towards higher release fractions, as all radionuclide releases are attributed to the melted fuel pins, even though additional fuel assemblies suffered fuel pin damage.

**Table 2-25: Fermi 1 Estimated Release Fractions Based on Findings in Ref [40]**

| *Isotope* | *Estimated Release Fraction to Primary Sodium* | |
|---|---|---|
| | *140 Pin Melt* | *280 Pin Melt* |
| *Kr-85* | *~50%* | *~10%* |
| *Xe-133* | *~100%** | *<50%*** |
| *Cs-137* | *~10%* | *~5%* |
| *Sr-89* | *Inconclusive* | *Inconclusive* |
| *I-131* | *~10%* | *~5%* |

* Assuming 0% $^{133}I$ release
** Assuming 10% $^{133}I$ release

[28] A previous RTDP report (ref [2]) indicated Fermi 1 fuel melting as equivalent to approximately one fuel assembly. Ref [2] was published before ref [40], indicating melting equivalent to two subassemblies, had been discovered.

### *2.2.3 EBR-II Failed Experimental Capsule*

From November 23, 1967 to March 1968 at EBR-II, an experimental capsule containing a fresh ternary metallic alloy fuel pin (U-15Pu-10Zr) was responsible for a series of radionuclide releases due to repeated melting of the fuel. The melting occurred due to flaws in the manufacturing process of the capsule, which resulted in loss of the capsule bond sodium. The lack of bond sodium reduced the heat transfer from the fuel [44], which led to inadequate cooling and subsequent melting. $Xe^{133}$, $Xe^{135}$, $I^{131}$, $I^{133}$, $Cs^{134}$, and $Cs^{137}$ were identified to have been released from the capsule prior to it being removed in May 1968, but release fraction calculations were not performed [45].

## *2.3 Other Sources*

### *2.3.1 EBR-I Incident*

The Experimental Breeder Reactor I (EBR-I) operated from 1951 to 1963 at the Argonne West site in Idaho. It was built to demonstrate fuel breeding, which was accomplished in 1952. The 1.4 $MW_{th}$ NaK-cooled reactor was operated with four core designs during its lifetime. The first three core designs contained U-235 (94% enriched) fuel, while the fourth design contained plutonium fuel. In November 1955, substantial fuel melting and pin failures occurred during a test to investigate a positive component of the power coefficient. In previous tests, this positive power coefficient had been identified when the coolant flow rate though the core was reduced. The meltdown occurred in the Mark II core design, which contained U-2Zr metal fuel (at less than 0.1% burnup) in stainless steel cladding [46]. Subsequent examinations of the fuel assemblies revealed that 40% to 50% of the core had melted [47].

A literature review performed as part of the current effort did not uncover any specific data on radionuclide release. Investigations into the amount of damage sustained during the meltdown were delayed until March of 1956, several months after the incident. It was noted that the delay in opening the reactor was to allow radioactive fission product gases to decay away, but not for health reasons [48]. It was feared that the fission product gases released from opening the reactor would interfere with the U.S. monitoring of fission product gases in the atmosphere, which were used for the monitoring of Russian nuclear bomb tests [48].

### *2.3.2 Dounreay Fast Reactor*

Limited data is available from the Dounreay Fast Reactor (DFR), which was a metal fuel (U-9Mo), NaK-cooled, fast reactor in the UK. Of particular interest was the use of vented fuel at DFR, which allowed primary NaK to flow within the fuel pin. This experience provides insight into radionuclides that may migrate to the bond sodium during irradiated of non-vented metal fuel pins. The radionuclides found during the operation of DFR are listed in Table 2-26. Uranium release into the sodium was noted at below the detectable limit of 0.01ppm [49].

**Table 2-26: Radionuclides Found at DFR [49] [50]**

| *Location* | *Isotopes* |
|---|---|
| *Coolant (NaK)* | *Ba-La$^{140}$, Ce$^{141}$, I$^{131}$, Cs$^{137}$* |
| *Cover Gas* | *Xe$^{133}$, Xe$^{135}$, Rb$^{88}$, Cs$^{138}$* |

# 3 Chemistry Modeling Summary

### *3.1 Overview of Modeling Effort*

Thermodynamic equilibrium speciation modeling was performed using the Gibbs free energy minimization module of the HSC Chemistry 8 software package [51]. The purpose of these calculations was to investigate the usefulness of equilibrium thermodynamics to better understand radionuclide releases from metal fuels during a fuel failure event. The generic components and work flows for a thermodynamic source term calculation, such as the one summarized in this report, are shown in Figure 3–1.

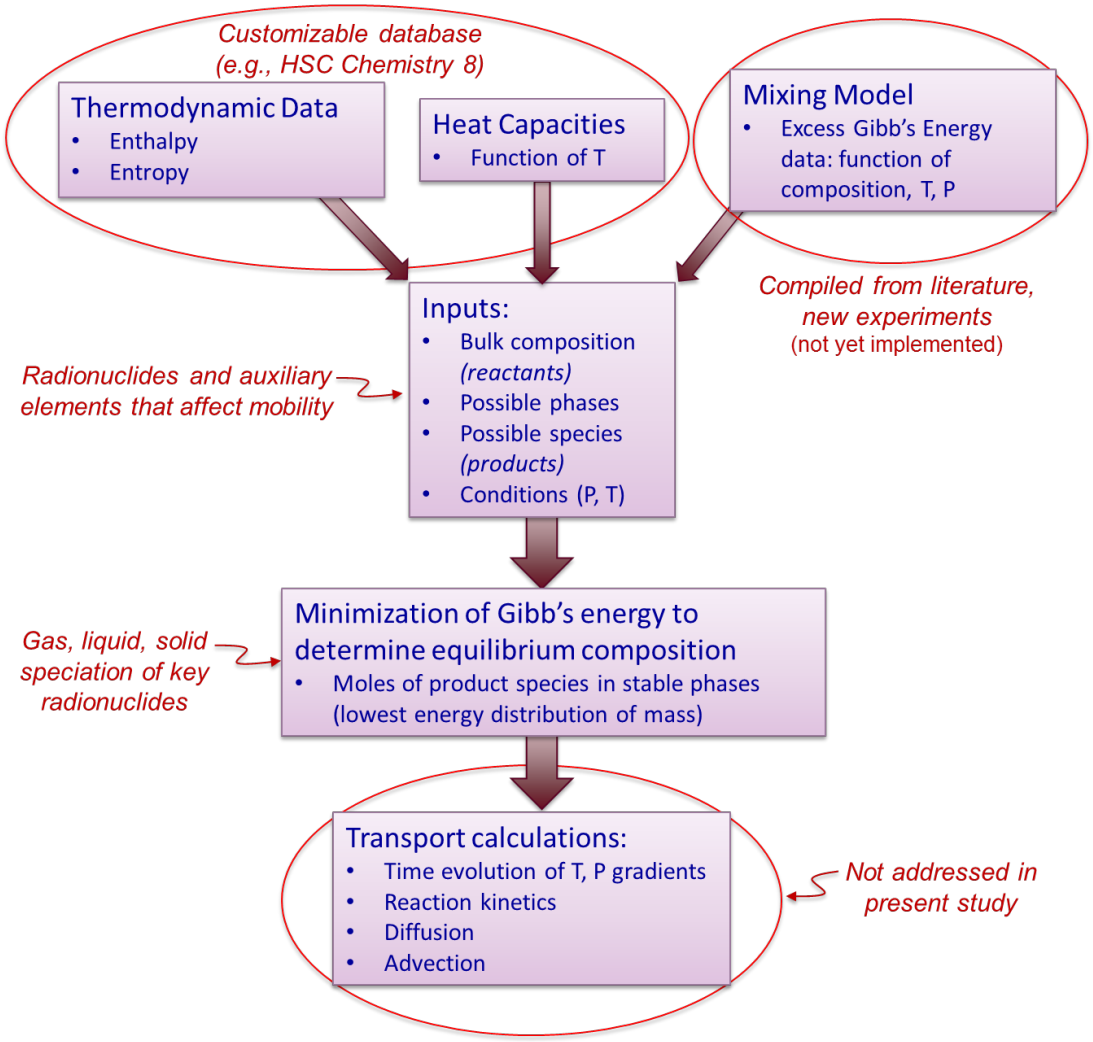


**Figure 3–1: Schematic Flow Diagram of a Generic Thermodynamic Model**

The keys to model accuracy and applicability are the thermodynamic databases that contain the constants (standard enthalpies and entropies) used to calculate the Gibbs free energy of the system and the heat capacities that are used to quantify temperature dependencies (top line Figure 3–1). To account for non-ideal mixing, Gibbs free energy excess functions must be obtained from the literature or by focused experimentation. Once the thermodynamic databases and mixing models are selected, the user specifies the bulk composition, pressure, and temperature of the system of interest. Thermodynamic codes commonly select all possible species and phases that can form for the given bulk composition; however, the user can suppress species and phases that are known not to form due to kinetic reasons. The Gibbs free energy of the system is then minimized using a numerical method such as the Lagrangian-multiplier

technique [52] and the result is the stable assemblage of species and phases for a given pressure and temperature.

Similar to many other thermodynamic modeling codes, HSC Chemistry 8 works by first identifying all possible chemical species and phases (in the HSC or user database) that could form from a user specified bulk chemical composition and then determining the equilibrium speciation (amounts of specific compounds) of the system by minimizing the total Gibbs free energy for a specified temperature and pressure. The user specified bulk composition represents the reactants in the system while the calculation results represent the assemblage of stable products for the specified bulk composition, pressure, and temperature conditions. A discussion of the theoretical basis, and the details of the results for this study are provided in Appendix C of this report.

*It is important to note that equilibrium models have inherent limitations stemming from several commonly unrealistic basic assumptions such as:*

- *The homogeneous mixing of all phases and species,*
- *The absence of chemical and thermal gradients,*
- *The absence of kinetic constraints on precipitation, melting, dissolution, vaporization, and the creation of reaction intermediates.*

With sufficiently thorough databases and experimental validation, however, equilibrium models offer the advantage of a predictive tool for assessing complex, multiphase systems that cannot be sufficiently characterized by site measurements and experimentation. Furthermore, equilibrium models can rapidly account for complex chemical interactions and interdependencies that may be missed in simplified experiments and accident site characterizations.

### *3.2 Model Scenarios and Assumptions*

Three scenarios were used to test the Gibbs free energy minimization modeling approach:

- **Scenario 1**: A simple ternary system consisting of 0.3 moles sodium, 0.02 moles cesium and 0.002 moles iodine was run from 400°C to 2000°C in 100 steps at a constant pressure of 1 bar.
    - ***Case 1a***: assumes all solids and liquids (melts) are pure phases.
    - ***Case 1b***: assumes a single melt phase that behaves as an ideal mixture.

- **Scenario 2**: A simplified metal fuel composition was run from 400°C to 2000°C in 100 steps at a constant pressure of 1 bar. The fuel composition is from the Advanced Liquid Metal Reactor source term study [53].
    - ***Case 2a***: assumes all solids and liquids (melts) are pure phases.

- **Scenario 3**: A metal fuel composition representing a Fermi 1 pin with a burnup of 0.48 MWd/kg was run from 400°C to 2000°C in 100 steps at a constant pressure of 1 bar. The fuel composition was calculated using ORIGEN2 (see Appendix C for details).
    - ***Case 3a***: assumes pure phase solids and liquids, no sodium present in the fuel.
    - ***Case 3b***: assumes pure phase solids and liquids, sodium is present in the fuel.

The details of the model scenarios, simulated fuel compositions, modeling assumptions, and a summary of the results are provided in Appendix C.

As discussed in Section 3.1 and Appendix C, the modeling results are strongly dependent on the assumptions made. Model runs for scenario 1 show that perhaps the most important assumption is whether the solids and liquids of the system are composed of pure phases (case 1a) or mixtures (case 1b). All of the cases for scenario 2 and 3 assume that the solids and liquids are composed of pure phases. The essential differences between the pure phase assumption used in case 1a and the mixture model assumption used in case 1b are summarized in Figure 3–2. The impact of using the mixing models summarized on the right side of Figure 3–2 is that the solubility, melting behavior, and vapor pressures for individual elements will be determined by properties of the mixture rather than properties of individual phases. This can have important implications on the predicted release fractions of key radionuclides from melted fuel. For example, as shown in Figure C-1 of Appendix C, if it is assumed that sodium and cesium are in an ideal mixture (molten phase), rather than pure separate phases, the model predicts that the vaporization of most of the cesium will occur at a temperature around 100°C lower than for the pure phase case.

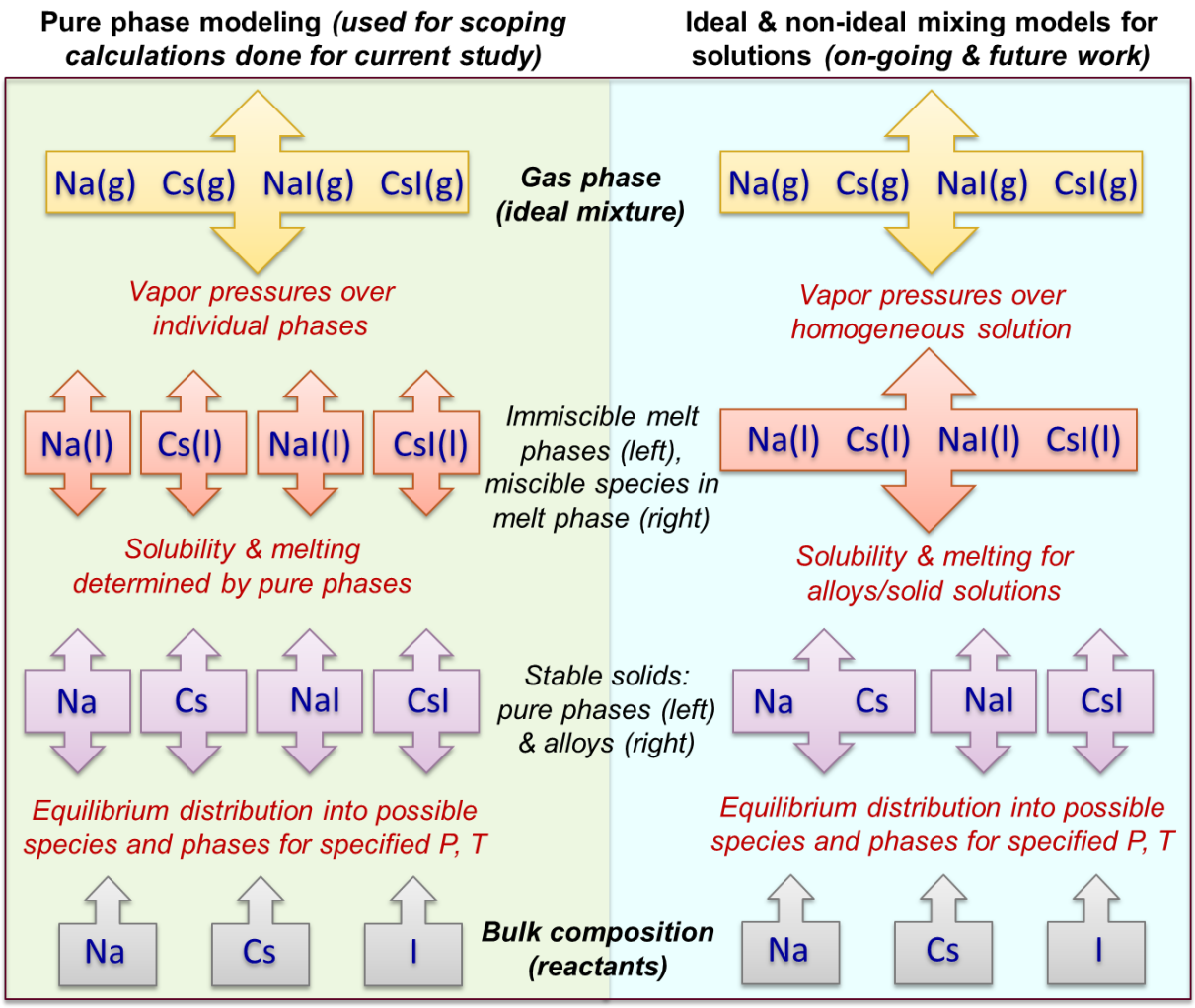


**Figure 3–2: Schematic Highlighting Differences between Pure Phase (L) and Mixture (R)[29]**

[29] Mixing models for complex systems such as mixed activation and fission products in used fuel, require knowledge of the miscibility of all relevant species in the liquid phase, as well as excess Gibbs free energy for non-ideal mixtures.

### *3.3 Conclusions of Initial Chemistry Modeling Effort*

The summary of the chemistry modeling results using HSC Chemistry 8 (provided in Appendix C) demonstrates that, while these types of calculations provide a powerful tool for explaining chemical interactions within complex mixed fission product – fuel systems, the assumptions of the calculations along with the limitations of the current database make quantitative assessments of fission product release difficult. This approach can be used to perform sensitivity analyses of radionuclide speciation for compositional and thermal variations, and may thus provide useful input for the planning and designing of release fraction experiments, but at the current time, these methods do not offer a direct way to fill gaps in the experimental and experience knowledgebase.

In particular, the assumptions related to homogenous mixing, lack of thermal gradients, and the omission of kinetics marks a significant departure from the complex constituent migration that occurs during metal fuel irradiation. The equilibrium approach has promise as a component of MST assessments for metal alloy fueled, SFRs; and may prove particularly useful in identifying knowledge gaps associated with the chemical forms and transport properties of key radionuclides in accident scenarios. The modeling approach should also be more directly useful in the analysis of radionuclide behavior once release to the primary sodium occurs, where the calculation assumptions are closer to reality.

The accurate prediction of the dominant radionuclide bearing species is a key criterion for success of a given thermodynamic modeling effort. Therefore, future modeling work will focus on collecting the data needed to formulate more complete mixing models and then comparing results to pure phase models under relevant experimental results. Future simulations that include more thorough mixing considerations will be directly compared to experimental and historical accident scenario results to provide a more quantitative model validation study.

# 4 Estimated Radionuclide Release Fraction from Metal Fuel

The following section discusses the radionuclide release fractions developed as part of the current effort. The first subsection provides the assumptions of the analysis, followed by summary results. The subsequent section provides an overview of gaps encountered during the determination of the radionuclide release fractions and possible closure pathways. Additional detail and discussion regarding how the release fractions were determined can be found in Appendix A.

## *4.1 Results*

Before radionuclide release fractions could be determined, the working assumptions were established, as shown in Table 4-1. First, the results are applicable to several metal fuel types, including unalloyed uranium metal and common uranium alloys. Second, while attempts were made to develop realistic release fractions, conservative results were assumed when data was sparse or uncertainty was high. The applicable burnup range is 0 – 10%, as this is the most typical burnup range for metal fuel and has the greatest amount of applicable data. Lastly, it is assumed that with cladding failure, the bond sodium and fission gases within the plenum regions of the pin will be released.

**Table 4-1: Release Fraction Determination Assumptions**

| *Assumptions* | *Notes* |
|---|---|
| *Metallic Fuel* | *Includes unalloyed uranium metal and typical SFR uranium alloys (U-Fs, U-Mo, U-Zr, U-Pu, U-Pu-Zr).* |
| *Level of Conservatism* | *The determined release fractions should be as realistic as possible. However, when insufficient or uncertain data exist, the release fraction should attempt to err conservatively (i.e., higher release fraction values).* |
| *Max 10% Burnup* | *The release percentages are given for metal fuel between 0 and 10% burnup, as this is the most common burnup range in modern metal fuel pool-type SFR designs.* |
| *Sodium Bond* | *Cladding failure provides a pathway for the release of bond sodium and fission gases within the plenum regions.* |

The radionuclides are divided into the eight groups identified in NUREG-1465 (the LWR Alternative Source Term) [54], provided in Table 4-2. Each following subsection provides a summary result table for each element, when possible. Some elements are treated together due to similar behavior or insufficient individual element information.

**Table 4-2: Radionuclide Grouping, Based on NUREG-1465 [54]**

| *Group* | *Elements* |
|---|---|
| *Noble Gases* | *Xe, Kr* |
| *Halogens* | *I, Br* |
| *Alkali Metals* | *Cs, Rb* |
| *Tellurium Group* | *Te, Sb, Se* |
| *Barium, Strontium* | *Ba, Sr* |
| *Noble Metals* | *Ru, Rh, Pd, Mo, Tc, Co* |
| *Lanthanides* | *La, Zr, Nd, Eu, Nb, Pm, Pr, Sm, Y, Cm, Am* |
| *Cerium Group* | *Ce, Pu, Np* |

The summary result table for each element contains the data listed in Table 4-3. The spectrum of temperatures has been split into four main categories, as seen in Figure 4–1. The purpose of the temperature categories is to identify the major differences in fuel behavior. The temperature ranges are approximate, as the eutectic formation and fuel melting temperatures will be different for each metal fuel

composition. The first category includes normal operating temperatures and slightly elevated temperatures. The second category includes appreciable eutectic formation, but below the melting temperature of the fuel matrix. The third category represents temperature ranges where fuel melting occurs, and the last category is high temperatures where fuel melting has occurred but below fuel vaporization.

**Table 4-3: Radionuclide Release Fraction Result Table Description**

| *Label* | *Notes* |
|---|---|
| *Temperature* | *Temperature range at which fuel failure occurs* |
| *Release Percentage* | *The release percentage from the fuel pin to the primary sodium for the radionuclide* |
| *Dependencies* | *Factors that may affect the release percentage (i.e., burnup level, time at temperature, fuel composition)* |
| *Uncertainty Level* | *A subjective measure of the uncertainty associated with the release percentage.* |
| *Sources* | *Quantitative*<br>*Sources that provide insight into the release percentage of the radionuclide*<br>*Qualitative*<br>*Sources that only provide indication of the radionuclide's release (or retention)* |

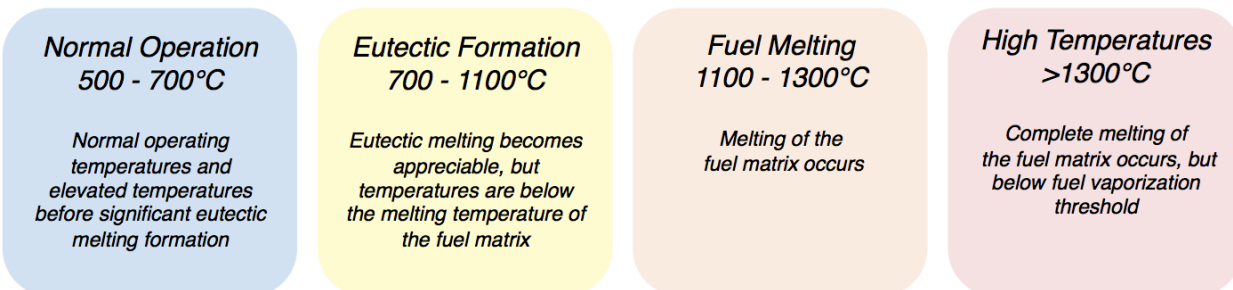


**Figure 4–1: Temperature Categories**[30]

The release percentage provides the *maximum* release to be expected in that temperature range. The release percentage may change according to the dependencies, which notes factors that may influence the release of the radionuclide. The minimum release fraction percentage used is 0.1%, and increments of 5% are used for larger release percentages. The main dependencies are burnup level, time at temperature, and fuel composition.

The uncertainty level is a subjective measure of the uncertainty associated with the release percentage. Table 4-4 provides an overview of the three uncertainty levels. The uncertainty may be high due to a lack of data sources in that temperature range, or due to conflicting sources of information. A lack of sources in a temperature range does not ensure a high uncertainty rating though, as it may be possible to bound the release percentage based on higher/lower temperature categories. For example, if it is known that complete fuel melting will only release 5% of a radionuclide, then it is very likely that melting in only eutectic regions will release less than 5% of the radionuclide, even if a data source is not available for that condition. The low uncertainty level is given when there are multiple, consistent data sources. Additional detail regarding how the uncertainty level was determined for each temperature category of each radionuclide is provided in Appendix A.

[30] Normal operation temperatures refer to fuel surface, as peak centerline temperature will be higher. Category temperatures are approximate, as fuel composition will effect eutectic formation and the fuel melting point.

**Table 4-4: Uncertainty Level Description**

| *Uncertainty Level* | *Description* |
|---|---|
| *High* | *No data sources (and unable to bound through the use of data sources in other temperature ranges), or highly conflicting data sources.* |
| *Medium* | *Data sources available, but may be limited by experiment/accident characteristics (such as burnup level), or multiple consistent data sources with a conflicting data source.* |
| *Low* | *Multiple data sources with consistent findings.* |

Lastly, the sources indicate what quantitative and qualitative information is available for each temperature range. Details on how the sources were used to develop the release percentages are available in Appendix A.

Table 4-5 specifies the section that contains the radionuclide release fractions for each element. In some cases, groups of elements are combined due to similar behavior or a lack differentiating data.

**Table 4-5: Release Fraction Result Sections**

| *Element* | *Notes* |
|---|---|
| *Xe, Kr* | *Section 4.1.1* |
| *I* | *Section 4.1.2* |
| *Br* | *Very limited data exists regarding bromine release (it can be difficult to track due to low fission yield and short half-lives). Use the release fractions of iodine.* |
| *Cs* | *Section 4.1.3* |
| *Rb* | *Very limited data regarding rubidium release and much lower fission yield than cesium. Use the release fractions of cesium.* |
| *Te* | *Section 4.1.4* |
| *Sb, Se* | *Very limited data regarding release, and have not been seen in past SFR accidents. Conservatively use release fraction of tellurium.* |
| *Ba* | *Section 4.1.5* |
| *Sr* | *Section 4.1.5* |
| *Ru* | *Section 4.1.6* |
| *Rh, Pd, Mo, Tc, Co* | *None of these noble metals have been seen released following past SFR accidents. Generally, noble metals behave similarly. Conservatively use ruthenium release fractions.* |
| *La, Zr, Nd, Nb, Pm, Pr, Sm, Y, Cm, Am* | *Section 4.1.7* |
| *Eu* | *The behavior of europium differs from the other lanthanides. However, available data on europium is insufficient for release fraction estimates. Conservatively use release fractions of cesium, as some similar behavior has been seen (METAPHIX tests).* |
| *Ce* | *Section 4.1.8* |
| *U, Pu* | *Section 4.1.8* |
| *Np* | *Very limited data regarding neptunium release, use U/Pu release fractions.* |

# **Noble Gases**: Xe & Kr

| **Temperature** | Normal Operation ~ 500°C | Eutectic Formation ~ 700°C | Fuel Melting ~ 1100°C | High Temperatures ≥ 1300°C |
|---|---|---|---|---|
| **Release Percentage** | ≤ 85% | ≤ 100% | ~ 100% | ~ 100% |
| **Dependencies** | Burnup | Burnup | Burnup | None |
| **Uncertainty Level** | Low | Medium | Low | Low |
| **Sources** | | | | |
| Quantitative | Metal Fuel PIE | | Fermi 1<br>ORNL Melt Tests<br>Hanford Melt Tests | AI Melt Tests |
| Qualitative | RBCB<br>EBR-II Leaker Tests | SRE | EBR-II Capsule<br>TREAT | |

# Halogens: I

| Temperature | Normal Operation ~ 500°C | Eutectic Formation ~ 700°C | Fuel Melting ~ 1100°C | High Temperatures ≥ 1300°C |
|---|---|---|---|---|
| Release Percentage | ≤ 15% | ≤ 20% | ≤ 30% | ≤ 100% |
| Dependencies | Burnup | Burnup | Burnup | Time, Temp. |
| Uncertainty Level | Medium | Medium | Medium | Low |

**Sources**

Quantitative

- EBR-II Reprocessing
- Metal Fuel PIE
- SRE
- Fermi 1
- Melt Refining Tests
- Hanford Melt Tests
- ORNL Melt Tests
- AI Melt Tests

Qualitative

- EBR-II Leaker Tests
- EBR-II Capsule

# Alkali Metals: Cs

| Temperature | Normal Operation ~ 500°C | Eutectic Formation ~ 700°C | Fuel Melting ~ 1100°C | High Temperatures ≥ 1300°C |
|---|---|---|---|---|
| Release Percentage | ≤ 55% | ≤ 60% | ≤ 100% | ≤ 100% |
| Dependencies | Burnup, Composition | Burnup, Composition | Burnup, Time, Composition | Time |
| Uncertainty Level | Low | Medium | Medium | Low |

**Sources**

Quantitative

- EBR-II Reprocessing
- Metal Fuel PIE
- SRE
- Fermi 1
- Melt Refining Tests
- Hanford Melt Tests
- ORNL Melt Tests

Qualitative

- RBCB
- EBR-II Capsule
- TREAT
- AI Melt Tests

# Tellurium Group: Te

| Temperature | Normal Operation ~ 500°C | Eutectic Formation ~ 700°C | Fuel Melting ~ 1100°C | High Temperatures ≥ 1300°C |
|---|---|---|---|---|
| Release Percentage | ≤ 1% | ≤ 1% | ≤ 5% | No Data |
| Dependencies | Composition | Composition | Composition | |
| Uncertainty Level | Medium | Medium | High | |
| Sources | | | | |
| Quantitative | | | Melt Refining Tests<br>Hanford Melt Tests | |
| Qualitative | RBCB | SRE | Fermi 1<br>EBR-II Capsule | |

# Barium/Strontium Group: Ba

| Temperature | Normal Operation ~ 500°C | Eutectic Formation ~ 700°C | Fuel Melting ~ 1100°C | High Temperatures ≥ 1300°C |
|---|---|---|---|---|
| Release Percentage | ≤ 5% | ≤ 10% | ≤ 15% | ≤ 20% |
| Dependencies | Unknown | Unknown | Unknown | Unknown |
| Uncertainty Level | Medium | Medium | High | Medium |
| Sources | | | | |
| Quantitative | Metal Fuel PIE; EBR-II Reprocessing | | Melt Refining Tests; Hanford Melt Tests | ORNL Melt Tests; AI Melt Tests |
| Qualitative | RBCB | SRE | Fermi 1; EBR-II Capsule | |

# Barium/Strontium Group: *Sr*

| Temperature | Normal Operation ~ 500°C | Eutectic Formation ~ 700°C | Fuel Melting ~ 1100°C | High Temperatures ≥ 1300°C |
|---|---|---|---|---|
| **Release Percentage** | ≤ 0.1% | ≤ 5% | ≤ 20% | ≤ 20% |
| **Dependencies** | None | None | None | None |
| **Uncertainty Level** | Medium | Medium | High | High |
| **Sources** | | | | |
| Quantitative | EBR-II Reprocessing | SRE | Fermi 1<br>Melt Refining Tests<br>Hanford Melt Tests | ORNL Melt Tests |
| Qualitative | RBCB | | EBR-II Capsule | |

# Noble Metals: Ru

| Temperature | Normal Operation ~ 500°C | Eutectic Formation ~ 700°C | Fuel Melting ~ 1100°C | High Temperatures ≥ 1300°C |
|---|---|---|---|---|
| Release Percentage | ≤ 0.1% | ≤ 1% | ≤ 5% | ≤ 5% |
| Dependencies | None | None | None | None |
| Uncertainty Level | Low | Medium | Medium | Medium |

**Sources**

Quantitative

- Metal Fuel PIE
- SRE
- Melt Refining Tests
- Hanford Melt Tests
- ORNL Melt Tests
- AI Melt Tests

Qualitative

- RBCB
- Fermi 1
- TREAT
- EBR-II Capsule

# Lanthanides[1]

| Temperature | Normal Operation ~ 500°C | Eutectic Formation ~ 700°C | Fuel Melting ~ 1100°C | High Temperatures ≥ 1300°C |
|---|---|---|---|---|
| **Release Percentage** | ≤ 0.1% | ≤ 1% | ≤ 30% | ≤ 30% |
| **Dependencies** | Unknown | Unknown | Unknown | Unknown |
| **Uncertainty Level** | Medium | High | High | High |
| **Sources** | | | | |
| Quantitative | Metal Fuel PIE | SRE (Zr-Nb) | | Al Melt Tests (Zr-Nb) |
| Qualitative | RBCB (Nb, Zr, Eu) | | Melt Refining Tests (La, Y, Eu, Nd)<br>Fermi 1 (Zr-Nb)<br>TREAT (Zr, Nb, Pr, Eu) | |

[1]The cesium release fractions should be used for europium (Eu).

# Cerium Group: *Ce*

| Temperature | Normal Operation ~ 500°C | Eutectic Formation ~ 700°C | Fuel Melting ~ 1100°C | High Temperatures ≥ 1300°C |
|---|---|---|---|---|
| **Release Percentage** | ≤ 1% | ≤ 5% | ≤ 10% | ≤ 15% |
| **Dependencies** | Burnup | Burnup | Burnup | Burnup |
| **Uncertainty Level** | Medium | High | High | High |

**Sources**

*Quantitative*

- Metal Fuel PIE
- SRE
- Melt Refining Tests
- ORNL Melt Tests

*Qualitative*

- RBCB
- Fermi 1
- TREAT
- EBR-II Capsule

# **Cerium Group:** *U and Pu*[1]

| **Temperature** | *Normal Operation ~ 500°C* | *Eutectic Formation ~ 700°C* | *Fuel Melting ~ 1100°C* | *High Temperatures ≥ 1300°C* |
|---|---|---|---|---|
| **Release Percentage** | ≤ 0.1% | ≤ 0.1% | ≤ 0.1% | ≤ 0.1% |
| **Dependencies** | Burnup | Burnup | Burnup | Burnup |
| **Uncertainty Level** | Low | Medium | Medium | Medium |

**Sources**

*Quantitative*

- *Metal Fuel PIE*
- *Melt Refining Tests*

*Qualitative*

- *RBCB*
- *SRE*
- *Fermi 1*
- *TREAT*
- *EBR-II Capsule*
- *AI Melt Tests*

[1]The release fractions for uranium and plutonium refer to dissolution in sodium.

### *4.2 Gaps and Possible Closure Pathways*

*Gaps in the current knowledgebase, along with possible closure pathways, are provided here. A prioritization of the closure efforts will be performed following the completion of a trial mechanistic source term calculation[30].*

The process of establishing radionuclide release fractions revealed several gaps in the current knowledgebase, which are reviewed in this section. These gaps have been segregated into two classes, based on possible closure pathways. The first group relates to the behavior of certain radionuclides during metal fuel irradiation, while the second gap concerns the radionuclide release from molten high burnup metal fuel. While the gaps and possible closure pathways are reviewed here, a prioritization of closure efforts will not be attempted until the conclusion of a trial mechanistic source tem calculation, which will provide insight into the importance of each radionuclide in regard to offsite consequence[31].

#### *4.2.1 Expanded Metal Fuel PIE*

Metal fuel PIE is a vital tool for assessing the behavior of radionuclides during the irradiation of metal fuel. As was shown in Section 2.1.5, there has been significant metal fuel PIE performed both domestically (for EBR-II, FFTF, and AFC fuel) and internationally (METAPHIX). However, the purpose of these examinations was typically to gauge fuel performance and fuel integrity, rather than assess the possible source term during accidents. Past metal fuel PIE provides valuable insight into the behavior of fission product radionuclides, such as cesium, ruthenium, and cerium, but only because these radionuclides were tracked for other reasons[32]. Additional PIE, with a focus on source term assessment, can close many of the gaps found during this work.

First, the behavior of iodine during irradiation is highly debated (more detail is provided in Appendix A.2). Particularly, it is unclear how much of the iodine inventory migrates to the bond sodium during irradiation. Currently, the only data point concerning this phenomenon is recent work conducted by INL as part of reprocessing efforts (Section 2.1.5.2). Additional PIE can confirm the findings of this study, which are notable, as they indicate that the migration of iodine to the bond sodium may be less than previously thought.

Second, there is "medium" to "high" uncertainty regarding the release of tellurium, barium, and strontium (europium also falls within the group) since there is little known regarding the migration of these elements to the bond sodium during irradiation. PIE of high burnup metal fuel regarding these elements would drastically reduce the uncertainty associated with their release. Many of these elements are soluble in sodium, which would indicate that migration to the bond sodium may be high, but past accident data does not necessarily support this conclusion. However, without PIE data to validate this viewpoint, it is difficult to justify low release fractions.

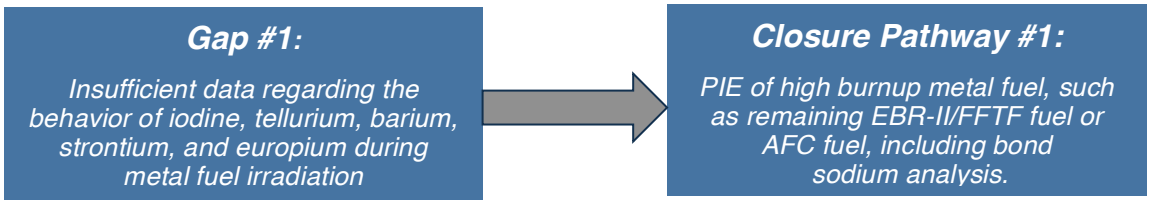


---

31 Argonne is currently conducting a trial mechanistic source term calculation to determine the importance of each radionuclide in regard to offsite consequences (dose and land contamination).

32 For example, cesium can represent the location of bond sodium and ruthenium can represent the location of the fuel matrix.

### *4.2.2 High Burnup Metal Fuel Melt Tests*

There are a series of knowledge gaps regarding the melting of high burnup metal fuel in sodium. There are past U.S. accidents involving metal fuel melting (such as Fermi 1), but at very low burnup. Additionally, there were many fuel melting tests conducted, but in inert gas atmospheres within oxide crucibles. A fuel melt test of high burnup metal fuel in sodium could provide closure to a number of open issues.

First, there were many metal fuel melt tests conducted as part of the EBR-II melt refining process (Section 2.1.1) and as part of source term assessments (Section 2.1.2). However, these tests were not performed in sodium, but typically in an inert gas. While this is an insightful measurement of volatilization, it does not directly translate to radionuclide release in liquid sodium. Many radionuclides in metal fuel are soluble in sodium, but are not likely to be volatilized at low fuel melting temperatures (~1100°C). Secondly, most of these tests were performed in oxide crucibles, meaning many elements formed oxides that would not occur in an SFR metal fuel incident. These are the elements in Category 2 of Table 2-1. The use of oxide crucibles in these experiments limits the applicability of the results for the determination of radionuclides release in SFR metal fuel accidents.

Additionally, the Fermi 1 accident and EBR-II capsule failure provide insight into radionuclide release during metal fuel melting in sodium. However, the fuel in both these incidents was at very low burnup. It is likely that the release of several radionuclides is strongly dependent on burnup level. For example, cerium is highly mobile in the fuel matrix, and will relocate to the cladding (as shown in Figure 2–6), but it is unknown if this cerium can be released during fuel melting, as there is no high burnup metal fuel melting experience. The same is true for many of the lanthanides. The AI melt tests, described in Section 2.1.2.3, examined metal fuel melting in sodium, but did not use typical metal fuel pins, but fuel discs.

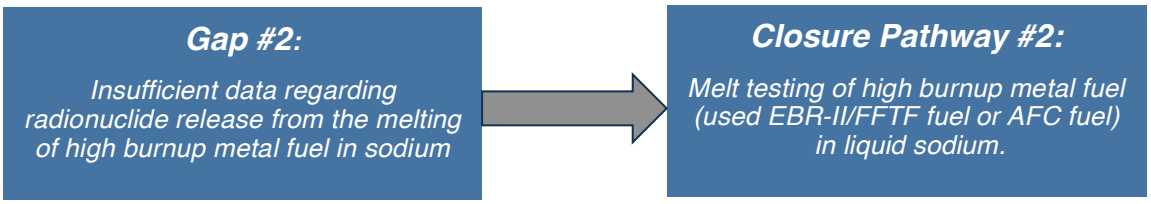

# 5 Conclusion

A study was conducted to determine the release fractions of radionuclides from metal fuel pins to the primary sodium during a variety of SFR accident conditions. This analysis utilized historical data to establish radionuclide release percentages and evaluated the usefulness of modern chemistry thermodynamic equilibrium computer codes for assisting in this effort. The focus of the effort was on common metal fuel types (metallic uranium, U-Fs, U-Mo, U-Zr, U-Pu, U-Pu-Zr) and their behavior during typical design basis and beyond design basis accidents at pool-type SFRs. The following figure highlights the major conclusions of the work.

***Conclusions:***

*1) There are many sources of data available regarding metal fuel behavior and the release of radionuclides during accident conditions.*

*2) Radionuclide release fractions from the fuel pin to the primary sodium were determined for the elements of interest, but gaps in the knowledgebase do exist:*

*2.a) Additional data is needed regarding the behavior of iodine, tellurium, barium, strontium, and europium during metal fuel irradiation. Further metal fuel post-irradiation examination could likely resolve this gap.*

*2.b) Additional data on the melting of high burnup metal fuel in liquid sodium would resolve or reduce many of the uncertainties related to the release of radionuclides at elevated temperatures.*

*3) Chemistry modeling, through thermodynamic equilibrium calculations, provides insight, but the necessary assumptions limit the applicability of the results for determining quantitative radionuclide release fractions for metal fuel.*

First, there are many sources of metal fuel data available. This includes a substantial database of metal fuel PIE and a variety of fuel melting tests. Additionally, there have been three U.S. metal fuel sodium reactor incidents that provide insight into accident behavior and radionuclide release.

Second, radionuclide release fractions were determined for the elements of interest for a metal fuel SFR source term assessment. However, several gaps were noted during this analysis. There is a lack of understanding regarding the migration of iodine, tellurium, barium, strontium, and europium to the bond sodium region of the fuel pin. The quantity of these radionuclides that transport to the bond sodium likely dominates the release fraction of these elements for several accident conditions. Fortunately, additional metal fuel post-irradiation examination can likely resolve this gap.

The second gap relates to information regarding radionuclide release from molten high burnup metal fuel. There has been significant fuel melting tests performed, but the conditions of these tests (oxide crucibles, fuel composition, inert gas atmospheres) limits their applicability for assessing high burnup metal fuel radionuclide release. Similarly, past U.S. accidents that have encountered fuel melting were at low burnup at the time of the incident. Many of these data deficiencies can be resolved through melt tests of high burnup fuel in liquid sodium.

Lastly, modern thermodynamic equilibrium chemistry codes provide insight into the behavior of radionuclides within the fuel pin. However, the assumptions regarding mixing, thermal gradients, and available compounds limits their applicability for determining quantitative radionuclide release fractions from the fuel. These codes are likely better suited for analyzing the behavior of radionuclides once they have been released to the primary sodium.

## Bibliography


[1] Code of Federal Regulations: 10 § 50.67 , "Accident Source Term," Amended 1999.

[2] Grabaskas, D., Brunett, A., Bucknor, M., Sienicki, J., and Sofu, T., "Regulatory Technology Development Plan: Sodium Fast Reactor - Mechanistic Source Term Development," ANL-ART-3, 2015.

[3] Stevenson, C., *The EBR-II Fuel Cycle Story*. La Grange Park, IL, USA: American Nuclear Society, Inc., 1987.

[4] Chellew, N. and Ader, M., "The Melt Refining of Irradiated Uranium: Application to EBR-II Fast Reactor Fuel. XI. Behavior of Iodine in Melt Refining," *Nuclear Science and Engineering*, vol. 9, pp. 82-86, 1961.

[5] Chellew, N., Honesty, C., and Steunenberg, R., "Laboratory Studies of Iodine Behavior in the EBR-II Melt Refining Process," ANL-6815 (TID-4500), 1964.

[6] Chellew, N., Bennett, G., and Trice, V., "The Melt Refining of Irradiated Uranium: Applications to EBR-II Fast Reactor Fuel: VII. The Behavior of Rare Earths, Yttrium, Barium, Strontium, and Cesium," *Nuclear Science and Engineering*, vol. 9, pp. 64-70, 1961.

[7] Chellew, N. and Bennett, G., "The Melt Refining of Irradiated Uranium: Application to EBR-II Fast Reactor Fuel. XII. The behavior of Ruthenium, Molybdenum, Palladium, Rhodium, Technetium, Antimony, Cadmium, and Tellurium," *Nuclear Science and Engineering*, vol. 9, pp. 87-90, 1961.

[8] Castleman, A. and Tang. I., "Chemical Considerations in Fast Reactor Safety," in *Proceedings of the Conference on Safety, Fuels, and Core Design in Large Fast Power Reactors*, 1965.

[9] Castleman, A. and Tang, J., "Vaporization of Fission Products from Irradiated Uranium - II," *Journal of Inorganic Nuclear Chemistry*, vol. 32, pp. 1057-1064, 1970.

[10] Burris, L., Steindler, M., and Miller, W., "Proposed Pyrometallurgical Process for Rapid Recycle of Discharged Fuel Materials from the Integral Fast Reactor," in *International Topical Meeting on Fuel Reprocessing and Waste Management*, 1984.

[11] Williamson, M., Private Communication, 2015.

[12] Parker, G., Barton, C., Creek, G., Martin, W., and Lorenz, R., "Out-of-Pile Studies of Fission-Product Release from Overheated Reactor Fuels at ORNL, 1955-1965," ORNL-3981, 1967.

[13] Creek, G., Martin, W., and Parker, G., "Experiments on the Release of Fission Products from Molten Reactor Fuels," ORNL-2616, TID-4500, 1959.

[14] Hilliard, R., "Fission Product Release from Uranium Heated in Air," HW-60689, 1959.

[15] Kunkel, W., "Fission Product Retention in Sodium - A Summary of Analytical and Experimental Studies at Atomics International," NAA-SR-11766, 1964.

[16] Kunkel, W., Elliott, D., and Gibson, A., "High-Temperature Experiments on Fission Product Retention in Sodium," NAA-SR-9287, 1965.

[17] Fryer, R., Ebersole, E., Henault, P., and Smith, R., "Symptoms and Detection of A Fission-Product Release from an EBR-II Fuel Element, Case 1: Defect Above Fuel Elevation," ANL-7605, 1970.

[18] Brunson, G., Fryer, R., and Strain, R., "Experimental Irradiation of Fuel Elements Having Known Cladding Defects in EBR-II," ANL-7782, 1971.

[19] Hofman, G., Walters, L., and Bauer, T., "Metallic Fast Reactor Fuels," *Progress in Nuclear Energy*, vol. 31, no. 1/2, pp. 83-110, 1997.

[20] Batte, G. , Hofman, G., and Pahl, R. , "Current Status of the Run-Beyond-Cladding-Breach (RBCB) Tests," ANL/FF/PP--68403, 1993.

[21] Bauer, T., Wright, A., Robinson, W., Holland, J., and Rhodes, E., "Behavior of Modern Metallic Fuel in TREAT Transient Overpower Tests," *Nuclear Fuel Cycles*, vol. 92, pp. 325-352, December 1990.

[22] Beck, W., Fousek, R., and Kittel, J, "The Irradition Behavior of High-Burnup Uranium Plutonium Alloy Prototype Fuel Elements," ANL-7388 (TID-4500), 1968.

[23] Pahl, R., Wisner, R., Billone, M., and Hofman, G., "Steady-State Irradiation Testing of U-Pu-Zr Fuel to >18% Burnup," in *1990 International Fast Reactor Safety Meeting*, 1990.

[24] Chang, Y., "Technical Rationale for Metal Fuel in Fast Reactors," *Nuclear Engineering and Technology*, vol. 39, no. 3, pp. 161-170, 2007.

[25] Kim, Y., Hofman, G., Hayes, S., and Sohn, Y., "Constituent Redistribution in U-Pu-Zr Fuel during Irradiation," *Journal of Nuclear Materials*, vol. 327, no. 1, pp. 27-36, 2004.

[26] Frank, S., "Summary of Iodine Partitioning in EBR-II Fuel," Inter-Lab Memo, Idaho National Laboratory to Argonne National Laboratory, 2016.

[27] Pahl, R., Lahm, C., and Hayes. S., "Performance of HT9 Clad Metallic Fuel at High Temperatures," in *International Symposium on Fuels for Liquid Metal Reactors ANS/ENS 1992 International Conference*, Chicago, 1992.

[28] Kim, Y., Hofman, G., and Yacout, A., "Migration of Minor Actnides and Lanthanides in Fast Reactor Metallic Fuel," *Journal of Nuclear Materials*, vol. 392, pp. 164-170, 2009.

[29] Meyer, M., Hayes, S., Carmack, W., and Tsai, H., "The EBR-II X501 Minor Actinide Burning Experiment," INL/EXT-08-13835, 2008.

[30] Porter, D. and Tsai, H., "Full-Length U-xPu-10Zr (x=0, 8, 19 wt.%) Fast Reactor Fuel in FFTF," *Journal of Nuclear Materials*, vol. 427, pp. 46-57, 2012.

[31] Ohta, H. et al., "Irradiation of Minor Actinide-Bearing Uranium-Plutonium-Zirconium Alloys up to ~2.5 at %, ~7 at %, and ~10 at % Burnup," *Nuclear Technology*, vol. 190, pp. 36 - 51, April 2015.

[32] Ohta, H. et al., "Low-Burnup Irradiation Behavior of Fast Reactor Metal Fuels Containing Minor Actinides," *Nuclear Technology*, vol. 165, pp. 96-110, January 2009.

[33] Carmack, J. and Pasamehmetoglu, K., "Review of Transmutation Fuel Studies," INL/EXT-08-13779, 2008.

[34] Chichester, H., Hayes, S., and Porter, D., "Irradiation and Postirradiation Examination of AFC-1 Transmutation Metallic Fuels for Fast Reactors," in *FR13: International Conference on Fast Reactors and Related Fuel Cycles: Safe Technologies and Sustainable Scenarios*, 2013.

[35] MacLean Chichester, H., "Irradiation and Postirradiation Examination of AFC-1 Transmutation Metallic Fuel for Fast Reactors," Presenation, 2013.

[36] Carmack, J. and Pasamehmetoglu, K., "Review of Transmutation Fuel Studies," INL/EXT-08-13779, 2008.

[37] Christian, J., "Chemical Behavior of Iodine-131 During SRE Fuel Element Damage in July 1959: Response to Plantiffs Expert Witness Arujn Makhijani," Prepare for in re Boeing Litigation, 2005.

[38] Atomics International, "SRE Fuel Element Damage," NAA-SR-4488, 1959.

[39] Hart, R., "Distribution of Fission Product Contamination in the SRE," Atomics International, NAA-SR-6890, 1962.

[40] Atomic Power Development Associates, "Report on the Fuel Melting Incident in the Enrico Fermi Atomic Power Plant on October 5, 1966," APDA-233, 1968.

[41] Atomic Power Development Associates, "Subassembly Thermocouple Analysis for the Fuel Melting Incident in the Enrico Fermi Reactor," APDA-LA-2, 1969.

[42] Atomic Power Development Associates, "Thermal-Hydraulic Analysis of the October 5, 1966 Fuel Melting Incident in the Enrico Fermi Reactor," APDA-LA-5, 1969.

[43] Mueller, R., Beaudry, R., and Feldes, J., "Results of the Fission-Product Activity Analysis to Determine the Extent of Fuel Failure in Fermi Accident," *Transactions of the American Nuclear Society*, vol. 10, no. 2, pp. 334-335, November 1967.

[44] Smith, R., Ebersole, E., Fryer, R., and Henault, P., "Fission-Product Release from an Encapsulated U-Pu-Zr Ternary Alloy," *Transactions of the American Nuclear Society*, vol. 12, no. 1, p. 180, June 1969.

[45] Smith, R., Ebersole, E., Fryer, R., and Henault, P., "Origin of Fission-Product Release in EBR-II November 23, 1967, to May 6, 1968," ANL-7604, 1970.

[46] Rice, R., Curran, R., McGinnis, F., Nevick, M., and Thalgett, F., "EBR-I, Mark III-Design Report," ANL-5836, 1958.

[47] Kittel, J., Novick, M., and Buchanan, R., "The EBR-I Meltdown - Physical and Metallurgical Changes in the Core. Final Report - Metallurgy Program 7.2.18," ANL-5731, 1957.

[48] Haroldsen, R., *The Story of the BORAX Reactor and the EBR-I Meltdown*., 2008.

[49] Matthews, R. et al., "Performance and Operation of the Dounreay Fast Reactor," in *Third United Nations International Conference on the Peaceful Uses of Atomic Energy*, 1964.

[50] Zwetzig, G., "Survey of Fission- and Corrosion-Product Activity in Sodium- or Nak-Cooled Reactors," AI-AEC-MEMO-12790, 1969.

[51] Outotec, "HSC Chemistry 8 User's Guide," 2014.

[52] Koukkari, P., "Introduction to Constrained Gibbs Energy Methods in Process and Materials Research," VTT Technical Research Centre of Finland, Report 160, 2014.

[53] Schram, R., Cordfunke, E., and Huntelaar, M., "Source Term Calculations of the ALMR," ECN-R--95-021, 1995.

[54] U.S. Nuclear Regulatory Commission, "Accident Source Terms for Light-Water Nuclear Power Plants," NUREG-1465, 1995.

[55] Walker, R. and Pratt, J., "The Solubilities of Bismuth and Tellurium in Liquid Sodium," *Journal of Nuclear Materials*, vol. 34, pp. 165-173, 1970.

[56] J., McFarlane,; J., LeBlanc,;, "Fission-Product Tellurium and Cesium Telluride Chemistry Revisted," AECL-11333, 1996.

[57] Collins, J., Osbourne, M., and Lorenz, R., "Fission Product Tellurium Release Behavior under Sever Light Water Reactor Accident Conditions," *Nuclear Technology*, vol. 77, no. 1, pp. 18-31, 1987.

[58] Pelton, A., "The Ba-Na (Barium-Sodium) System," *Bullentin of Alloy Phase Diagrams*, vol. 6, no. 1, pp. 26-29, 1985.

[59] Pelton, A. , "The Na-Sr (Sodium-Strontium) System," *Bulletin of Alloy Phase Diagrams*, vol. 6, no. 1, pp. 43-45, 1985.

[60] Mariani, R., Porter, D., O'Holleran, T., Hayes, S., and Kennedy, J., "Lanthanides in Metallic Nuclear Fuels: Their Behavior and Methods for their Control," *Journal of Nuclear Materials*, vol. 419, pp. 263-271, 2011.

[61] Bozzolo, G., Hofman, G., Yacout, A., and Mosca, H., "Lathanide Migration and Immobilization in U-Zr Nuclear Fuels," *Journal of Nuclear Materials*, vol. 425, pp. 188-192, 2012.

[62] Lamprecht, G. and Crowther, P., "Solubility of Metals in Liquid Sodium: The Systems Na-Ag, Na-Zn, and Na-Ce," *Trans. Metallic. Soc. AIME*, vol. 242, no. 10, pp. 2169-2171, 1968.

[63] Caputi, R. and Adamson, M., "Experimental Determination of Plutonia and Urania Solubility in Liquid Metal," GEFR-SP-202, 1980.

[64] Douglas, T., "A Cryoscopic Study of the Solubility of Uranium in Liquid Sodium at 97.8 C," *Journal of Research of the National Bureau of Standards*, vol. 52, no. 5, pp. 223-226, 1954.

[65] Toshiba, "4S Safety Analysis," AFT-2009-000155, 2009.

[66] Trice, V. and Chellew, N., "The Melt Refining of Irradiated Uranium: Application to EBR-II Fast Reactor Fuel. VI. The Behavior of Plutonium in the Melt-Refining Process," *Nuclear Science and Engineering*, vol. 9, pp. 55-58, 1961.

[67] Hilton, B., Porter, D., and Hayes, S., "AFC-1 Transmutation Fuel Post-Irradiation Hot Cell Examination 4 to 8 at.% Final Report," INL/EXT-05-00785, 2006.

[68] Okamoto, H., "Ru-U (Ruthenium-Uranium)," *Journal of Phase Equilibria and Diffusion*, vol. 33, no. 6, p. 499, 2012.

# Appendix A: Radionuclide Release Fraction Determination

The following sections describe the sources and reasoning used to construct the release fraction tables in Section 4.1. Each section is divided into the four temperature ranges presented in the summary tables. As with the results presented in Section 4.1, the discussion is separated by element, if adequate information is available.

***Note**: For radionuclides, the element symbol (Xx) is used to refer to the elemental state or a particular isotope, otherwise the element name is used.*

## *A.1 Noble Gases*

**Noble Gases: Normal Operation 500 – 700°C**

The metal fuel PIEs (Section 2.1.5) provide the best quantitative data for the release fraction of noble gases in this temperature range. As the early experiments at EBR-II show (Section 2.1.5.1), the release of noble gases is highly burnup dependent (*i.e.*, dependent on fuel expansion), but likely hits a maximum of 80 – 85% as burnup increases. This was true for multiple types of metal fuel, and has been reinforced by more recent testing (Sections 2.1.5.2 through 2.1.5.5). The balance of the noble gases remain trapped within the fuel matrix.

Qualitatively, the leaker and RBCB tests at EBR-II, discussed in Section 2.1.3, saw the release of noble gases with cladding failure at normal operating temperatures. While release fractions were not calculated, the noble gas behavior is consistent with the quantitative sources

*Summary*: The available data sources demonstrate that the release of noble gases between 500 - 700°C is highly burnup dependent, but that a release of greater than 85% of the noble gas inventory is unlikely. The uncertainty regarding this estimate is considered "low," as there is significant data available from multiple sources regarding fission product behavior during metal fuel irradiation.

**Noble Gases: Eutectic Formation 700 – 1100°C**

The only data point in this temperature range is the qualitative experience from the SRE accident, reviewed in Section 2.2.1. Noble gases were released from the failed fuels pins, but release fractions were not calculated.

*Summary*: The increase in fuel temperature, and small amount of fuel melting in eutectic regions of the fuel matrix, should only increase the amount of noble gases released when compared to fuel failure near normal operating temperatures, as fuel melting liberates noble gases that remain trapped within the fuel matrix.

Therefore, the release of noble gases remains highly burnup dependent, but may be slightly higher than the maximum of 85% seen at lower temperatures. A release percentage of up to 100% of the noble gas inventory is noted (up to 85% of the total inventory released from the plenum, and up to 15% released from the fuel matrix). The uncertainty level is considered "medium," as there is no quantitative data source to indicate how much of the noble gases may be liberated through eutectic melting.

**Noble Gases: Fuel Melting 1100 – 1300°C**

Release fractions for the noble gases were calculated following the Fermi 1 incident, described in Section 2.2.2. Post accident analysis indicated the release of approximately 50% of the noble gases. While this release percentage seems low, it is important to note that the Fermi 1 fuel was at low burnup (< 0.05 a/o), which based on the results of the fission gas release experiments described in Section 2.1.5.1, imply that only a small percentage of the noble gases had escaped the fuel matrix prior to the incident. This suggests that the noble gases that were released from the failed fuel pins were liberated from the fuel matrix during the fuel melting process, and had not previously been released to the fission gas plenum.

The fuel melt tests conducted at ORNL (Section 2.1.2.1) confirm the results seen at Fermi 1. As Figure 2–2 shows, the release of noble gases reaches over 98% within minutes after melting, even for low burnup fuel. It is assumed that fuel at higher burnup will have only greater release percentages, since much of the noble gases will have already escaped the fuel matrix and be released from the fuel pin as soon as the cladding fails. These tests also show that dependency of the release on time is small, as the majority of the noble gas release happens quickly after melting.

Hanford melt tests (Section 2.1.2.2) saw smaller releases of xenon with fuel melt in helium (~10%) for 25 minutes. The exact burnup of the test fuel is unknown, and a review by ORNL questioned the initial gas concentration of the sample [12]. As will be discussed in subsequent sections, the results of this test are considered less reliable due to the lack of repeated experiments, and the conflicting results when compared to multiple other data sources.

The EBR-II experimental capsule failure, reviewed in Section 2.2.3, provides a qualitative indicator, as the noble gases were found in the cover gas region of the reactor following the extensive melting of the experimental metal fuel element.

*Summary*: Several data points indicate that fuel melting can liberate any noble gases that have not already escaped the fuel matrix during irradiation. When coupled with the noble gases that were released from the fuel matrix during irradiation, a release of up to 100% of the noble gases is possible. The dependence on fuel burnup is unclear, as Fermi 1 had a release of approximately 50% of the noble gases at low burnup, but ORNL melt testing liberated 100% of the noble gases also at low burnup. The uncertainty is considered "low," as there are multiple data sources demonstrating similar noble gas behavior.

**Noble Gases: Very High Temperatures ≥1300°C**

At very high temperatures (1700 - 1800°C) for short time periods (<1 min), the ORNL fuel melt experiments described in Section 2.1.2.1 saw complete release of the noble gases with fuel at 15% burnup.

Additionally, melt tests of uranium metal in sodium conducted by AI (Section 2.1.2.3) saw the complete release of xenon from the fuel samples when melted at extremely high temperatures (>2300°C) over very small time periods (<20 ms).

*Summary*: Both ORNL and AI melt tests indicate that complete (100%) noble gas release should be expected at very high temperatures, with no dependency on fuel burnup or time at elevated temperature. The uncertainty is again considered "low" due to multiple, consistent data sources.

## *A.2 Halogens*

**Iodine: Normal Operation 500 – 700°C**

First, reprocessing experience at the FCF at EBR-II, described in Section 2.1.5.1, provides insight into the behavior of iodine during metal fuel irradiation. During used fuel preparation for melt refining, approximately 10% of the iodine inventory was identified in the bond sodium of the fuel pin, with the remainder in the fuel matrix. However, the burnup level of the fuel at the time of reprocessing was low (~1%).

The only other quantitative measurement of iodine migration to the bond sodium comes from the recent INL examination (Section 2.1.5.2). Here, it was determined that approximately 10% of the iodine inventory had migrated to the regions outside the fuel region (the upper/lower plenums and end cap) after irradiation to 11.5% burnup. It is not known how much of the remaining 90% of the iodine inventory in the fuel region was within the fuel matrix, or in the bond sodium dispersed within the fuel matrix.

The EBR-II leaker tests, described in Section 2.1.3.1, provide a qualitative indicator of iodine release during fuel pin failure at operational temperatures, as the bottom leaker experiment resulted in iodine release to the primary sodium. Also, a relationship between the iodine release rate and the sodium flowrate was observed. This is likely a result of internal pin pressure changes and bond sodium movement. This would appear to confirm that the release of iodine is due to iodine within the bond sodium region, not from iodine within the fuel matrix.

*Summary*: The behavior of iodine during metal fuel irradiation has been highly debated. Multiple sources of information and data must be considered to determine appropriate release fractions for iodine in this temperature range.

It has long been thought that a fraction of the iodine inventory will bond with cesium in the fuel matrix to form CsI, which is the most thermodynamically preferential iodide of those possible in the fuel. As will be described in Section A.3, cesium can migrate to the bond sodium of the fuel pin during irradiation, and dissolve in the sister alkali metal. It is possible that some of the iodine found in the bond sodium region during the FCF experience and INL examination was transported as CsI, and then dissociated to Cs and NaI in the sodium bond.

FCF experience provides one data point, as the migration of iodine to the bond sodium is limited to approximately 10% of the iodine inventory at ~1% burnup, while the INL examination found about 10% of the iodine outside the fuel region at 11.5% burnup (as described in Section 2.1.5.4, by 11.5% burnup, it is likely that ~90% of the bond sodium had been displaced from the fuel region). These two data points appear to indicate that iodine does not behave in direct proportion to cesium, as Section A.3 will show that the cesium fraction outside the fuel region (in the plenums) increases with burnup and reaches ~50% by 10% burnup. There are typically more atoms of cesium in the fuel matrix than iodine due to their differing fission yields. If all the iodine within the fuel matrix bonded with cesium to form CsI (a one to one atomic ratio), then it would be expected that the fraction of iodine in the plenum regions would be *at least* as high as the cesium fraction. The data appears to indicate that iodine is likely forming a bond other than CsI in the fuel (possibly $UI_3$), which does not migrate to the bond sodium.

While uranium iodides are not as thermodynamically preferential as other fission product-iodine compounds, the much greater quantity of uranium in the fuel matrix compared to fission products would appear to make this compound likely. The fuel melt tests conducted by BNL, summarized in Table 2-6, appear to support this conclusion, as it was found that iodine volatizes from the fuel as a uranium iodide at temperatures above the fuel melting point, and as following sections will describe, the release of iodine from the fuel matrix during fuel melt tests has been found to be small unless very high temperatures (>1300°C) are reached.

Therefore, based on the limited available data, it appears that the majority of the iodine inventory within the fuel pin is in a form that does not readily migrate to the bond sodium region. The two data points show a similar iodine fraction in the plenum regions (~10%) despite significant differences in burnup level (~1% and 11.5%). The release percentage is set at up to 15% of the iodine inventory, which accounts for 10% of the iodine inventory in the plenum region, which would be released with pin failure, plus an addition 5% that may be within the bond sodium that is dispersed within the fuel matrix. The assumption regarding the iodine fraction in the bond sodium within the fuel region is difficult to justify, and accounts for the "medium" level of uncertainty regarding the release percentage. Also, the data does not show a strong dependence on burnup level once 1% burnup has been reached. The SRE accident in the following temperature range appears to show that a lower release fraction is likely if burnup is very low (~0.1%).

**Iodine: Eutectic Formation 700 – 1100°C**

The only data point within this temperature region is the SRE accident. As described in Section 2.2.1, only 0.3 - 0.7% of the iodine inventory was estimated to be released from the failed fuel pins at SRE. It is important to note that the burnup at SRE at the time of the accident was on average ~0.1%.

*Summary*: The low release rate of iodine seen at SRE was likely a result of the very low fuel burnup, which limited initial iodine migration to the NaK bond region. However, the SRE results do demonstrate that iodine release from the fuel matrix at this temperature range is small, even with significant eutectic melt regions forming.

Therefore, the release fractions for iodine with fuel pin failure in this temperature range will likely be only slightly higher than the fraction of iodine contained within the bond sodium region. Based on the assumptions of the previous temperature category, a release percentage of up to 20% is assumed (15% from iodine in the bond sodium, plus 5% release from eutectic regions or dispersed bond sodium liberated by the eutectic melting). The lack of high burnup fuel data in the region merits a "medium" uncertainty level. As explained in the preceding temperature category, the dependence on burnup appears minimal after the 1% level is reached.

**Iodine: Fuel Melting 1100 – 1300°C**

The release fraction of iodine was calculated following the Fermi 1 incident, described in Section 2.2.2. Depending on the fuel melt assumptions[33], approximately 5 – 10% of the iodine inventory was released from the affected pins despite significant melting and relocation. The burnup of the Fermi 1 fuel was very low at the time (<0.05 a/o).

Melt refining tests at EBR-II, described in Section 2.1.1.1, were conducted within this temperature range (1250 °C) and also at very high temperatures (1300 - 1400°C, described in the following subsection). As shown in Table 2-2, when held at 1250°C for four hours, less than 1% of the iodine was volatized from the metal fuel sample in an inert atmosphere.

Conversely, melt experiments at Hanford (described in Section 2.1.2.2) found over 40% of the iodine volatized from a pure metallic uranium sample when heated to 1215°C for 25 minutes. There is very little supporting data regarding this test in ref [14], as the main focus of the melt tests were on oxidation of uranium metal in air. It is unclear why the result of this test is substantially different from other experience (for various radionuclides).

Lastly, the EBR-II experimental capsule failure, described in Section 2.2.3, resulted in iodine in the primary sodium, but the exact fractional release was not calculated.

---

[33] As noted in Section 2.2.2, the total number of melted fuel pins was likely between 140 and 280.

*Summary*: From the melt refining tests conducted for EBR-II reprocessing, it appears that very little iodine is volatized from the fuel matrix in this temperature range, even if held at elevated temperatures for several hours. However, these tests were conducted in an inert gas atmosphere, not in liquid sodium. The Fermi 1 accident saw a release of 5 – 10% of the iodine inventory even though the fuel was at very low burnup. This likely indicates that the iodine was liberated from the fuel matrix, as migration to the bond sodium prior to the melting event was likely limited. Without additional supporting evidence, the Hanford melt test is considered less reliable, as it disagrees with the multiple fuel melt tests conducted at EBR-II.

Therefore, the release percentage is set at up to 30% for this temperature range (15% in the bond sodium, plus an additional 15% for iodine release from the fuel matrix or from bond sodium that was dispersed in the fuel matrix, but that was liberated by fuel melting). The uncertainty level remains "medium," as data regarding high burnup fuel behavior is lacking.

**Iodine: Very High Temperatures ≥1300°C**

Many iodine volatilization tests have been conducted in this temperature range. The EBR-II melt refining tests and FCF reprocessing experience, described in Section 2.1.1.1, saw the majority of the iodine volatized at heating to 1300°C for several hours, with essentially complete volatilization with heating to 1400°C for several hours. This process formed the basis of iodine removal during reprocessing at FCF, which was successfully utilized for over 35,000 used fuel pins.

Similarly, the melt tests conducted at ORNL in air and in steam environments (results in Table 2-8) saw on average 26 – 46% of the iodine volatized when at 1700 - 1800°C for less than a minute. This appears to indicate some amount of time dependence, as complete volatilization of iodine did not occur immediately, even with some oxidation occurring, which likely increases volatilization.

Lastly, the AI melt tests, described in Section 2.1.2.3, provide perhaps the best comparison to an SFR accident, as the fuel melting was conducted in sodium. The results, shown in Table 2-11, find iodine release fractions between 44% and 72%. While the time at temperature for these tests was very short (<20ms), the complete melting and disintegration of the fuel likely aided in iodine release.

*Summary*: The ORNL and AI melt tests saw fairly high iodine release percentages when at high temperatures for short time periods. The EBR-II melt refining tests and FCF experience demonstrates essentially complete iodine volatilization when at held at high temperatures for an extended period. Therefore, it is likely that complete iodine release will occur from the fuel pin when at temperatures above 1400°C for a time period beyond several minutes. At 1300°C, a slightly smaller release may occur, but a substantial amount of iodine will still be released. Therefore, the iodine release fraction is set at up to 100% of the inventory, with a small dependence on time at temperature. The uncertainty is considered "low" due to the multiple consistent data sources and substantial FCF reprocessing experience.

### *A.3 Alkali Metals*

**Cesium: Normal Operation 500 – 700°C**

There are a variety of factors that must be considered to determine the release percentage of cesium in this temperature range. First, reprocessing experience at the FCF at EBR-II (Section 2.1.1.2) and the metal fuel PIE (Section 2.1.5) provide data on the fraction of cesium that migrates to the plenum region of the fuel pin (in the bond sodium). Table A-1 provides a review of this data[34], which has been plotted in Figure A-1. As can be seen, the data shows a fairly consistent trend regarding the migration of cesium to the upper plenum. There is a strong dependence on burnup level (which likely implies a dependence on fuel expansion) as the cesium escapes the fuel matrix and migrates to the bond sodium in the plenum region. The increase of cesium in the plenum occurs fairly rapidly with increasing burnup at low burnup values, but begins to slow at higher burnup values.

**Table A-1: Cesium Migration Data**

| *Experiment/ Experience* | *Burnup* | *Cesium in Plenum (%)* |
|---|---|---|
| *FCF* | *~1%* | *~ 15%* |
| *METAPHIX-1* | *2.5 – 2.7%* | *30 – 38%* |
| *METAPHIX-2* | *6.6 – 7.2%* | *40 – 46%* |
| *X501* | *7.6%* | *~ 40%* |
| *METAPHIX-3* | *9.3 – 10.2%* | *48 – 53%* |
| *AFC-1H4* | *26.7%* | *~ 70%* |

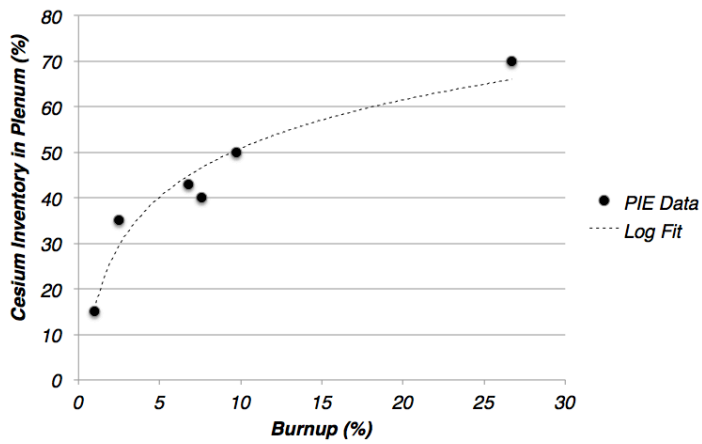


**Figure A-1: Cesium Migration Data with Log Fit**

The percentage of cesium in the plenum may not be the only cesium available for release during pin failure at this temperature range though. As noted in the METAPHIX PIE results (Section 2.1.5.4), a fraction of the bond sodium remains dispersed within the fuel matrix, even at high burnup. From the data, it appears this fraction ranges from 40% of the bond sodium at ~1% burnup, to ~10% of the bond sodium at 10% burnup. There may be additional cesium contained within this dispersed bond sodium. However, the X447 experiment at EBR-II (Section 2.1.5.2) appears to provide a resolution to this issue.

In X447, two fuel pins breached between 9.5% and 10% burnup. Subsequent gamma scans indicated that approximately 50% of the cesium inventory had been released during the breach. According to the PIE information plotted in Figure A-1, it is likely that ~50% of the cesium inventory was located in the upper plenum region of the fuel pin. This would appear to indicate that the release of additional cesium (from the fuel matrix or from the ~10% bond sodium[35] dispersed within the fuel matrix) was small.

Qualitatively, the RBCB tests at EBR-II (Section 2.1.3.2) found cesium released from the fuel pin after cladding failure. While quantitative measurements of the released cesium were recorded, an effort to determine release fractions was not made.

*Summary*: As mentioned in the discussion of iodine release in this temperature range, cesium will migrate from the fuel matrix to the bond sodium region as burnup increases and the fuel expands. Once there, the miscible cesium will form elemental Cs and remain in the sodium. The migration of cesium is strongly

[34] There are *many* additional PIE gamma scans of EBR-II metal fuel experiments, which could be analyzed to provide additional validation of the trend noted here.

[35] Estimate of sodium bond dispersed within fuel matrix is based on METAPHIX PIE at ~10% burnup (Table 2-21).

dependent on fuel expansion, which in turn depends on fuel burnup level and fuel composition (as was seen in the METAPHIX tests). For the current study, a maximum burnup of 10% is assumed, which from past testing, likely limits cesium migration to the plenum to about 50% of the total cesium fuel inventory. If the pin cladding were to fail, this cesium could be released to the primary sodium as the bond sodium in the plenum escapes the fuel pin. Also, as shown at the X447 experiment, additional cesium release from the fuel matrix or the bond sodium dispersed within the fuel matrix appears small.

Therefore, the release percentage of cesium is highly dependent on burnup level, as shown in Table A-1, with a maximum release of ~55% at 10% burnup. There may also be a dependence on fuel composition (as it can affect fuel expansion). The uncertainty is rated as "low" since there are multiple PIE results, which appear to provide a consistent trend, and there is quantitative breach experience with X447.

**Cesium: Eutectic Formation 700 – 1100°C**
The only data point within this temperature range is the incident at SRE (Section 2.2.1). Following the accident, calculations determined that approximately 1.0 - 1.05% of the cesium was released from the affected pins. Again, SRE was at very low burnup (0.1%) at the time of the incident, which likely limited the amount of cesium that had migrated to the NaK bond region.

*Summary*: The SRE incident appears to indicate that cesium release from the fuel matrix is small, even with significant eutectic melt formation. Thus, the determining factor is the quantity of cesium that has migrated to the bond sodium and plenum regions. Therefore, cesium release percentage is set at up to 60% (up to 55% from the sodium bond, and <5% from the fuel matrix). The dependence on burnup remains, as it will determine the amount of cesium in the bond sodium and plenum regions. Uncertainty is considered "medium," due to the lack of high burnup fuel information.

**Cesium: Fuel Melting 1100 – 1300°C**
Following the Fermi 1 accident (Section 2.2.2), release fractions for cesium were estimated to be approximately 5 - 10%[36]. The very low burnup (<0.05 a/o) of Fermi 1 fuel likely limited the amount of cesium that was in the bond sodium during the accident, and therefore limited the release of cesium from the fuel pin.

Melt refining tests at EBR-II (Section 2.1.1.1) found the volatilization of cesium at 1200°C was both time and concentration dependent, with release percentages from 27% to essentially 100% with greater time and initial concentration.

Conversely, the melt test at Hanford in a helium environment (Section 2.1.2.2) saw only 1.2% of the cesium volatized at 1250°C for 25 minutes, but as mentioned in the iodine discussion, the results of this test are considered less reliable.

Qualitatively, the EBR-II experimental capsule failure (Section 2.2.3) resulted in cesium release to the primary sodium, and cesium was found in the test loop following the TREAT M-Series tests (Section 2.1.4).

*Summary*: The cesium volatilization tests for EBR-II indicate that significant cesium volatilization (27 – 100%) is possible in this temperature range (assuming the single Hanford test is an outlier). However, the Fermi 1 incident saw a smaller cesium release fraction (5 – 10%) with significant melting in sodium, rather than in an inert gas atmosphere. In either case, it is possible that up to 55% of the cesium may already be present in the bond sodium of the fuel pin (at ~10% burnup). Any cesium release from the fuel matrix during fuel melting will only be in addition to the amount released from the bond sodium.

---

[36] As noted in Section 2.2.2, the total number of melted fuel pins was likely between 140 and 280, which accounts from the distribution between five and ten percent.

Therefore, the cesium release percentage in this temperature range is set as 100% or less of the cesium inventory (up to 55% from the sodium bond, and up to 45% from the fuel matrix). The dependence on burnup continues, as it will determine the amount of cesium in the bond sodium, and the EBR-II melt refining tests appear to indicate a dependence on time at elevated temperature. The uncertainty level in this temperature range is considered "medium," as the EBR-II melt tests, Hanford melt tests, and Fermi 1 experience all provide somewhat conflicting information regarding the amount of cesium volatized from the fuel.

**Cesium: Very High Temperatures ≥1300°C**

For five years, the FCF at EBR-II (Section 2.1.1) reprocessed 35,000 used metal fuel pins by heating them to 1400°C for 4 hours and volatizing the cesium inventory in an inert gas atmosphere. This experience indicates that approximately all the cesium is volatilized from the fuel at this temperature and time range.

The only other quantitative data point at this temperature range is the cesium volatilization melt tests conducted by ORNL (Section 2.1.2.1). Natural uranium held at very high temperatures (1700 - 1800°C) for less than a minute resulted in the volatilization of 10 – 20% of the cesium inventory, despite some amount of oxidization occurring.

Surprisingly, the AI melt tests (Section 2.1.2.3) did not find cesium in the sodium following the melt tests (and the small quantity of cesium that was found in the cover gas space was likely the result of xenon decay [15]).

*Summary*: The FCF experience at EBR-II clearly demonstrates that complete cesium volatilization is possible when at 1400°C for multiple hours. The ORNL melt tests show that release fractions may be smaller if the time period is short, even at very high temperatures. Therefore, the cesium release percentage is set at up to 100%, with a dependence on time at elevated temperature. The uncertainty level is considered "low" due to the substantial experience at the FCF.

### *A.4 Tellurium Group*

**Tellurium: Normal Operation 500 – 700°C**

No tellurium release was noted following the RBCB tests at EBR-II (Section 2.1.3.2), and available literature does not indicate significant tellurium release from the vented fuel pins at DFR. There is some indication from FCF reprocessing that tellurium will interact with the cladding during irradiation.

*Summary*: There is limited data available regarding the behavior of tellurium in irradiated metal fuel. However, some insight can be inferred from the limited data and operational experience. First, the solubility of tellurium in sodium is high [55], and its low elemental Te melting point (449°C) would indicate high mobility. Oxide fuel experience has shown tellurium bonding with fission product cesium and zirconium [56]. The fission yield of $Te^{132}$ in a metal fuel SFR is very similar to that of $Cs^{137}$.

Although tellurium properties would appear to suggest the possibility of significant release of tellurium to the bond sodium, the limited available data (RBCB at EBR-II and DFR) does not support this conclusion. Instead, there is indication of tellurium interaction with the cladding (FCF experience). Although its fission yield is similar to cesium, its behavior within the fuel pin appears very different. It is also possible that tellurium is bonding with zirconium within the fuel matrix (for U-Zr fuel pins), which may account for its retention. Zirconium tellurides have been shown to retain tellurium up to 1700°C [57]. All but one of the EBR-II RBCB tests used a 10Zr fuel, which may explain why tellurium release was not noted.

Therefore, the release percentage for tellurium with pin failure at this temperature range is set to a maximum of 1%. Although tellurium release has not been seen in the available metal fuel data and its retention appears to be explained by zirconium telluride formation, its low melting point and high solubility in sodium may allow some migration to the bond sodium. The uncertainty level is considered "medium," as no metal fuel PIE was found that validates the assumptions made here. A dependence on composition is noted, as an increase in zirconium content in the fuel matrix will likely aid in tellurium retention.

**Tellurium: Eutectic Formation 700 – 1100°C**

Following the accident at SRE (Section 2.2.1), tellurium was not recorded as being found in the primary system or sodium.

*Summary*: The SRE incident appears to indicate that significant eutectic melting does not cause the liberation of a significant amount of tellurium. It should also be noted that many of the damaged SRE pins did *not* use a uranium zirconium alloy, which would aid tellurium retention through zirconium tellurides.

With little additional data, the release percentage for tellurium in this temperature range is set at up to 1% of the total inventory (based on similar assumptions as the preceding temperature range). It appears that eutectic formation does not result in the release of additional tellurium, as even the non-zirconium fuel at SRE did not appear to release an appreciable amount of tellurium. Uncertainty is noted as "medium," due to the lack of available data regarding high burnup fuel in this temperature range.

**Tellurium: Fuel Melting 1100 – 1300°C**

The EBR-II melt refining tests (Section 2.1.1.1) examined the volatilization of tellurium at 1200 and 1400°C, and found volatized quantities below 5%. However, the use of an oxide crucible makes the applicability of these results for metal fuel melting questionable, as the majority of the tellurium reacted with the crucible.

The Hanford melt test in helium (Section 2.1.2.2) provides another quantitative indication of tellurium volatilization, with 4.2% of the tellurium inventory volatized when at 1215°C for 25 minutes. However, like the EBR-II melt refining tests, the use of a zirconia ($ZrO_2$) boat as the melting vessel may have affected the results through the formation of oxides.

Qualitatively, no tellurium release was noted following the Fermi 1 accident (Section 2.2.2) and the EBR-II experimental capsule failure (Section 2.2.3).

*Summary*: The EBR-II and Hanford melt tests provide limited insight, as oxide crucibles affect the applicability of the results. However, the Fermi 1 accident and EBR-II capsule failure appears to reinforce the notion that the tellurium release is limited. The EBR-II experimental capsule used a U-Pu-Zr fuel element, and the presence of zirconium may account for the retention of tellurium. Fermi 1 utilized a U-Mo fuel, but did have a zirconium cladding, although the low burnup may have limited tellurium migration to the cladding.

Therefore, the release percentage for tellurium in this temperature range is set at up to 5%. Although tellurium release was not noted following the Fermi 1 incident and the EBR-II experimental capsule failure, the EBR-II melt refining tests saw some volatilization (below 5%) even with an oxide crucible. The uncertainty is considered "high," as it is unclear whether efforts were made to measure tellurium following the Fermi 1 incident and EBR-II capsule failure. The dependence on composition (and zirconium) continues, as zirconium tellurides can retain tellurium up to 1700°C [57].

**Tellurium: Very High Temperatures ≥1300°C**
There is no metal fuel tellurium release data available in this temperature range.

*Summary*: Although it has been shown that zirconium tellurides can retain tellurium up to 1700°C [57], the lack of supporting evidence for metal fuel behavior precludes the assessment of a release percentage.

### *A.5 Barium, Strontium*

**Barium: Normal Operation 500 – 700°C**

Reprocessing experience at the FCF at EBR-II (Section 2.1.1.2) typically found approximately 100% of the barium inventory within the fuel matrix at the end of fuel pin life (at ~1% burnup). The metal fuel PIE (Section 2.1.5) saw minor barium concentration regions during radial scans.

Barium ($Ba^{140}$ and its daughter $La^{140}$) was found in almost all radionuclide surveys following the RBCB tests at EBR-II (Section 2.1.3.2), although no release fraction determination was made. Barium was also found in the primary coolant of DFR, which operated with vented fuel (Section 2.3).

*Summary*: Due to a lack of information regarding the location of barium within the fuel pin at high burnup levels, it is difficult to determine an appropriate release percentage. Barium is quite soluble in sodium [58], and its elemental Ba melting point is 727°C. The fission yield of $Ba^{140}$ is similar to that of $Cs^{137}$. The RBCB tests demonstrate that barium can escape the fuel matrix at these temperature levels, which is not surprising given its high solubility in sodium. The difficulty is determining the fraction of the barium inventory that will be present in the bond sodium at higher burnup levels (the FCF experience at EBR-II was only at very low burnups levels, and barium was only tracked during radial scans at EBR-II, not axial scans).

Therefore, the release fraction of barium at this temperature range is assumed to be up to 5% of the pin inventory. This estimation is based on available information in this temperature range but also the AI melt tests discussed in the ≥1300°C range, which appears to set an upper bound on release. The 5% of barium released is assumed to be from migration to the bond sodium due to its high solubility, even though appreciable relocation was not seen in the available data. The uncertainty is considered "medium," due to the lack of high burnup metal fuel PIE regarding barium migration.

**Barium: Eutectic Formation 700 – 1100°C**

The only qualitative data point in this temperature range is the SRE incident (Section 2.2.1), where a release fraction of 0.22 – 0.7% was estimated. Again, the burnup of SRE was very low (0.1%).

*Summary*: SRE appears to indicate that barium release in this temperature range is small, but the low burnup of the fuel limits its range of applicability, as barium migration to the NaK bond may not have occurred (if it occurs at all). It is assumed that the barium release noted at SRE was from barium within the fuel matrix, not the bond.

Therefore, a release percentage estimate for barium of up to 10% is assumed (up to 5% in bond sodium, plus up to 5% from the fuel matrix), based on the assumptions of the preceding temperature range and the SRE result. The uncertainty continues to be "medium," as the lack of data regarding high burnup fuel continues.

**Barium: Fuel Melting 1100 – 1300°C**

Melt refining experiments at EBR-II (Section 2.1.1.1) found essentially complete retention of barium when heated to 1300°C for 2.3 hours. However, barium is one of the "reactive" elements that formed oxides with the crucible.

The Hanford melt test in helium (Section 2.1.2.2) saw only 0.08% of the barium volatized at 1250°C for 25 minutes, but again, an oxide crucible was used. As mentioned in the sections on iodine and cesium, the Hanford tests are also questionable due to the lack of supporting data and repeatability.

During the Fermi 1 accident (Section 2.2.2), barium was found in the primary sodium, but a quantitative release fraction was not calculated. Following the TREAT M-Series tests (Section 2.1.4), $La^{140}$ was found

in the sodium loop, which is a daughter of $Ba^{140}$. No barium release was noted following the EBR-II experimental capsule failure (Section 2.2.3).

*Summary*: Despite the formation of oxides in the EBR-II and Hanford melt tests, the low volatilization of barium is consistent with its high elemental boiling point (1897°C). However, as the Fermi 1 accident shows, barium release to the primary sodium is still possible in this temperature range. Continuing the assumptions from the lower temperature ranges, it may be possible that up to 5% of the barium inventory is already in the bond sodium, so releases from the melted fuel matrix will only add to that amount. However, since appreciable volatilization of barium appears unlikely in this temperature range, barium in the fuel matrix would likely have to come in contact with sodium to escape the fuel matrix. As will be seen in the next subsection on very high temperatures, the AI melt tests in sodium found less than 5% of the barium released from completely molten and dispersed fuel. This data point helps bound the amount of barium that can be released from molten fuel.

Therefore, a release percentage of barium at up to 15% is estimated (up to 5% from the bond sodium, and a conservative 10% through non-volatile release from the fuel matrix). The uncertainty is considered "high," as the applicability of the EBR-II melt refining tests and Hanford test is questionable due to their use of oxide crucibles. Also, the lack of quantitative data from Fermi 1, TREAT, and the EBR-II capsule limits their insight.

**Barium: Very High Temperatures ≥1300°C**

EBR-II melt refining tests (Section 2.1.1.1) at 1400°C for three hours found about 1% of the barium volatized, with the rest of the inventory bonding with the oxide crucible.

ORNL melt tests (Section 2.1.2.1) found only 0.2 – 0.4% of barium volatized in steam and in air at 1700 – 1800°C for less than a minute, but in an oxide crucible.

Perhaps the most relevant test, the AI melt tests in sodium (Section 2.1.2.3) found 2.1 – 5.4% of the barium released at very high temperatures with fuel dispersal (and some vaporization) in sodium.

*Summary*: The EBR-II and ORNL melt tests indicate very little barium volatilization, even at temperatures approaching the boiling point of barium (1897°C), but with oxide crucibles. Perhaps most notable, the AI melt test in sodium found a relatively small fraction of barium released, despite very high temperatures and complete fuel dispersal in sodium. This would appear to indicate that barium release from the fuel matrix to the sodium is small, even when molten.

Therefore, the determined release fraction is 20% (up to 5% from the sodium bond, and a conservative 15% through volatile and non-volatile release from the fuel matrix). The uncertainty is considered "medium," as the AI melt tests provides fairly comprehensive data regarding barium release from molten metal fuel in sodium. However, there is still uncertainty regarding the applicability of the results to high burnup fuel.

**Strontium: Normal Operation 500 – 700°C**
Reprocessing experience at the FCF at EBR-II (Section 2.1.1.2) typically found approximately 100% of the strontium inventory within the fuel matrix at the end of fuel pin life (~1% burnup). No strontium was noted following the RBCB tests at EBR-II (Section 2.1.3.2). It also appears that no appreciable amount of strontium was released from the vented fuel at DFR (Section 2.3).

*Summary*: While the solubility of strontium in sodium is high [59], it does not appear to escape the fuel matrix in significant amounts at this temperature range. The fission yield of $Sr^{90}$ is similar to that of $Cs^{137}$, but experience at the FCF, DFR, and the RBCB test at EBR-II did not see appreciable migration from the fuel matrix to the sodium. However, due to its high solubility in sodium, the possibility that a small fraction of the strontium may dissolve in the sodium at fuel matrix/bond sodium interfaces cannot be discounted.

Therefore, the release percentage for strontium is estimated at up to 0.1% of the inventory, based on the high solubility of strontium in sodium. Although there are multiple data points indicating that the release of strontium is small, the lack of high burnup metal fuel PIE showing the exact location of the strontium inventory results in a "medium" uncertainty level.

**Strontium: Eutectic Formation 700 – 1100°C**
Following the accident at SRE (Section 2.2.1), it was calculated that approximately 1% of the strontium inventory of the affected fuel pins had been released.

*Summary*: It appears that a small release of strontium is possible in this temperature range, likely due to exceeding the melting point of elemental Sr (768°C) and the formation of eutectic melt regions in the fuel, which may allow strontium migration to the sodium, where it is soluble. While the SRE experiment was at very low burnup, based on the preceding temperature category, it does not appear that increasing burnup would necessary lead to greater fractional strontium releases.

Therefore, the strontium release percentage is set at less than 5% of the strontium inventory, with no apparent dependencies. Again, the lack of data regarding the location of strontium in high burnup fuel pins is continued at this temperature range, resulting in a "medium" uncertainty designation.

**Strontium: Fuel Melting 1100 – 1300°C**
The Fermi 1 accident (Section 2.2.2) provides a conflicting data point regarding strontium release. Very large strontium activity was detected in the primary sodium following the accident. As Table 2-24 shows, even assuming a 100% release percentage from the affected fuel pins, this total would amount to over 300 melted fuel pins (only 140 – 280 fuel pins actually melted during the incident). At a 10% release percentage, the number of affected fuel pins would have been over 3000. It is unclear why the strontium reading was so high, and no explanation is provided in the original reporting documents.

The EBR-II melt refining tests (Section 2.1.1.1) examined the volatilization of strontium at 1200 - 1400°C, and found essentially complete retention of the strontium. However, as is the case with other elements in the "reactive" group, the use of an oxide crucible makes the applicability of these results for metal fuel melting questionable, as the majority of the strontium reacted with the crucible.

The Hanford melt test in helium (Section 2.1.2.2) saw 0.18% of the strontium inventory volatized when at 1215°C for 25 minutes, but again, the $ZrO_2$ crucible may have resulted in the formation of oxides.

Qualitatively, no strontium release was noted followed the EBR-II experimental capsule failure (Section 2.2.3), and no strontium release was noted following the TREAT M-Series tests (Section 2.1.4).

*Summary*: The melt tests at EBR-II and Hanford appear to reinforce the assumption that strontium volatilization is very low at this temperatures in this range, which are below the boiling point of elemental Sr (1382°C). However, the use of oxide crucibles makes these results suspect. The Fermi 1 accident adds another conflicting data point, as the recorded levels of strontium are too high to be attributed solely to the melted pins. The ORNL melt tests (described in the following temperature range) appear to indicate that strontium volatility at even higher temperatures is fairly low.

Therefore, the release percentage of strontium is estimated to be up to 20% of the total inventory. This number is based largely on the bounds of the ORNL melt tests, but adjusted higher due to the Fermi 1 experience. The conflicting Fermi 1 data, coupled with the questionable applicability of the melt tests in oxide crucibles, results in a "high" uncertainty designation.

**Strontium: Very High Temperatures ≥1300°C**

The only data point at this temperature range is the melt tests performed by ORNL in air and in steam (Section 2.1.2.1). These tests found on average 1 – 2% of the strontium inventory volatized when heated to 1700 - 1800°C for a minute or less. As noted previously, some amount of oxidation likely occurred during these tests. Also, the use of a quartz ($SiO_2$) crucible may have resulted in the formation of some oxides. However, the relatively short time period of the experiment may have lessened this effect when compared to the Hanford melt test and EBR-II melt refining tests.

*Summary*: The ORNL melt tests appear to indicate a strontium release percentage below 5%. However, due to the conflicting Fermi 1 data from the previous temperature category, the release percentage is set at up to 20%. The uncertainty regarding this estimate is "high" due to the use of oxide crucibles and the lack of supporting evidence from other data sources.

### *A.6 Noble Metals*

**Ruthenium: Normal Operation 500 – 700°C**

The metal fuel PIEs (Section 2.1.5) provide the best data point for this temperature range. Many PIEs purposefully scan for ruthenium as a method of tracking fuel location, since ruthenium is essentially completely retained within the fuel matrix.

Only a single experiment of the RBCB tests at EBR-II (Section 2.1.3.2) found a very small amount of ruthenium released from the fuel pin.

*Summary*: The fact that ruthenium is purposefully tracked in metal fuel PIEs as a method to locate fuel is a strong indication the ruthenium release from the fuel matrix in this temperature range is very small.

Therefore, the minimum release percentage of up to 0.1% is assumed for ruthenium. The uncertainty level is considered "low" due to the substantial amount of metal fuel PIE using ruthenium as a fuel location indicator.

**Ruthenium: Eutectic Formation 700 – 1100°C**

During the accident at SRE (Section 2.2.1), it was calculated that approximately 0.09 – 0.2% of the ruthenium inventory of the affected fuel pins had been released.

*Summary*: The SRE incident provides another data point indicating that ruthenium release is apparently very small when below fuel melting temperatures. The eutectic melt regions may account for the liberation of some ruthenium from the fuel matrix.

Therefore, the release percentage for ruthenium is set at less than 1% of the ruthenium inventory. The uncertainty level is considered "medium," as there is no additional data to validate these findings at high burnup levels.

**Ruthenium: Fuel Melting 1100 – 1300°C**

The EBR-II melt refining tests (Section 2.1.1.1) provide meaningful data on ruthenium release, since it is a noble metal that does not interact with the oxide crucible. The testing results indicate complete retention in the fuel ingot, with no volatilization when at high temperatures for several hours.

The Hanford melt test in helium (Section 2.1.2.2) also saw very small (0.09%) volatilization of ruthenium when at 1250°C for 25 minutes.

After the Fermi 1 accident (Section 2.2.2) ruthenium was found on primary system structure, but no quantitative release fractions were calculated. Following the TREAT M-Series tests (Section 2.1.4), ruthenium was found in the sodium loop. However, ruthenium was also used as an indicator of fuel fragments in the loop. So while ruthenium was found during radiological analysis, it may have still been within a fuel fragment. Qualitatively, no ruthenium release was noted followed the EBR-II experimental capsule failure (Section 2.2.3).

*Summary*: The melt tests at EBR-II and Hanford provide clear data that ruthenium volatilization in this temperature range is very small (which is consistent with the elemental Ru melting point of 2334°C[37]). Without a quantitative measurement from the Fermi 1 accident, it is difficult to determine the amount of ruthenium that may be transported to the primary sodium through a process other than volatilization. However, the AI melt tests (discussed in the next temperature category) provide an upper bound of approximately 2% of the ruthenium inventory.

---

[37] The ruthenium melting point can be lower when in solution with uranium [68].

Therefore, the ruthenium release percentage is estimated at up to 5% of the ruthenium inventory. The uncertainty level is considered "medium" due to the lack of high burnup fuel data.

**Ruthenium: Very High Temperatures ≥1300°C**
The AI melt tests in sodium (Section 2.1.2.3) found a ruthenium release of 0.66 – 1.9% with complete fuel melting and dispersal (and some fuel vaporization).

*Summary*: As with the previous temperature category, the AI melt tests appear to provide an upper bound on the possible release amount of ruthenium in sodium.

Therefore the release percentage of ruthenium is again estimated to be up to 5% of the ruthenium inventory. The uncertainty level is again considered "medium" due to the lack of high burnup data and the lack of experimental melt testing with a prototypic fuel element (the AI melt test used a non-sodium bonded fuel disc).

### *A.7 Lanthanides*

**Lanthanides[38]: Normal Operation 500 – 700°C**

The behavior of lanthanides in metal fuel is extremely complex, and many studies have been performed attempting to understand the phenomena related to their movement, as their interaction with the cladding can cause degradation. Significant metal fuel PIE (Section 2.1.5) has been conducted regarding the migration of lanthanides in metal fuel during irradiation. There are far too many studies to review all the pertinent findings here. Refs [25], [28], [60], and [61] provide more detail on the migration of lanthanides and current efforts to create metal fuel compositions that limit their mobility. The most pertinent finding for the study here is that the lanthanides exhibit liquid-like transport within the fuel matrix [60], and generally migrate to the periphery of the fuel pin (as shown in the PIE in Section 2.1.5.2). Figure 2–6 shows how La, Pr, Nd, and Sm all migrate into the cladding structure, while Zr concentrates at the center and edges of the fuel matrix.

Other than metal fuel PIE, the only other data point in this temperature range are the RBCB tests at EBR-II (Section 2.1.3.2), which saw Nd, Zr, and Eu released from the fuel pins.

*Summary*: The lanthanides appear to be very mobile within the fuel matrix. Other than europium[39], which is an outlier of lanthanide behavior, the solubility of lanthanides in sodium is believed to be low [60]. Coupled with the fact that lanthanide interaction with the cladding has been seen in numerous experiments, the data implies that lanthanide release to the bond sodium should be small.

Due to the lack of quantitative lanthanide release information, the release percentage is estimated to be up to 1% of the inventory. The uncertainty level is considered "medium," as there is substantial data related to lanthanide movement, but the focus has generally been on cladding integrity, not lanthanide release.

**Lanthanides: Eutectic Formation 700 – 1100°C**

During the accident at SRE (Section 2.2.1), it was calculated that approximately 0.18 – 0.4% of the Zr/Nb inventory of the affected fuel pins had been released.

*Summary*: The SRE accident appears to confirm the findings of the RBCB tests at EBR-II, where Zr was also found released from the failed fuel pins. It is difficult to assess how the low burnup of the SRE fuel affected the release of Zr/Nb. With higher burnup, more of the Zr inventory may have migrated, but lanthanide interaction with the cladding may have increased, resulting in less mobile lanthanides.

Therefore, a likely conservative release percentage of up to 1% of the lanthanide inventory is assigned. Even though lanthanide solubility in sodium is generally low, the SRE data does indicate that some Zr/Nb can escape the fuel matrix. The uncertainty is considered "high" due to the lack of available data and general lack of understanding regarding the availability of the lanthanides to be liberated from the fuel matrix/cladding.

**Lanthanides: Fuel Melting 1100 – 1300°C**

The EBR-II melt refining tests (Section 2.1.1.1) examined the release of La, Y, Eu, and Nd during melt refining. However, the lanthanides are quick to form oxides with the crucible, limiting the applicable insight from these experiments.

After the Fermi 1 accident (Section 2.2.2), Zr/Nb was found but no quantitative release fractions were calculated. Following the TREAT M-Series tests (Section 2.1.4), Zr, Nb, Pr, and Eu were found in the

---

[38] The elemental symbols (Xx) are used in this section for brevity.

[39] Europium release should be approximated with the cesium release fractions, as similar behavior has been seen, and detailed europium analysis is not available.

sodium loop. Qualitatively, no lanthanide release was noted followed the EBR-II experimental capsule failure (Section 2.2.3).

*Summary*: The Fermi 1 and TREAT tests are in agreement with the RBCB tests and SRE accident in that some release of the lanthanides is possible. However, there is no reliable quantitative data regarding lanthanide release in this temperature range. Fortunately, the AI melt tests in the following temperature category tracked Zr/Nb release. As will be seen, 10 – 24% releases were seen for Zr/Nb in that experiment.

Lacking further quantitative data, the AI melt test information is used to bound this temperature category. A release percentage of up to 30% is estimated, with a "high" uncertainty rating.

**Lanthanides: Very High Temperatures ≥1300°C**
The AI melt tests in sodium (Section 2.1.2.3) found a Zr/Nb release of 10 – 24% with complete fuel melting and dispersal (and some fuel vaporization).

*Summary*: The AI melt tests offer valuable quantitative insight into lanthanide release in this temperature range. A release percentage of up to 30% is estimated based on these findings. This release percentage is likely very conservative for many of the lanthanides, but without additional data, it is difficult to justify lower release fractions. The uncertainty level is again determined to be "high," since data is only available for Zr/Nb.

### *A.6 Cerium Group and Uranium*

**Cerium: Normal Operation 500 – 700°C**

The metal fuel PIEs (Section 2.1.5) provide the best data point for this temperature range. The FFTF PIEs show very little of the cerium escapes the fuel matrix, but extensive cerium axial migration within the fuel matrix occurs with increasing burnup. The axial scans also appear to show that very little cerium is present in the plenum regions and therefore in the bond sodium. The EBR-II PIEs show that cerium migrates and interacts with the cladding (as shown in Figure 2–6 and Figure 2–7).

Cerium release was noted in two of the RBCB tests at EBR-II (Section 2.1.3.2), and was also found in the primary sodium during DFR operation with vented fuel (Section 2.3).

*Summary*: As with the discussion of lanthanides in this temperature range, the behavior of cerium is complex. Cerium appears to be mobile in the fuel matrix (radially and axially), and can relocate to the fuel/clad interface, but the exact mechanism of mobility is not yet known [30]. Cerium is very insoluble in sodium [62], which should limit its migration to the bond sodium. This is consistent with FFTF PIEs, which show very little cerium in the plenum regions. However, the presence of cerium at DFR and the RBCB tests indicates that some amount of cerium can be released in this temperature range.

Therefore, absent more detailed information, the cerium release percentage is set at up to 1% of the inventory. There is a probable dependence on burnup level (and cerium migration), but the exact extent is unclear. The uncertainty level is "medium," as the FFTF PIEs appear to show that there is very little cerium in the plenum sodium, but release were observed at EBR-II and DFR.

**Cerium: Eutectic Formation 700 – 1100°C**

During the accident at SRE (Section 2.2.1), it was calculated that approximately 0.22 – 0.7% of the cerium inventory of the affected fuel pins had been released.

*Summary*: The fact that cerium was released from the damaged fuel pins at SRE (although in a small amount) is consistent with evidence from DFR and the RBCB tests, and the FFTF PIE. If cerium has migrated to the fuel/clad interface, eutectic melting in this temperature range may increase the release fraction.

Therefore, the cerium release percentage is estimated to be up to 5% (up to 1% from the bond sodium, with additional cerium liberated from eutectic melting of the cladding region). The uncertainty is considered "high," as it is unclear whether releases would be greater with high burnup fuel, as there may be a larger quantity of cerium in the cladding, where eutectic melting may occur.

**Cerium: Fuel Melting 1100 – 1300°C**

The EBR-II melt refining tests (Section 2.1.1.1) saw very little cerium volatilization at 1200°C, but cerium interacts with the oxide crucible, which limits the applicability of these results.

After the Fermi 1 accident (Section 2.2.2) cerium was found on primary system structure, but no quantitative release fractions were calculated. Similarly, following the TREAT M-Series tests (Section 2.1.4), cerium was found in the test loop. No cerium release was noted followed the EBR-II experimental capsule failure (Section 2.2.3).

*Summary*: Testing appears to show that cerium volatilization is very unlikely in this temperature range, which is consistent with the elemental Ce boiling point (3443°C). However, with higher burnup, there is likely to be significant cerium concentration in the cladding. If melting occurs in the region, it may liberate the cerium. This behavior would be consistent with Fermi 1 and TREAT, where cerium releases were seen with fuel melting.

Determining a release percentage for this temperature range is difficult. It does not appear that a significant amount of cerium is released (as it was not a primary radioactive source following the Fermi 1 accident), but it is challenging to bound the release percentage. At high burnup, there is likely a significant fraction of cerium in the cladding, but it is unclear what would happen to the cerium if the cladding were to melt. Therefore, a release percentage of up to 10% is estimated, but with "high" uncertainty. The dependence on burnup remains, as this will dictate the migration of cerium.

**Cerium: Very High Temperatures ≥1300°C**

The ORNL melt tests in sodium (Section 2.1.2.1) found a cerium release of 0.004 – 0.3% when at 1700 – 1800°C for less than a minute in air and in steam, but in an oxide crucible.

*Summary*: Although the ORNL melt tests were performed in an oxide crucible, the short timeframe may have limited cerium oxide formation, meaning some insights may still be valid. It appears that cerium volatilization, even at this temperature range, is small. This is consistent with its very high elemental boiling point (3443°C). This likely implies that the release of cerium is dominated by the mechanisms discussed in the preceding temperature ranges: migration to the bond sodium, and liberation from melted cladding.

Determining an appropriate cerium release percentage in this temperature range continues to be difficult. Volatilization is likely small, but that does not guarantee that the overall cerium release will be small. Therefore, a release percentage of up to 15% is estimated, but with "high" uncertainty. The dependence on burnup remains, as this will dictate the migration of cerium to the cladding, where melting *may* result in increased cerium release.

**Uranium and Plutonium[40]: Normal Operation 500 – 700°C**
The metal fuel PIEs (Section 2.1.5) show very little fuel migration to the bond sodium (through the tracking of ruthenium).

Very small amounts of uranium and plutonium were released during the RBCB tests at EBR-II (Section 2.1.3.2).

*Summary*: One of the advantages of metal fuel is the known compatibility between the bond sodium and the metallic uranium. The solubility of uranium and plutonium in sodium is apparently very small [63] [64], and testing has demonstrated that plutonium dissolution in the sodium bond of the fuel pin should be less than 0.1% over the lifetime of the fuel pin [65]. The very small amounts of uranium and plutonium detected at the RBCB tests appear to confirm these results.

Therefore, the release percentage of uranium and plutonium at this temperature range is set up to 0.1% of the inventory (which is likely conservative, but is the minimum fraction for the current work), with a dependence on burnup, as longer pin lifetime may allow greater dissolution into the sodium bond. The uncertainty is considered "low," as there is significant experience with sodium-bonded metal fuel, and uranium/plutonium release to the sodium has not been an issue.

**Uranium and Plutonium: Eutectic Formation 700 – 1100°C**
No uranium release was noted following the accident at SRE (Section 2.2.1).

*Summary*: It is unlikely that the release of uranium or plutonium will increase in this temperature range, as melting will only occur in eutectic regions. Also, the following temperature ranges will show that uranium/plutonium releases at higher temperatures is small, which bound the estimate for this temperature range.

Therefore, the release percentage is maintained at up to 0.1%, with a dependence on burnup. The uncertainty level is considered "medium," as there is limited data regarding potential uranium/plutonium release with high burnup fuel in this temperature range.

**Uranium and Plutonium: Fuel Melting 1100 – 1300°C**
Melt refining reprocessing at the FCF at EBR-II (Section 2.1.1) was based on the principle that uranium would not volatize in this temperature range (up to 1400°C) or react with the oxide crucible in appreciable quantities (plutonium interacted with the crucible in greater quantities) [66].

During the Fermi 1 accident (Section 2.2.2) fuel melted and slumped within the fuel assembly. There is no indication that fuel was transported beyond the fuel assembly. Uranium and plutonium were noted in the test loop following the TREAT M-Series tests (Section 2.1.4), likely as pieces of fuel that were extruded through the cladding failure. It is estimated that up to 50% of the fuel was released from the fuel pin, and were found as fragments throughout the test loop. The EBR-II experimental capsule failure (Section 2.2.3) saw fuel relocation, but no transport of uranium or fuel material within the primary system was noted.

*Summary*: It appears that essentially no uranium or plutonium volatizes in this temperature range, and the transport of uranium or plutonium within the primary system would only be due to fuel fragment transport, not dissolution. Therefore, it is unlikely that additional uranium and plutonium would be in solute in the sodium. The release fraction remains up to 0.1%, with a dependence on burnup. The uncertainty level is considered "medium," as there are not quantitative measurements from Fermi 1, TREAT, or the EBR-II capsule regarding the dissolution of uranium/plutonium.

---

[40] The focus of this section is on uranium/plutonium dissolution into sodium, rather than fuel fragment relocation.

**Uranium and Plutonium: Very High Temperatures ≥1300°C**
The AI melt tests in sodium (Section 2.1.2.3) saw the fuel material reduced to very small fragments (on the order of 100 microns) with some fuel vaporization at temperatures up to 3600°C. Fuel temperatures in this range are highly unlikely for most SFR accidents.

*Summary*: The AI tests demonstrate that even with very high fuel temperatures and some fuel vaporization, uranium and plutonium dissolution in sodium is small, as fuel remains in fragments. Therefore the 0.1% release percentage is continued, with a dependence on fuel burnup level at the start of the accident. The uncertainty level is again considered "medium," as the AI melt tests are the only data point, and this tests did not use a sodium-bonded metal fuel pin.

# Appendix B: Literature Review Information Tables

The following tables summarize the documents reviewed as part of the literature search. The documents listed here contain data or information which were part of the quantitative or qualitative data sources used to determine the radionuclide release fractions in Section 4.1. The tables contain document titles and type, along with details on the type of fuel investigated and burnup levels. Any known access limitations related to the document, such as the DOE Applied Technology designation, are also listed. Lastly, if a quality assurance (QA) protocol was followed for the experiment, it is also noted. However, for many older experiments, it is unknown if a specific QA protocol was used, as typically no information regarding the topic was recorded.

**EBR-II Melt Refining Reprocessing and Experiments**[41]

| Document Number | Reference Number and Document Title[1] | Document Type | Date | Location/Facility/Test | Fuel Type of Interest | Fuel Burnup | Access Status | QA |
|---|---|---|---|---|---|---|---|---|
| N/A | [11] Private communication with Mark Williamson[2] | Communication | 2015 | FCF – Argonne West | Various | ~1.0% | Unlimited | Unknown |
| N/A | [7] The Melt Refining of Irradiated Uranium: Application to EBR-II Fast Reactor Fuel. XII. The Behavior of Ruthenium, Molybdenum, Palladium, Rhodium, Technetium, Antimony, Cadmium, and Tellurium | Journal Article | 1/1961 | Argonne West | Uranium Metal<br>U-Zr<br>U-Fs | Various | Unlimited | Unknown |
| N/A | The Melt Refining of Irradiated Uranium: Application to EBR-II Fast Reactor Fuel. VII. The Evolution of Xenon and Krypton | Journal Article | 1/1961 | Argonne West | Uranium Metal<br>U-Fs | Various | Unlimited | Unknown |
| N/A | The Melt Refining of Irradiated Uranium: Application to EBR-II Fast Reactor Fuel. VI. The Behavior of Plutonium in the Melt-Refining Process | Journal Article | 1/1961 | Argonne West | U-Pu<br>U-Pu-Fs | Various | Unlimited | Unknown |
| N/A | [4] The Melt Refining of Irradiated Uranium: Application to EBR-II Fast Reactor Fuel. XI. Behavior of Iodine in Melt Refining | Journal Article | 1/1961 | Argonne West | U-Fs | Various | Unlimited | Unknown |
| N/A | [6] The Melt Refining of Irradiated Uranium: Application to EBR-II Fast Reactor Fuel. VIII. The Behavior of Rare Earths, Yttrium, Barium, Strontium, and Cesium | Journal Article | 1/1961 | Argonne West | Uranium Metal<br>U-Zr<br>U-Fs | Various | Unlimited | Unknown |
| ANL-6815 (TID-4500) | [5] Laboratory Studies of Iodine Behavior in the EBR-II Melt Refining Process | Report – Argonne | 1/1964 | Argonne West | Uranium Metal<br>U-Zr<br>U-Fs | Various | Unlimited | Unknown |

[1]Not all documents were directly referenced within the body of the current work.
[2]A document summarizing FCF experience could not be found, but is currently being investigated.

[41]The journal articles listed in the table contain summaries of the melt refining experimental results, in addition to project conclusions. The journal articles cite numerous Argonne reports (ANL-5000 series) that contain the original experimental data. Also, the ANL-6000 series reports contain additional information related to melt refining testing and operation of the FCF.

## Fuel Melt Experiments

| Document Number | Reference Number and Document Title | Document Type | Date | Location/Facility/Test | Fuel Type of Interest | Fuel Burnup | Access Status | QA |
|---|---|---|---|---|---|---|---|---|
| N/A | [8] Chemical Considerations in Fast Reactor Safety | Conference Article | 10/1965 | BNL | U-3.5Mo | Various | Unlimited | Unknown |
| N/A | [9] Vaporization of Fission Products from Irradiated Uranium - II | Journal Article | 5/1969 | BNL | U-3.5Mo | Various | Unlimited | Unknown |
| ORNL-3981 | [12] Out-of-Pile Studies of Fission-Product Release from Overheated Reactor Fuels at ORNL, 1955-1965 | Report – ORNL | 7/1967 | ORNL | Uranium Metal | 0.1% | Unlimited | Unknown |
| ORNL-2616 (TID-4500) | [13] Experiments on the Release of Fission Products from Molten Reactor Fuels | Report – ORNL | 12/1959 | ORNL | U-Zr | 15% | Unlimited | Unknown |
| HW-60689 | [14] Fission Product Release from Uranium Heated in Air | Report – Hanford | 12/1960 | Hanford | Uranium Metal | $2.4\times10^{14}$ n/cm$^2$ | Unlimited | Unknown |
| NAA-SR-11766 | [15] Fission Product Retention in Sodium - A Summary of Analytical and Experimental Studies at Atomics International | Report – AI | 12/1966 | KEWB Pulsed Reactor – Santa Susana Field Laboratory | Uranium Metal | Irradiated (unknown) | Unlimited | Unknown |
| NAA-SR-9287 | [16] High-Temperature Experiments on Fission Product Retention in Sodium | Report – AI | 2/1965 | KEWB Pulsed Reactor – Santa Susana Field Laboratory | Uranium Metal | Irradiated (unknown) | Unlimited | Unknown |

## Cladding Breach Experiments at EBR-II

| Document Number | Reference Number and Document Title | Document Type | Date | Location/Facility/Test | Fuel Type of Interest | Fuel Burnup | Access Status | QA |
|---|---|---|---|---|---|---|---|---|
| ANL-7782 | [18] Experimental Irradiation of Fuel Elements Having Known Cladding Defects in EBR-II | Report - Argonne | 12/1971 | EBR-II – Argonne West | U-5Fs | 0.55 – 1.52% | Unlimited | Unknown |
| ANL/FF/PP--68403 | [20] Current Status of the Run-Beyond-Cladding-Breach (RBCB) Tests | Report – Argonne (additional data in Argonne Applied Technology document) | 9/1993 | EBR-II – Argonne West | U-5Fs<br>U-19Pu-10Zr<br>U-8Pu-10Zr | 6.0 – 14.4% | Unlimited | Unknown |

**TREAT M-Series**

| Document Number | Reference Number and Document Title[1] | Document Type | Date | Location/Facility/Test | Fuel Type of Interest | Fuel Burnup | Access Status[2] | QA |
|---|---|---|---|---|---|---|---|---|
| TREAT – 1 | | Argonne | 04/30/1985 | Argonne/TREAT/Mark-IIIC Loop (Serial# 010, 011)/M2 and M3 Experiments | U-5Fs | 4.4%<br>7.9% | AT | Unknown |
| TREAT – 2 | | Argonne | 03/04/1986 | Argonne/TREAT/Mark-IIIC Loop (Serial# 010)/M2 Experiment | U-5Fs | 4.4%<br>7.9% | AT | Unknown |
| TREAT – 3 | | Argonne | 03/04/1986 | Argonne/TREAT/Mark-IIIC Loop (Serial# 011)/M4 Experiment | U-5Fs | 2.4% | AT | Unknown |
| TREAT – 4 | | Argonne | 06/18/1987 | Argonne/TREAT/Mark-IIIC Loop (Serial# 010, 011)/M2, M4, M6 Experiments | U-5Fs<br>U-19Pu-10Zr | 2.4%<br>5.3% | AT | Unknown |
| TREAT – 5 | | Argonne | 07/01/1987 | Argonne/TREAT/Mark-IIIC Loop (Serial# 010)/M6 Experiment | U-19Pu-10Zr | 5.3% | AT | Unknown |
| TREAT – 6 | | Argonne | 11/12/1987 | Argonne/TREAT/Mark-IIIC Loop (Serial# 010)/M7 Experiment | U-19Pu-10Zr | 9.8% | AT | Unknown |
| TREAT – 7 | | Argonne | 12/17/1987 | Argonne/TREAT/Mark-IIIC Loop (Serial# 010)/M7 Experiment | U-19Pu-10Zr | 9.8% | AT | Unknown |
| TREAT – 8 | | Argonne | 06/1985 | Argonne/TREAT/HFEF/ Mark-IIIC Loop (Serial# 010)/M2 Experiment | U-5Fs | 4.4%<br>7.9% | AT | Unknown |
| TREAT – 9 | | Argonne | 01/1986 | Argonne/TREAT/HFEF/ Mark-IIIC Loop (Serial# 011)/M4 Experiment | U-5Fs | 2.4% | AT | Unknown |
| TREAT – 10 | | Argonne | 02/1987 | Argonne/TREAT/HFEF/ Mark-IIIC Loop (Serial# 010)/M6 Experiment | U-19Pu-10Zr | 5.3% | AT | Unknown |
| TREAT – 11 | | Argonne | 09/1988 | Argonne/TREAT/HFEF/ Mark-IIIC Loop (Serial# 010)/M7 Experiment | U-19Pu-10Zr | 9.8% | AT | Unknown |

[1]Due to Applied Technology restrictions, only the limited information presented here can be listed. The numbering of the TREAT documents is a placeholder created as part of the current effort.
[2]AT – Applied Technology

**Metal Fuel Post-Irradiation Examination**[42]

| Document Number | Reference Number and Document Title | Document Type | Date | Location/Facility/Test | Fuel Type of Interest | Fuel Burnup | Access Status | QA |
|---|---|---|---|---|---|---|---|---|
| ANL-7388 (TID-4500) | [22] The Irradition Behavior of High-Burnup Uranium Plutonium Alloy Prototype Fuel Elements | Report – Argonne | 12/1969 | EBR-II – Argonne West | U-Fs<br>U-Pu-Fs<br>U-Pu-Zr | 2.7 – 12.5% | Unlimited | Unknown |
| N/A | [23] Steady-State Irradiation Testing of U-Pu-Zr Fuel to >18% Burnup | Conference Paper | 8/1990 | EBR-II – Argonne West | U-10Zr<br>U-8Pu-10Zr<br>U-19Pu-10Zr | ~1 – 18.4% | Unlimited | Unknown |
| N/A | [26] Summary of Iodine Partitioning in EBR-II Fuel | Inter-Lab Memo | 2016 | INL | U-19Pu-10Zr | 11.5% | Internal | QRL3 |
| N/A | [27] Performance of HT9 Clad Metallic Fuel at High Temperatures | Conference Paper (Similar information in Argonne Applied Technology document) | 11/1992 | EBR-II – Argonne West | U-10Zr | ~10% | Unlimited | Unknown |
| N/A | [30] Full-Length U-xPu-10Zr (x=0, 8, 19 wt.%) Fast Reactor Fuel in FFTF | Journal Article | 2012 | Irradiation: FFTF – Hanford<br>PIE: INL | U-10Zr<br>U-8Pu-10Zr<br>U-19Pu-10Zr | ~7 – 10% | Unlimited | Unknown |
| N/A | [31] Irradiation of Minor Actinide-Bearing Uranium-Plutonium-Zirconium Alloys up to ~2.5 at %, ~7 at %, and ~10 at % Burnup | Journal Article | 2015 | Irradiation: Phénix - France<br>PIE: CRIEPI - Japan | U-19Pu-10Zr (some with minor actinide and rare earth additions) | 2, 5, 8% | Unlimited | Unknown |
| N/A | [32] Low-Burnup Irradiation Behavior of Fast Reactor Metal Fuels Containing Minor Actinides | Journal Article | 2009 | Irradiation: Phénix - France<br>PIE: CRIEPI - Japan | U-19Pu-10Zr (some with minor actinide and rare earth additions) | ~2% | Unlimited | Unknown |
| INL/EXT-05-00785 | [67] AFC-1 Transmutation Fuel Post-Irradiation Hot Cell Examination 4 to 8 at.% Final Report[1] | Report – INL | 2006 | Irradiation: ATR – INL<br>PIE: INL | Various (see Table 2-22) | Various (see Table 2-22) | Unlimited | |

[1]There are many additional AFC series documents available, with varying access limitations.

42 There are many individual EBR-II PIE documents, which are not listed here. Argonne is currently developing an "EBR-II Fuels Irradiation and Physics Database," which contains documentation (including PIE) on many of the EBR-II experiments. For additional information regarding the database, contact Adbellatif Yacout (yacout@anl.gov).

### SRE Accident

| Document Number | Reference Number and Document Title | Document Type | Date | Location/Facility/Test | Fuel Type of Interest | Fuel Burnup | Access Status | QA |
|---|---|---|---|---|---|---|---|---|
| NAA-SR-4488 | [38] SRE Fuel Element Damage – Final Report | Report – Atomics International | 11/1959 | SRE – Santa Susana Field Laboratory | Uranium Metal, Various Uranium Alloys | ~0.1% | Unlimited | Unknown |
| NAA-SR-6890 | [39] Distribution of Fission Product Contamination in the SRE | Report – Atomics International | 3/1962 | SRE – Santa Susana Field Laboratory | Uranium Metal, Various Uranium Alloys | ~0.1% | Unlimited | Unknown |

### Fermi 1 Accident

| Document Number | Reference Number and Document Title | Document Type | Date | Location/Facility/Test | Fuel Type of Interest | Fuel Burnup | Access Status | QA |
|---|---|---|---|---|---|---|---|---|
| APDA-233 | [40] Report on the Fuel Melting Incident in the Enrico Fermi Atomic Power Plant on October 5, 1966 | Report – Atomic Power Development Associates | 12/1968 | Fermi 1 – Enrico Fermi Nuclear Generating Station | U-10Mo | <0.05% | Unlimited | Unknown |
| APDA-LA-2 | [41] Subassembly Thermocouple Analysis for the Fuel Melting Incident in the Enrico Fermi Reactor | Report – Atomic Power Development Associates | 7/1969 | Fermi 1 – Enrico Fermi Nuclear Generating Station | U-10Mo | <0.05% | Unlimited | Unknown |
| APDA-LA-5 | [42] Thermal-Hydraulic Analysis of the October 5, 1966 Fuel Melting Incident in the Enrico Fermi Reactor | Report – Atomic Power Development Associates | 7/1969 | Fermi 1 – Enrico Fermi Nuclear Generating Station | U-10Mo | <0.05% | Unlimited | Unknown |
| N/A | [43] Results of the Fission-Product Activity Analysis to Determine the Extent of Fuel Failure in Fermi Accident | Journal Article | 11/1967 | Fermi 1 – Enrico Fermi Nuclear Generating Station | U-10Mo | <0.05% | Unlimited | Unknown |

### EBR-II Experiment Capsule Failure

| Document Number | Reference Number and Document Title | Document Type | Date | Location/Facility/Test | Fuel Type of Interest | Fuel Burnup | Access Status | QA |
|---|---|---|---|---|---|---|---|---|
| N/A | [44] Fission-Product Release from an Encapsulated U- Pu-Zr Ternary Alloy | Journal Article | 6/1969 | EBR-II – Argonne West | U-15Pu-10Zr | ~0% | Unlimited | Unknown |
| ANL-7604 | [45] Origin of Fission-Product Release in EBR-II November 23, 1967, to May 6, 1968 | Report - Argonne | 12/1970 | EBR-II – Argonne West | U-15Pu-10Zr | ~0% | Unlimited | Unknown |

## Other Sources

| Document Number | Reference Number and Document Title | Document Type | Date | Location/Facility/Test | Fuel Type of Interest | Fuel Burnup | Access Status | QA |
|---|---|---|---|---|---|---|---|---|
| A/CONF.28/P/130 | [49] Performance and Operation of the Dounreay Fast Reactor | Conference Article | 5/1964 | DFR – Dounreay Nuclear Power Development Establishment UK | U-9Mo | Various | Unlimited | Unknown |

# Appendix C: Chemistry Modeling Details

## C.1 Model Scenarios: Simulated Fuel Compositions

Scenario 1:

This modeling scenario was performed to elucidate how basic assumptions influence the speciation predicted by the model. It was defined as a simple ternary system consisting of 0.3 moles sodium, 0.02 moles cesium and 0.002 moles iodine and was run from 400°C to 2000°C in 100 steps at a constant pressure of 1 bar. The moles of each element were based on the fuel composition from the ALMR source term study shown in Table C-1. The two cases run for scenario 1 were as follows:

- *Case 1a*: assumes all solids and liquids (melts) are pure phases.
- *Case 1b*: assumes a single melt phase that behaves as an ideal mixture.

Scenario 2

This scenario involved a simplified metal fuel composition that was run from 400°C to 2000°C in 100 steps at a constant pressure of 1 bar. The fuel composition (Table C-1) is from the ALMR mechanistic source term study [53]. Only a single modeling case was run with this composition.

- *Case 2a*: assumes all solids and liquids (melts) are pure phases.

Scenario 3:

This scenario involved a metal fuel composition representing a Fermi 1 pin with a burn-up of 0.48 MWd/kg and was run from 400°C to 2000°C in 100 steps at a constant pressure of 1 bar. The fuel composition was calculated using ORIGEN2. The ORIGEN2 input parameters are listed in Table C-2 and the resulting fuel composition is shown in Table C-3. Two cases were run for this composition:

- *Case 3a*: assumes pure phase solids and liquids, no sodium present in the fuel.
- *Case 3b*: assumes pure phase solids and liquids, sodium is present in the fuel.

**Table C-1. Composition of Fuel used for Preliminary Thermodynamic Speciation Calculations**[43]

| *Element* | *Moles* | *Moles per gram of fuel* |
|---|---|---|
| *Ar* | *2.3E-03* | *6.3E-06* |
| *Kr* | *1.9E-03* | *5.2E-06* |
| *Xe* | *2.2E-02* | *6.1E-05* |
| $I_2$ | *1.8E-03* | *5.1E-06* |
| $Br_2$ | *1.0E-04* | *2.9E-07* |
| *Rb* | *1.6E-03* | *4.3E-06* |
| *Cs* | *1.9E-02* | *5.1E-05* |
| *Te* | *3.2E-03* | *8.9E-06* |
| *Sb* | *3.6E-04* | *1.0E-06* |
| *Se* | *3.2E-04* | *8.9E-07* |
| *Ba* | *6.4E-03* | *1.8E-05* |
| *Sr* | *3.6E-03* | *1.0E-05* |
| *Ru* | *2.0E-02* | *5.6E-05* |
| *Mo* | *2.0E-02* | *5.6E-05* |
| *La* | *5.4E-03* | *1.5E-05* |
| *Ce* | *1.1E-02* | *3.0E-05* |
| *Eu* | *5.5E-04* | *1.5E-06* |
| *Y* | *1.9E-03* | *5.2E-06* |
| *Zr* | *1.8E-02* | *5.06E-05* |
| *Pu* | *2.4E-01* | *6.6E-04* |
| *U* | *1.1* | *3.1E-03* |

**Table C-2: ORIGEN2 Inputs for Fermi 1 Fuel Composition used for Model Scenario 3**

| *Code: ORIGEN2 with the FFTF libraries*<br>*Fuel: U-10wt% Mo fuel (Zr clad)* | |
|---|---|
| *Number of fuel assemblies* | *105* |
| *Mass U-235/assembly (kg)* | *4.75* |
| *Fraction U-235* | *0.256* |
| *Mass U/subassembly (kg)* | *18.6* |
| *Number of pins per assembly* | *140* |
| *Mass U/pin (g)* | *132.53* |
| *Total Burn up (MWd/kg)* | *0.48* |
| *Cumulative (MWd)* | *942* |
| *Mass fissioned (g)* | *993* |
| *Mass fissioned (%)* | *0.052* |
| *Maximum Specific power density (W/g)* | *15.91* |

43 This composition was used for the ALMR source term study [53].

**Table C-3: ORIGEN2 Results Shown as Moles of Element within a Single Fuel Pin[44]**

| Element (moles/pin) | Charged | No cooling | 1.0 second | 1.0 minute | 1.0 hour | 12.0 hours | 1.0 day | 30.0 days | 1.0 year | 5.0 years | 20.0 years | 50.0 years |
|---|---|---|---|---|---|---|---|---|---|---|---|---|
| U | 5.6E-01 | 5.6E-01 | 5.6E-01 | 5.6E-01 | 5.6E-01 | 5.6E-01 | 5.6E-01 | 5.6E-01 | 5.6E-01 | 5.6E-01 | 5.6E-01 | 5.6E-01 |
| Pu | 0.0E+00 | 1.3E-04 | 1.3E-04 | 1.3E-04 | 1.3E-04 | 1.3E-04 | 1.3E-04 | 1.3E-04 | 1.3E-04 | 1.3E-04 | 1.3E-04 | 1.3E-04 |
| Zr | 0.0E+00 | 8.3E-05 | 8.3E-05 | 8.3E-05 | 8.3E-05 | 8.3E-05 | 8.3E-05 | 8.3E-05 | 8.3E-05 | 8.4E-05 | 8.8E-05 | 9.3E-05 |
| Mo | 0.0E+00 | 6.3E-05 | 6.3E-05 | 6.3E-05 | 6.3E-05 | 6.3E-05 | 6.3E-05 | 6.4E-05 | 6.8E-05 | 6.8E-05 | 6.8E-05 | 6.8E-05 |
| Xe | 0.0E+00 | 6.2E-05 | 6.2E-05 | 6.2E-05 | 6.2E-05 | 6.2E-05 | 6.2E-05 | 6.2E-05 | 6.2E-05 | 6.2E-05 | 6.2E-05 | 6.2E-05 |
| Cs | 0.0E+00 | 5.2E-05 | 5.2E-05 | 5.2E-05 | 5.2E-05 | 5.2E-05 | 5.2E-05 | 5.2E-05 | 5.2E-05 | 5.1E-05 | 4.6E-05 | 4.1E-05 |
| Nd | 0.0E+00 | 4.7E-05 | 4.7E-05 | 4.7E-05 | 4.7E-05 | 4.7E-05 | 4.7E-05 | 4.8E-05 | 5.2E-05 | 5.6E-05 | 5.6E-05 | 5.6E-05 |
| Ce | 0.0E+00 | 4.1E-05 | 4.1E-05 | 4.1E-05 | 4.1E-05 | 4.1E-05 | 4.1E-05 | 4.0E-05 | 3.5E-05 | 3.2E-05 | 3.2E-05 | 3.2E-05 |
| Ru | 0.0E+00 | 3.8E-05 | 3.8E-05 | 3.8E-05 | 3.8E-05 | 3.8E-05 | 3.8E-05 | 3.7E-05 | 3.6E-05 | 3.6E-05 | 3.6E-05 | 3.6E-05 |
| Sr | 0.0E+00 | 2.6E-05 | 2.6E-05 | 2.6E-05 | 2.6E-05 | 2.6E-05 | 2.6E-05 | 2.5E-05 | 2.4E-05 | 2.3E-05 | 1.9E-05 | 1.4E-05 |
| Ba | 0.0E+00 | 1.9E-05 | 1.9E-05 | 1.9E-05 | 1.9E-05 | 1.9E-05 | 1.8E-05 | 1.8E-05 | 1.9E-05 | 2.0E-05 | 2.5E-05 | 3.0E-05 |
| La | 0.0E+00 | 1.8E-05 | 1.8E-05 | 1.8E-05 | 1.8E-05 | 1.8E-05 | 1.8E-05 | 1.8E-05 | 1.8E-05 | 1.8E-05 | 1.8E-05 | 1.8E-05 |
| Tc | 0.0E+00 | 1.6E-05 | 1.6E-05 | 1.6E-05 | 1.6E-05 | 1.6E-05 | 1.6E-05 | 1.6E-05 | 1.6E-05 | 1.6E-05 | 1.6E-05 | 1.6E-05 |
| Pr | 0.0E+00 | 1.6E-05 | 1.6E-05 | 1.6E-05 | 1.6E-05 | 1.6E-05 | 1.6E-05 | 1.6E-05 | 1.6E-05 | 1.6E-05 | 1.6E-05 | 1.6E-05 |
| Y | 0.0E+00 | 1.3E-05 | 1.3E-05 | 1.3E-05 | 1.3E-05 | 1.3E-05 | 1.3E-05 | 1.3E-05 | 1.2E-05 | 1.2E-05 | 1.2E-05 | 1.2E-05 |
| Kr | 0.0E+00 | 1.1E-05 | 1.1E-05 | 1.1E-05 | 1.1E-05 | 1.1E-05 | 1.1E-05 | 1.1E-05 | 1.1E-05 | 1.0E-05 | 1.0E-05 | 1.0E-05 |
| Rb | 0.0E+00 | 9.6E-06 | 9.6E-06 | 9.6E-06 | 9.6E-06 | 9.6E-06 | 9.6E-06 | 9.6E-06 | 9.7E-06 | 9.8E-06 | 1.0E-05 | 1.0E-05 |
| Rh | 0.0E+00 | 9.1E-06 | 9.1E-06 | 9.1E-06 | 9.1E-06 | 9.1E-06 | 9.1E-06 | 9.4E-06 | 9.8E-06 | 9.8E-06 | 9.8E-06 | 9.8E-06 |
| Te | 0.0E+00 | 8.1E-06 | 8.1E-06 | 8.1E-06 | 8.1E-06 | 8.1E-06 | 8.1E-06 | 8.1E-06 | 8.1E-06 | 8.3E-06 | 8.5E-06 | 8.5E-06 |
| Pd | 0.0E+00 | 7.6E-06 | 7.6E-06 | 7.6E-06 | 7.7E-06 | 7.7E-06 | 7.7E-06 | 7.7E-06 | 8.4E-06 | 9.1E-06 | 9.1E-06 | 9.1E-06 |
| Sm | 0.0E+00 | 6.7E-06 | 6.7E-06 | 6.7E-06 | 6.7E-06 | 6.7E-06 | 6.7E-06 | 6.8E-06 | 8.0E-06 | 1.1E-05 | 1.2E-05 | 1.2E-05 |
| Pm | 0.0E+00 | 5.5E-06 | 5.5E-06 | 5.5E-06 | 5.5E-06 | 5.5E-06 | 5.5E-06 | 5.4E-06 | 4.3E-06 | 1.5E-06 | 2.8E-08 | 1.0E-11 |
| I | 0.0E+00 | 4.5E-06 | 4.5E-06 | 4.5E-06 | 4.5E-06 | 4.5E-06 | 4.5E-06 | 4.5E-06 | 4.5E-06 | 4.5E-06 | 4.5E-06 | 4.5E-06 |
| Sn | 0.0E+00 | 2.8E-06 | 2.8E-06 | 2.8E-06 | 2.8E-06 | 2.8E-06 | 2.8E-06 | 2.8E-06 | 2.8E-06 | 2.8E-06 | 2.8E-06 | 2.8E-06 |
| Nb | 0.0E+00 | 2.3E-06 | 2.3E-06 | 2.3E-06 | 2.3E-06 | 2.3E-06 | 2.3E-06 | 1.9E-06 | 6.7E-08 | 4.7E-11 | 1.6E-10 | 4.0E-10 |
| Cd | 0.0E+00 | 1.8E-06 | 1.8E-06 | 1.8E-06 | 1.8E-06 | 1.8E-06 | 1.8E-06 | 1.8E-06 | 1.8E-06 | 1.8E-06 | 1.8E-06 | 1.8E-06 |
| Se | 0.0E+00 | 1.7E-06 | 1.7E-06 | 1.7E-06 | 1.7E-06 | 1.7E-06 | 1.7E-06 | 1.7E-06 | 1.7E-06 | 1.7E-06 | 1.7E-06 | 1.7E-06 |
| Np | 0.0E+00 | 1.3E-06 | 1.3E-06 | 1.3E-06 | 1.4E-06 | 1.4E-06 | 1.4E-06 | 1.2E-06 | 1.2E-06 | 1.2E-06 | 1.2E-06 | 1.2E-06 |
| Sb | 0.0E+00 | 1.1E-06 | 1.1E-06 | 1.1E-06 | 1.1E-06 | 1.1E-06 | 1.1E-06 | 1.1E-06 | 1.0E-06 | 8.2E-07 | 7.0E-07 | 7.0E-07 |
| Eu | 0.0E+00 | 7.8E-07 | 7.8E-07 | 7.8E-07 | 7.8E-07 | 7.8E-07 | 7.8E-07 | 7.8E-07 | 7.7E-07 | 7.5E-07 | 8.1E-07 | 1.0E-06 |
| Br | 0.0E+00 | 6.6E-07 | 6.6E-07 | 6.6E-07 | 6.6E-07 | 6.6E-07 | 6.6E-07 | 6.6E-07 | 6.6E-07 | 6.6E-07 | 6.6E-07 | 6.6E-07 |
| Ag | 0.0E+00 | 6.4E-07 | 6.4E-07 | 6.4E-07 | 6.4E-07 | 6.4E-07 | 6.4E-07 | 6.4E-07 | 6.4E-07 | 6.4E-07 | 6.4E-07 | 6.4E-07 |
| In | 0.0E+00 | 3.3E-07 | 3.3E-07 | 3.3E-07 | 3.3E-07 | 3.3E-07 | 3.3E-07 | 3.3E-07 | 3.3E-07 | 3.3E-07 | 3.3E-07 | 3.4E-07 |
| Gd | 0.0E+00 | 2.0E-07 | 2.0E-07 | 2.0E-07 | 2.0E-07 | 2.0E-07 | 2.0E-07 | 2.0E-07 | 2.2E-07 | 2.8E-07 | 3.6E-07 | 3.7E-07 |
| H | 0.0E+00 | 5.5E-08 | 5.5E-08 | 5.5E-08 | 5.5E-08 | 5.5E-08 | 5.5E-08 | 5.5E-08 | 5.2E-08 | 4.2E-08 | 1.8E-08 | 3.3E-09 |
| Ge | 0.0E+00 | 4.8E-08 | 4.8E-08 | 4.8E-08 | 4.8E-08 | 4.8E-08 | 4.8E-08 | 4.8E-08 | 4.8E-08 | 4.8E-08 | 4.8E-08 | 4.8E-08 |
| As | 0.0E+00 | 1.5E-08 | 1.5E-08 | 1.5E-08 | 1.5E-08 | 1.5E-08 | 1.5E-08 | 1.5E-08 | 1.5E-08 | 1.5E-08 | 1.5E-08 | 1.5E-08 |
| Tb | 0.0E+00 | 1.3E-08 | 1.3E-08 | 1.3E-08 | 1.3E-08 | 1.3E-08 | 1.3E-08 | 1.3E-08 | 1.3E-08 | 1.3E-08 | 1.3E-08 | 1.3E-08 |
| Dy | 0.0E+00 | 6.2E-09 | 6.2E-09 | 6.2E-09 | 6.2E-09 | 6.2E-09 | 6.2E-09 | 6.2E-09 | 6.2E-09 | 6.2E-09 | 6.2E-09 | 6.2E-09 |

44 The "No cooling" composition was used for modeling scenario 3 discussed in Section 3 of this report. For model scenarios 3, case 3b, 0.17 moles/pin bond sodium was included in the chemical system (amount based on proportion of sodium in an ALMR pin [53]).

**C.2 Results/Summary of Findings**

Results from cases 1a and 1b are instructive for showing the types of information that equilibrium models provide, as well as demonstrating the effect of the basic assumptions described in Figure 3-2. Representative results from scenario 1 are shown in Figure 3-3.

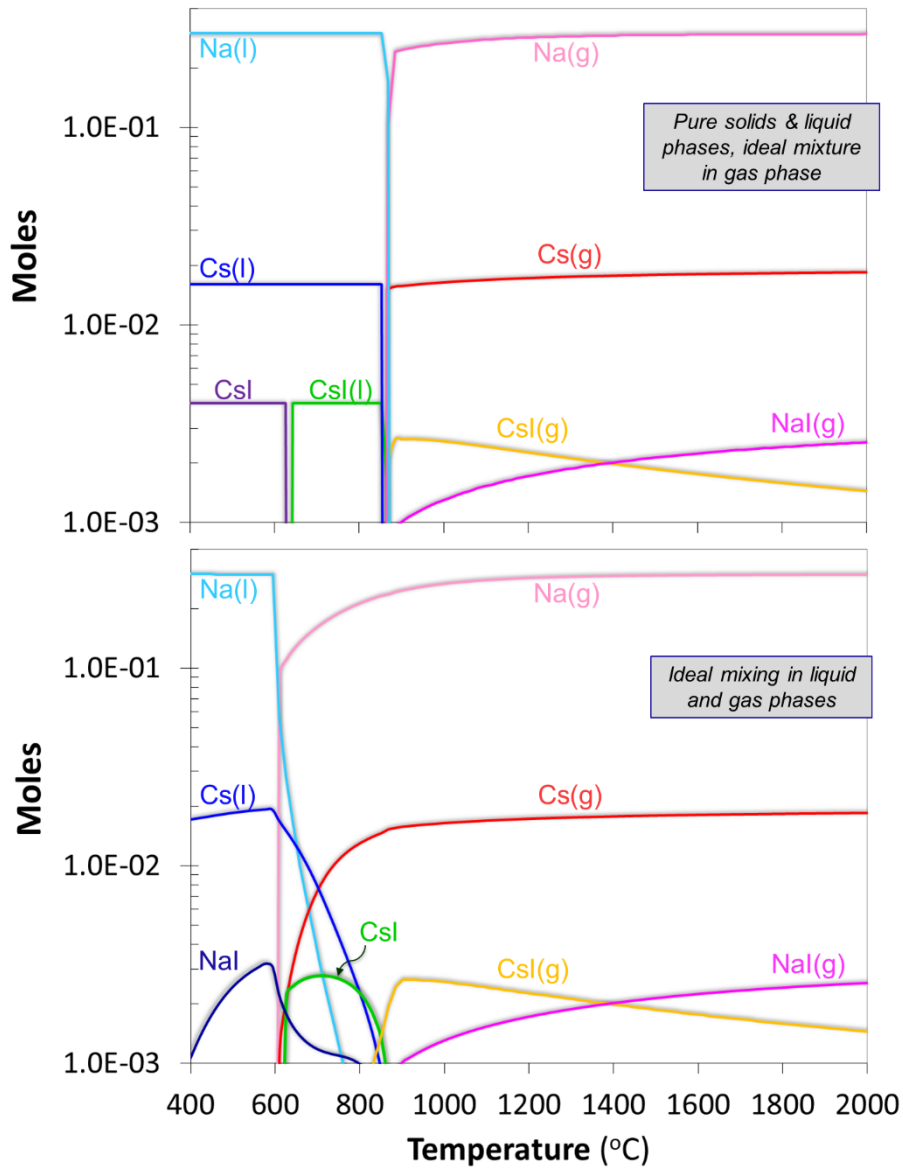


**Figure C-1: Example Results from the Case 1a and 1b Model Runs[45]**

Figure C-1 shows that for the pure phase solids and liquid assumption, the molten phases of Na, Cs, and CsI transition to Na, Cs, CsI, and NaI gas species at around 880°C. Assuming ideal mixing within the molten phase leads to the stabilization of NaI and CsI below 850°C and decreases the temperature at which both Na and Cs become mostly gaseous species. These results, therefore, indicate that the use of mixing models or pure phase assumptions lead to distinct iodine bearing species (NaI vs. CsI). This is an

[45] Plots show the equilibrium composition of the Na-Cs-I system as a function of temperature assuming pure phase equilibrium (top) and ideal mixing in the liquid (melt) phase (bottom). The bulk composition for the system is 0.3 moles sodium, 0.02 moles cesium and 0.002 moles iodine

important observation that could influence predicted release fractions of cesium and iodine if the fuel was to come in contact with hot sodium coolant.

To further demonstrate the type of information that equilibrium models provide for complex mixed fission product and fuel systems, a summary of pertinent observations are bulleted below. As shown in Figures C-2 to C-8[46], the results for modeling scenario 2 lead to the following general observations:

- Actinides such as uranium are predicted to be associated with noble metal elements such as ruthenium, rhodium, and palladium.
- The important radionuclide cesium is predicted to be present mainly as molten cesium metal with lesser amounts of solid cesium telluride and iodide below 700°C. At temperatures greater than 850°C cesium and cesium iodide gas species are dominant.
- Rubidium is predicted to be present as a melt and rubidium bromide below 800°C. Above 850°C rubidium is present as rubidium and rubidium bromide and iodide gas species.
- The speciation of the key radionuclide iodine is predicted to be present as cesium and rubidium iodide below 800°C. At temperatures from around 800°C to 1200°C iodine is predicted to partition into a barium iodide melt phase. Above 1200°C gaseous cesium iodide, strontium iodide, and rubidium iodide are predicted to dominate.
- Barium is predicted to remain largely in the elemental state as a solid and melt over the entire temperature range. From around 640°C up to 1500°C a barium iodide melt phase is also predicted to be stable. Also above 1500°C barium gas species are present in measurable quantities.
- Strontium is predicted to remain as an elemental solid and melt to temperatures up to 1100°C where it partitions in to a gas phase containing mainly elemental strontium and strontium iodide.
- The lanthanide elements cerium and lanthanum are predicted to be present as stable selenide and telluride compounds. Europium is somewhat unique in that it is predicted to volatilize at temperatures greater than 1600°C.

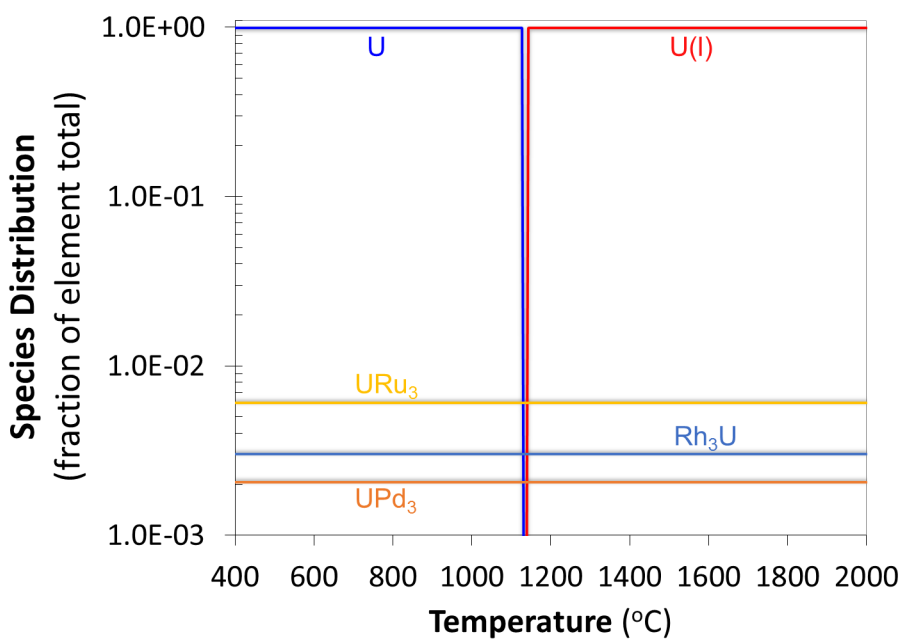


**Figure C-2: Uranium Speciation for Model Scenario 2**

[46] Not all the elements listed in Table C-3 are plotted in Figure C-1 to C9, as the purpose of these plots is to highlight the chemical trends for key elements rather than track the behavior of each element listed.

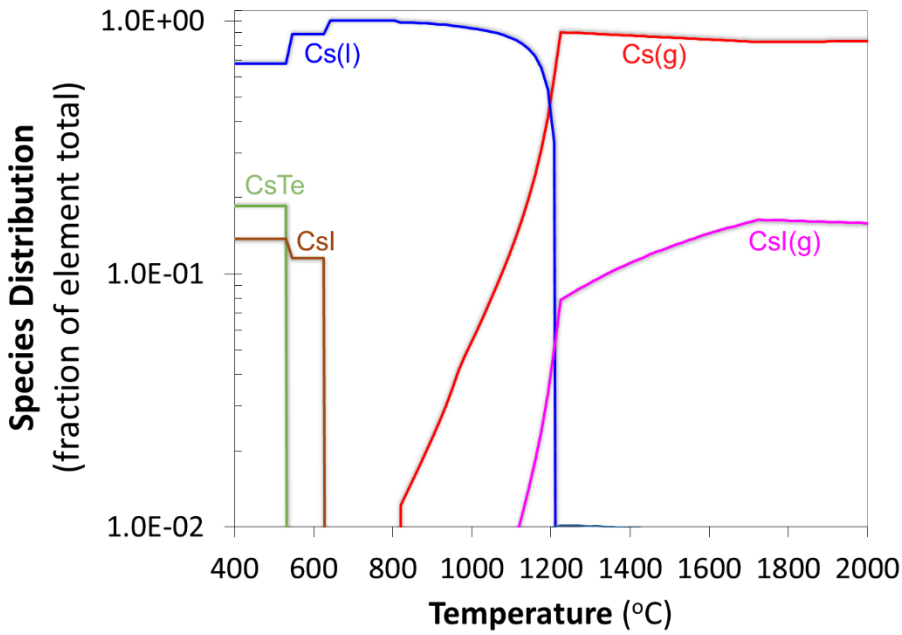


**Figure C-3: Cesium Speciation for Model Scenario 2**

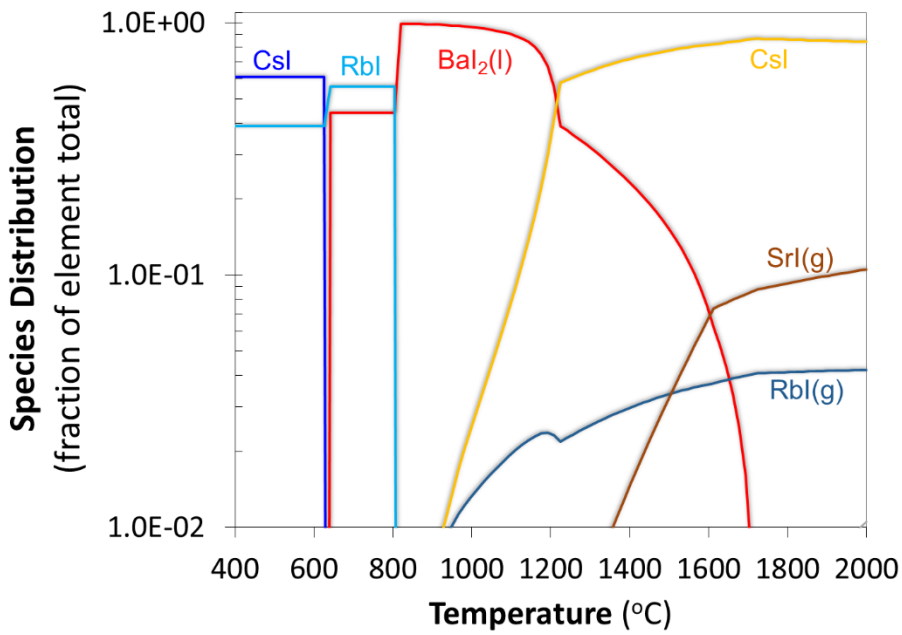


**Figure C-4: Iodine Speciation for Model Scenario 2**

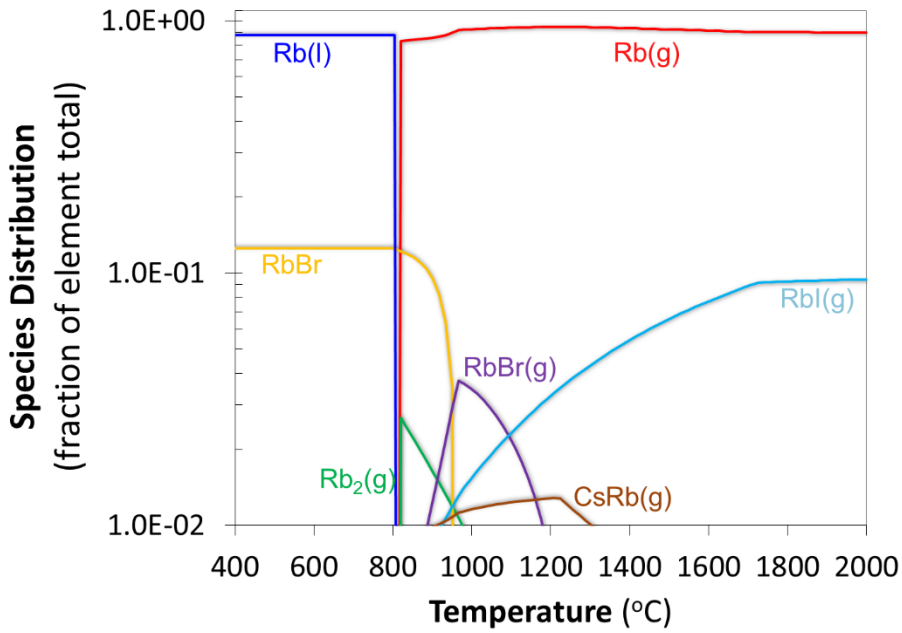


**Figure C-5: Rubidium Speciation for Model Scenario 2**

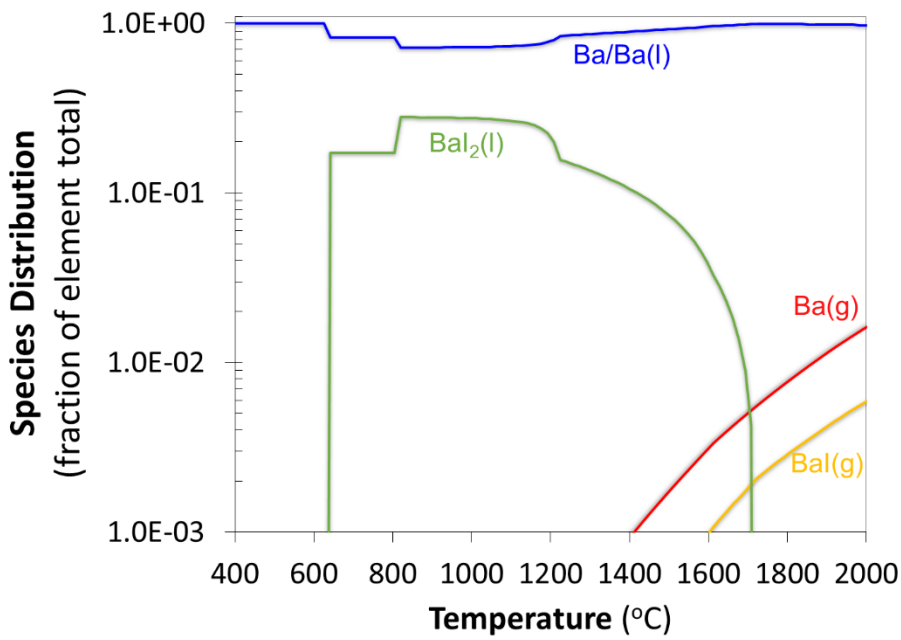


**Figure C-6: Barium Speciation for Model Scenario 2**

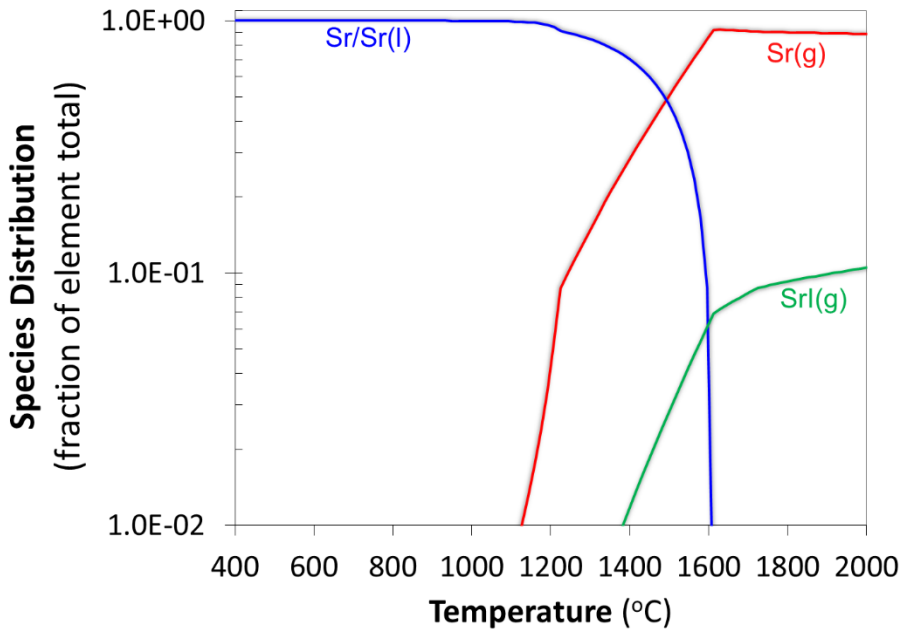


**Figure C-7: Strontium Speciation for Model Scenario 2**

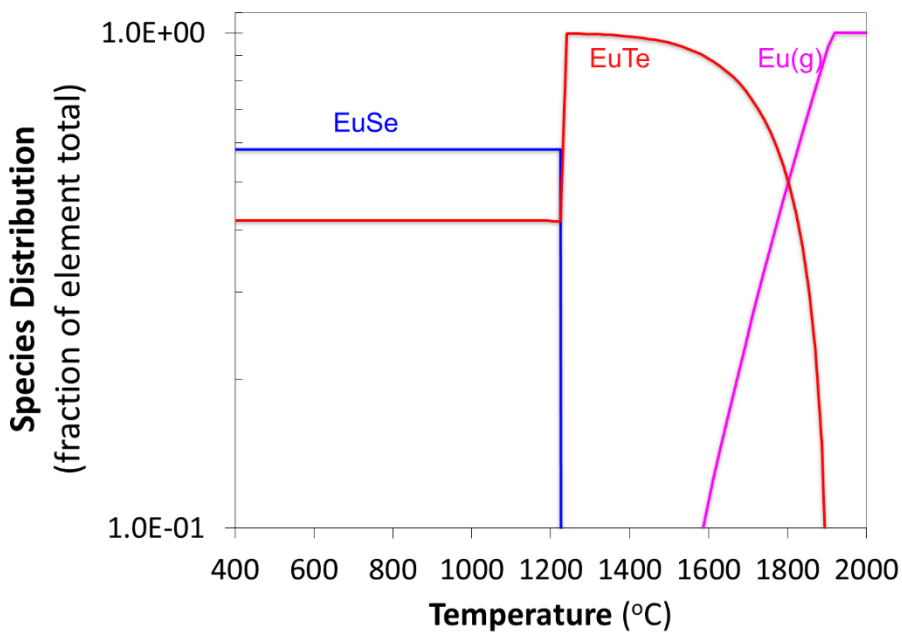


**Figure C-8: Europium Speciation for Model Scenario 2**

For model scenario 3, the Fermi 1 simulation, two cases were run to investigate the role that sodium within the pin (bond sodium) is predicted to play in terms of equilibrium speciation. The following general observations were made (Figures C-9 To C-12[47]).

[47] Not all the elements listed in Table C-3 are plotted in Figure C-9 to C12, as the purpose of these plots is to highlight the chemical trends for key elements rather than track the behavior of each element listed.

- As with scenario 2, the key element cesium is predicted to be present as a melt with lesser amounts of cesium iodide and telluride below 1000°C. The presence of sodium is predicted to lower the temperature at which cesium volatilizes (Figure C-9) as well as suppress the formation of cesium iodide in the gas phase due to the stability of sodium iodide.
- Iodide speciation is also dramatically influenced by the presence of sodium. For the no-sodium case iodine is predicted to be present as cesium and rubidium compounds below 800°C, barium iodide up to 1200°C and cesium and strontium gases species above that. If sodium is present, however, iodine speciation becomes dominated by sodium iodide at temperatures greater than 900°C (Figure C-10).
- Sodium also plays a key role in barium speciation due to the suppression of barium iodide by the formation of sodium iodide. It is interesting to note that for the sodium case, barium is predicted to volatilize at temperatures greater than 1100°C. Also of note is the stability of a barium – tin compound at temperatures from 400°C to 1400°C. Strontium is noted to follow the same trends at barium with the absence of the tin phase.
- An example of tellurium speciation for scenario 3 shows the dominance of cesium telluride at temperatures less than 550°C and lanthanide tellurides form 550°C up to 1800°C where tellurium gas species becomes dominant.

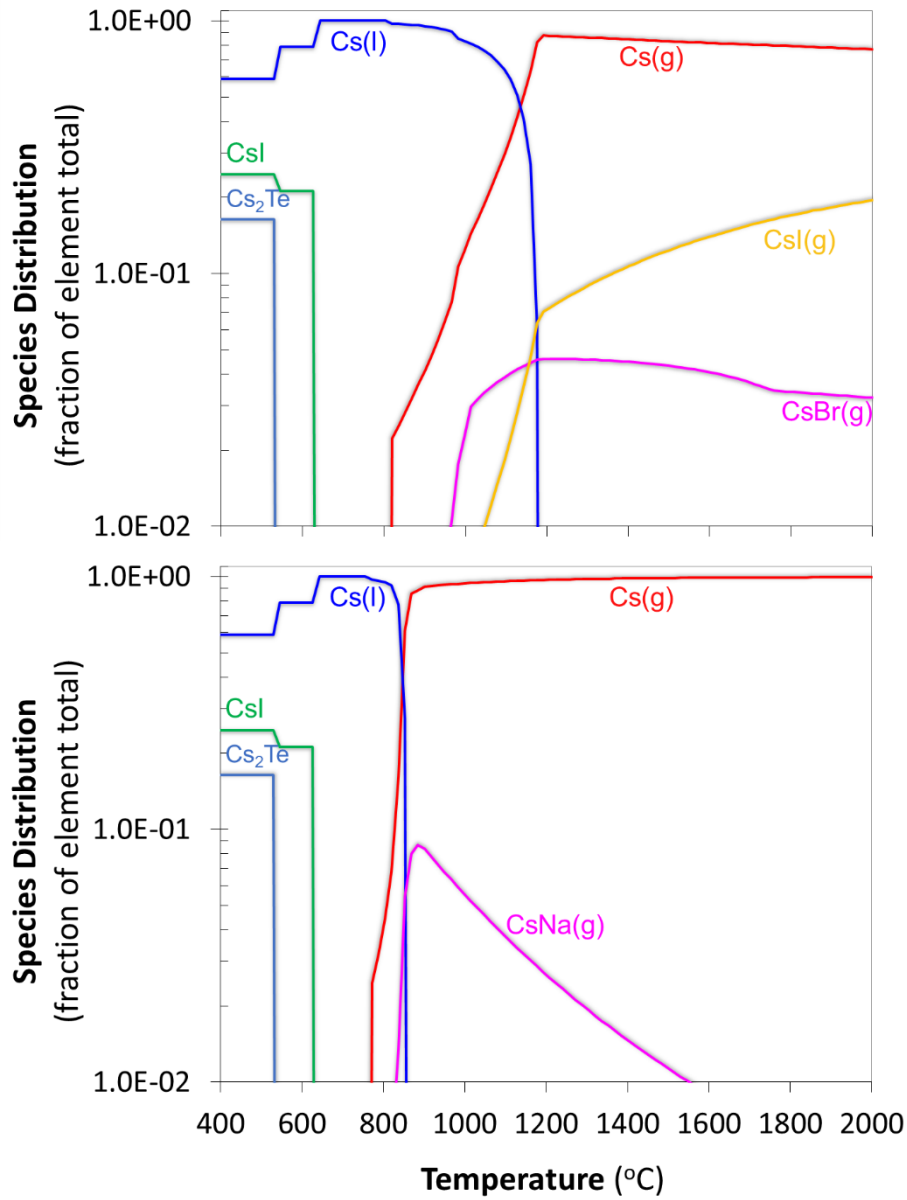


**Figure C-9: Comparison of Cesium Speciation for Model Scenario 3, case 3a – No Sodium Case (top plot) and Case 3b – Bond Sodium included in System (bottom plot)**

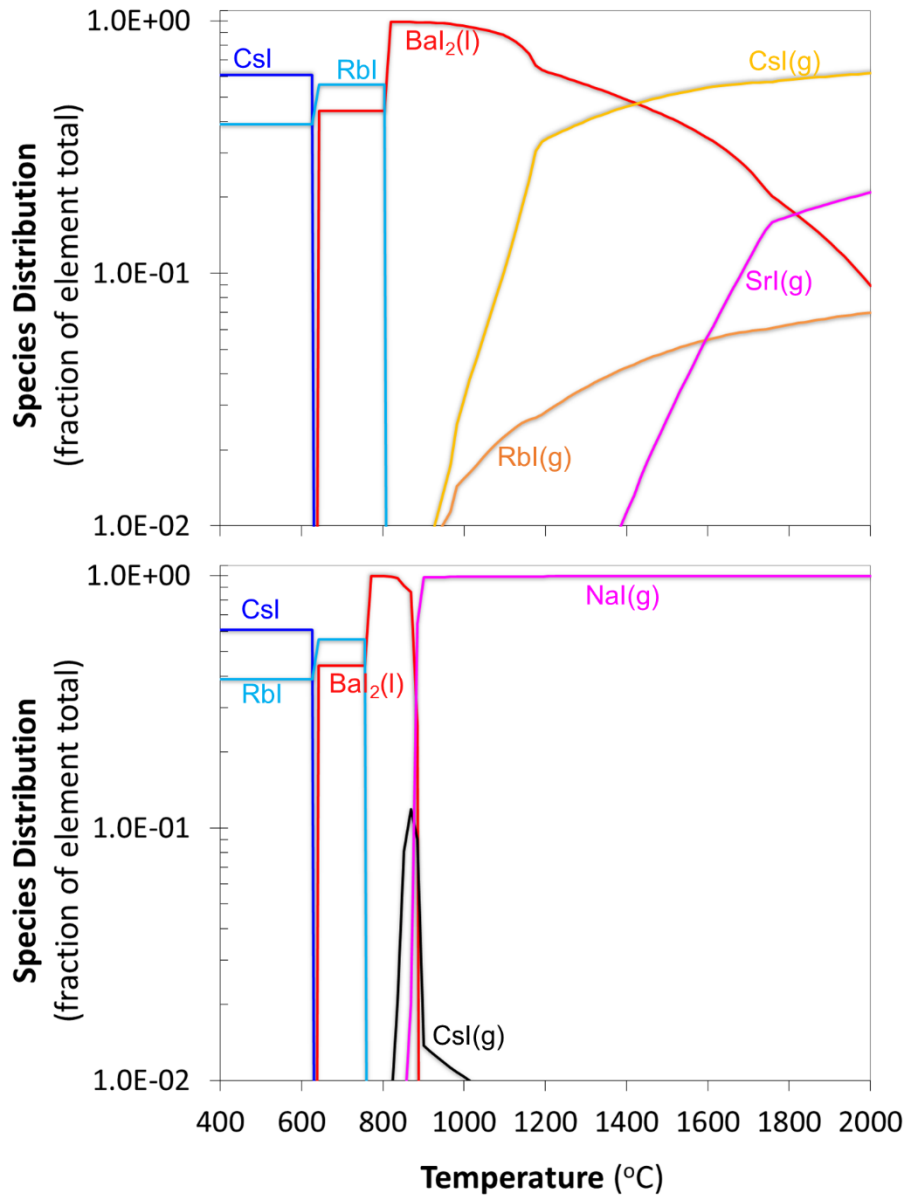


**Figure C-10: Comparison of Iodine Speciation for Model Scenario 3, case 3a – No Sodium Case (top plot) and Case 3b – Bond Sodium included in System (bottom plot)**

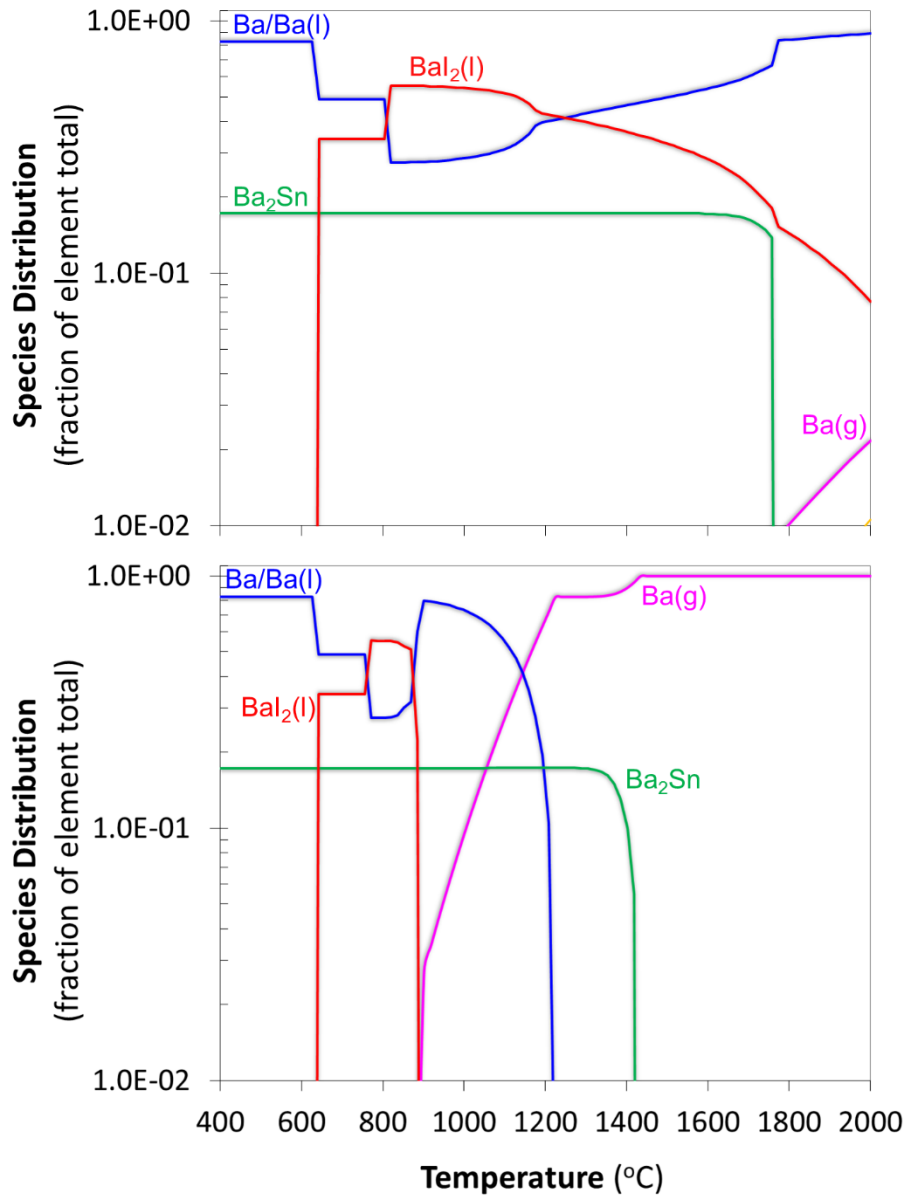


**Figure C-11: Comparison of Barium Speciation for Model Scenario 3, case 3a – No Sodium Case (top plot) and Case 3b – Bond Sodium included in System (bottom plot)**

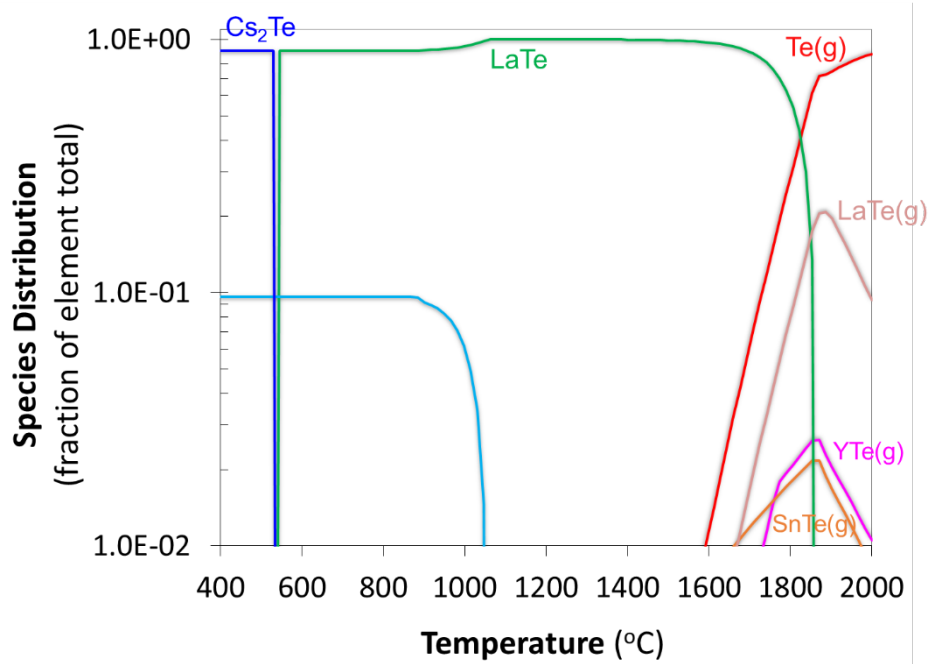


**Figure C-12: Tellurium Speciation for Model Scenario 3, case 3a**

The results from this study do not include mixing models for the complex mixed fission product-fuel systems of model scenarios 1 and 2. However, the qualitative comparison of the results to experiments and historical accidents suggests that the pure phase models may provide bounding cases for the volatilization of key radionuclides. The pure phase models are generally conservative relative to the mixing models in terms of the volatilization of key radionuclides such as cesium, iodine, rubidium, strontium and barium. However, the magnitude of this conservatism needs to be quantified.

Due to the uncertainties involved in the scoping model runs performed as part of this work, it is premature to expect the results to predict the behaviors of key radionuclides in specific experiments or accident scenarios. However, it is noted that using the pure phase assumption tends to over-predict volatilization of cesium, iodine, barium and strontium relative to measured release fractions.

**Nuclear Engineering Division**
Argonne National Laboratory
9700 South Cass Avenue, Bldg. 208
Argonne, IL 60439-4842

www.anl.gov

Argonne National Laboratory is a U.S. Department of Energy
laboratory managed by UChicago Argonne, LLC